Acetylcholine mediates protective immune responses against the rodent filarial nematode *Litomosoides sigmodontis*

Dissertation

zur

Erlangung eines Doktorgrades (Dr. rer. nat.)

der

Mathematisch-Naturwissenschaftlichen Fakultät

der

Rheinischen Friedrich-Wilhelms-Universität Bonn

vorgelegt von

Anna Lena Neumann

aus

Moers

Bonn, August 2021

Angefertigt mit der Genehmigung der Mathematisch-Naturwissenschaftlichen Fakultät der Rheinischen Friedrich-Wilhelms-Universität Bonn

1. Gutachter: Prof. Dr. Marc Hübner

2. Gutachter: Prof. Dr. Walter Witke

Tag der Promotion: 07.02.2022

Erscheinungsjahr: 2022

Summary

A variety of tropical infectious diseases are caused by parasitic helminths. These include filarial infections causing lymphatic filariasis and onchocerciasis (river blindness). Filariae have the ability to modulate the immune response of their host in such a way that they can survive in their host for many years. On the one hand, this is a disadvantage for the infected individuals, as they may suffer from the symptoms of the disease and social stigmatization. On the other hand, human and animal studies suggested that helminth infections or worm proteins have a protective effect on allergies and autoimmune diseases. For a better understanding of the protective immune response against filariae and their ability to modulate immune mechanisms of the host, the rodent filarial nematode *Litomosoides sigmodontis* was used. Previous studies showed that the immune system and the nervous system interact with each other to ensure proper regulation of inflammatory processes. The aim of this thesis was to investigate the contribution of acetylcholine (ACh) signalling through muscarinic receptors in regulating the immune response against *L. sigmodontis*. Since it is already known that the enzyme choline acetyltransferase (ChAt) is needed for ACh synthesis, ChAt reporter mice were naturally infected via the mite vector (*Ornithonyssus bacoti*) for identification of ACh producing cells during *L. sigmodontis* infection. At day 5 post infection, when the migrating L3 larvae reach the thoracic cavity, $CD4^+$ T cells and $CD8^+$ T cells showed an increased ChAt expression in the thoracic cavity of infected animals compared to naïve mice. In addition, at 35 days post infection when L4 larvae have finally moulted into adult worms, ChAt expression of $CD8^+$ T cells, B cells and neutrophils was increased. Since ACh was produced by immune cells such as $CD4^+$ T cells and neutrophils, which are essential for the protective immune response against filariae and at an important time of filarial development, natural infection with *L. sigmodontis* in BALB/c wild-type mice was studied when the cholinergic signalling was inhibited using aclidinium bromide (AB). Cholinergic inhibition resulted in an increased worm recovery at day 9 of a natural infection. This time point is shortly after the infective L3 larvae reached their final location, the thoracic cavity, indicating that protective immune responses occurred during the migration of the L3 larvae. Circumventing the migration of L3 larvae through the skin by an intravenous injection led to a comparable worm burden in mice treated with or without muscarinic inhibitor, indicating that the protective immune responses within the skin were compromised by the inhibition of ACh signalling. Analysis of the immune response in the skin, the first barrier L3 larvae have to penetrate, showed that neutrophil recruitment is delayed in AB-treated animals.

Confirmation of the involvement of ACh in protective immune responses against *L. sigmodontis* was further provided in muscarinic receptor type 3 (M3R) knockout mice. The M3R is a muscarinic ACh receptor that is necessary to ensure smooth muscle contraction and is present in the central nervous system, the lung and on immune cells. In comparison to wild-type mice, $M3R^{-/-}$ mice had a lower worm burden at day 9 but an increased worm burden 15 and 37 days after natural infection. Immunological analysis showed that, natural infection with *L. sigmodontis* was accompanied by decreased numbers of eosinophils, neutrophils, and significantly reduced $CD4^+$ and $CD8^+$ T cell numbers in the thoracic cavity of $M3R^{-/-}$ mice compared to wild-type mice at day 9 post infection. At day 15 post infection, T cell numbers were still reduced, but increased at day 37 post infection and tended to be higher in $M3R^{-/-}$ mice compared to wild-type mice. Interestingly, delayed larval migration in $M3R^{-/-}$ mice was abolished after intravenous infection, which revealed comparable differences on the cellular level in the thoracic cavity of both infected groups as natural infection. As intravenous infection circumvented the reduced worm recovery in $M3R^{-/-}$ mice, either L3 migration through the skin or the lymphatics might have been affected. Therefore, the local immune response in the skin was analysed as the majority of penetrating L3 larvae are already eliminated there. Neutrophils, eosinophils and $CD4^+$ T cells are essential for the protective immune response against *L. sigmodontis*. After 3 hours of intradermal infection with infective L3 larvae neutrophils were recruited in both WT and $M3R^{-/-}$ mice compared to their corresponding controls. However, $M3R^{-/-}$ mice revealed reduced eosinophil recruitment accompanied by an impaired activation of eosinophils and neutrophils compared to WT mice. Furthermore, the vascular permeability was investigated as it is known that histamine induces vasodilation, which facilitates larval migration due to an increased vascular permeability. Basophils are the main producers of histamine in the plasma. Therefore, when histamine release was investigated after 30 minutes of an intravenous infection, reduced histamine levels in the plasma of $M3R^{-/-}$ mice compared to WT mice were observed. Reduced histamine release contradicts the theory of enhanced vascular permeability in the $M3R^{-/-}$ mice. However, when vascular permeability was examined for confirmation, a significantly increased vascular permeability in the M3R deficient mice was noticed. *In vitro* analysis further revealed that activation was impaired in neutrophils and basophils derived from $M3R^{-/-}$ mice. These data suggest that ACh is involved in protective immune responses against filariae by facilitating the migration of L3 larvae to the thoracic cavity and is associated with neutrophil activation and recruitment.

Zusammenfassung

Eine Vielzahl tropischer Infektionskrankheiten wird durch parasitäre Helminthen verursacht. Hierzu zählen Infektionen mit Filarien die Erkrankungen wie die lymphatische Filariose und Onchozerkose (Flussblindheit) verursachen. Filarien haben die Fähigkeit, die Immunantwort ihres Wirtes so zu modulieren, dass sie viele Jahre in ihm überleben können. Einerseits ist dies zum Nachteil der infizierten Personen, da diese unter den Krankheitssymptomen und der sozialen Stigmatisierung leiden können. Andererseits haben einige Studien an Menschen und Tieren bestätigt, dass Infektionen mit Helminthen oder deren Proteine einen schützende Wirkung gegen Allergien und Autoimmunerkrankungen haben können. Um die Immunantwort gegen Filarien und deren Fähigkeit das Immunsystem des Wirtes zu modulieren besser zu verstehen, wird die Nagetier Filarie *Litomosoides sigmodontis* verwendet. Frühere Studien haben gezeigt, dass das Immunsystem und das Nervensystem miteinander interagieren, um eine angemessene Regulierung von Entzündungsprozessen zu gewährleisten. Ziel dieser Arbeit war es, den Einfluss der Acetylcholin (ACh)-Signalübertragung durch muskarinische Rezeptoren bei der Regulierung der Immunantwort gegen *L. sigmodontis* zu untersuchen. Choline Acetyltransferase (ChAt) Reportermäuse wurden hier mit Hilfe des Milbenvektor (*Ornithonyssus bacoti*) natürlicherweise mit *L. sigmodontis* infiziert und Immunzellen wurden auf ihre Fähigkeit hin, ACh zu produzieren untersucht. Das Enzym ChAt ist notwendig für die Synthese von ACh. Im Vergleich zu naïven Tieren, konnte an Tag 5 der Infektion, der Zeitpunkt an dem L3 Larven den Ort der Infektion erreichen (Pleurahöhle), eine erhöhte ChAt Expression in $CD4^+$ T Zellen und $CD8^+$ T Zellen aus der Pleurahöhle beobachtet werden. Zudem zeigten $CD8^+$ T Zellen, B Zellen und Neutrophile eine erhöhte ChAt Expression an Tag 35, wenn sich die L4 Larven zu adult Würmen weiterentwickeln. ACh wurde von Immunzellen wie $CD4^+$ T Zellen und Neutrophilen produziert, die für die schützende Immunantwort gegen Filarien essentiell sind und dies an Zeitpunkten die für die Filarienentwicklung wichtig sind. Daher wurde die natürliche Infektion mit *L. sigmodontis* in BALB/c Wildtyp Mäusen untersucht während die cholinerge Signalübertragung mit Aclidiniumbromid (AB) gehemmt wurde. Die Hemmung des cholinergen Signals führte zu einer erhöhten Wurmlast an Tag 9 der natürlichen Infektion. Dieser Zeitpunkt liegt kurz nachdem die infektiösen L3 Larven ihren endgültigen Aufenthaltsort, die Pleurahöhle, erreicht hatten, was darauf hindeutet, dass schützende Immunreaktionen während der Wanderung der L3 Larven stattfinden. Analysen der Immunreaktionen in der Haut, welche die erste Barriere der migrierenden L3 Larven darstellt,

zeigten, dass die Rekrutierung von Neutrophilen bei mit Aclidiniumbromid behandelten Tieren verzögert ist. Umgeht man die natürliche Wanderung der L3 Larven durch die Haut mittels einer intravenösen Injektion führte dies zu einer vergleichbaren Wurmlast bei Mäusen, die mit oder ohne muskarinischen Inhibitor behandelt wurden. Dies deutet darauf hin, dass die schützenden Immunreaktionen in der Haut durch die Hemmung der ACh-Signalübertragung verhindert wurden. Die Beteiligung von ACh an schützenden Immunreaktionen gegen *L. sigmodontis* wurde außerdem durch Knockout Mäuse mit dem muskarinischen Typ 3 Rezeptor (M3R) bestätigt. Der M3R gehört zu den muskarinischen ACh Rezeptoren, kommt hauptsächlich im zentralen Nervensystem, in der Lunge und auf Immunzellen vor und ist für die Kontraktion der glatten Muskulatur notwendig. *L. sigmodontis* infizierte $M3R^{-/-}$ Mäuse hatten im Vergleich zu den Wildtyp Kontrollen an Tag 9 der Infektion eine geringere Wurmlast, wohingegen an Tag 15 und 37 der natürlichen Infektion eine erhöhte Wurmlast beobachtet werden konnte. Immunologische Analysen zeigten zudem, dass eine natürliche Infektion mit *L. sigmodontis* an Tag 9 mit einer verringerten Anzahl von Eosinophilen und Neutrophilen sowie einer signifikant reduzierten Anzahl von $CD4^+$ und $CD8^+$ T Zellen in der Pleurahöhle von $M3R^{-/-}$ Mäusen im Vergleich zu Wildtyp Mäusen einherging. An Tag 15 konnte weiterhin eine Reduktion bei der T Zell Anzahl festgestellt werden, welche dann allerdings an Tag 37 in der Gruppe der $M3R^{-/-}$ Mäuse, verglichen mit den Wildtyp Kontrollen tendenziell erhöht war. Interessanterweise war die verzögerte Wanderung der L3 Larven bei $M3R^{-/-}$ Mäusen nach einer intravenösen Infektion aufgehoben. Auf zellulärer Ebene wurden verglichen mit der natürlichen Infektion, vergleichbare Unterschiede in der Pleurahöhle von beiden infizierten Gruppen festgestellt. Da eine intravenöse Infektion die reduzierte Wurmlast an Tag 9 in den $M3R^{-/-}$ Mäusen aufgehoben hat, könnte entweder die Wanderung der L3 Larven durch die Haut oder die Lymphgefäße betroffen sein. Aus diesem Grund wurde im nächsten Schritt die lokale Immunreaktion in der Haut analysiert. Neutrophile, Eosinophile und $CD4^+$ T Zellen sind entscheidend an der schützende Immunantwort gegen *L. sigmodontis* beteiligt. Drei Stunden nachdem infektiöse L3 Larven in die Haut der Tiere injiziert wurden, infiltrierten Neutrophile die Injektionsstelle sowohl bei Wildtyp Mäusen als auch bei $M3R^{-/-}$ Mäusen verglichen mit den entsprechenden Kontrollen. Interessanterweise, wiesen $M3R^{-/-}$ Mäuse verglichen mit den Kontrollen eine verminderte Rekrutierung von Eosinophilen auf, die mit einer geringeren Aktivierung von Eosinophilen und Neutrophilen einherging. Darüber hinaus wurde die vaskuläre Permeabilität untersucht, da bekannt ist, dass Histamin eine Vasodilatation induziert, welche die Migration der Larven aufgrund einer erhöhten vaskulären Permeabilität erleichtert. Basophile Zellen sind die Hauptproduzenten von Histamin im

Plasma. Daher wurde die Histaminfreisetzung 30 Minuten nach einer intravenösen Infektion untersucht. Es hat sich gezeigt, dass der Histamingehalt im Plasma der $M3R^{-/-}$ Mäuse im Vergleich zu Wildtyp Mäusen reduziert war. Obwohl die verringerte Histaminfreisetzung in $M3R^{-/-}$ Mäusen der Theorie einer erhöhten Gefäßpermeabilität wiederspricht wurde zur Bestätigung die Gefäßpermeabilität untersucht. Interessanterweise zeigte sich trotz reduzierten Histamingehaltes eine signifikant erhöhte Gefäßpermeabilität bei den $M3R^{-/-}$ Mäusen. *In vitro* Analysen zeigten außerdem, dass die Aktivierung von Neutrophilen und Basophilen aus $M3R^{-/-}$ Mäusen beeinträchtigt war. Zusammenfassend deuten diese Daten darauf hin, dass ACh an schützenden Immunreaktionen gegen Filarien beteiligt ist, indem es die Migration von L3 Larven in die Pleurahöhle erleichtert und mit der Aktivierung und Rekrutierung von Neutrophilen einhergeht.

Table of Contents

1. Introduction 1

1.1 Parasites 1

1.2 Neglected tropical diseases 1

1.3 *L. sigmodontis* - an experimental mouse model to study filarial immune responses 3

1.4 General immune response against pathogens 5

1.5 Immune response against helminths 6

1.6 Neuro-immune interaction 8

1.7 The cholinergic anti-inflammatory pathway 9

1.8 The neurotransmitter acetylcholine 10

1.9 Aim 13

2. Material and methods 14

2.1 Housing of animals 14

2.2 Life cycle of *L. sigmodontis* 14

2.3 Experimental infection with *L. sigmodontis* 14

2.3.1 Natural infection 14

2.3.2 Subcutaneous infection 15

2.3.3 Intradermal infection 15

2.3.4 Intravenous infection 16

2.4 *L. sigmodontis* adult worm extract (LsAg) preparation 16

2.5 Bradford assay 17

2.6 General experimental *in vivo* set up 17

2.7 Analysis of microfilariae counts 17

2.8 Analysis of embryogenesis 17

2.9 Plasma isolation 18

2.10 Isolation of spleen cells 18

2.11 Isolation of thoracic cavity cells 18

2.12 Bronchio-alveolar cell isolation 19

2.13 Lung cell isolation 19
2.14 Cell staining for flow cytometry 20
2.16 Filarial analysis 24
2.17 Enzyme-linked immunosorbent assay (ELISA) 25
2.18 RNA isolation and detection of ChAt expression by PCR analysis 25
2.19 Isolation of bone marrow-derived neutrophils 26
2.20 *In vitro* activation assay and co-culture 27
2.21 Whole blood activation assay 27
2.22 DNA quantification 28
2.23 Vascular permeability assay 28
2.24 Statistical analysis 28
3. Results 29
3.1 Expression of choline acetyltransferase in immune cells during *L. sigmodontis* infection 29
3.2 Influences of cholinergic signalling during *L. sigmodontis* infection in BALB/c mice 32
3.2.1 Cholinergic inhibition with aclidinium bromide increases the worm burden following natural *L. sigmodontis* infection 32
3.2.2 Intravenous infection with *L. sigmodontis* abolishes the higher worm recovery 33
3.2.3 Cholinergic inhibition with aclidinium bromide during intradermal *L. sigmodontis* infection 36
3.3 Lack of muscarinic type 3 receptor signalling during *L. sigmodontis* infection 37
3.3.1 Lack of M3R leads to a delayed but higher worm recovery after natural *L. sigmodontis* infection 37
3.3.2 Cellular recruitment to different body compartments at 9 days post natural *L. sigmodontis* infection 40
3.3.3 Cellular composition in different body compartments at 15 days of natural *L. sigmodontis* infection 44
3.3.4 Cellular composition in different body compartments at 37 days of natural *L. sigmodontis* infection 47

3.3.5 Cellular composition in different body compartments at 70 days of natural *L. sigmodontis* infection 52

3.4 Summary of the cellular analysis at the different time points of *L. sigmodontis* infection 57

3.5 Intravenous *L. sigmodontis* infection abolishes the higher worm recovery in $M3R^{-/-}$ mice 58

3.4.1 Cellular recruitment to different body compartments at 9 days post intravenous *L. sigmodontis* infection 59

3.5 Innate lymphoid cells during natural and intravenous *L. sigmodontis* infection 63

3.6 Intradermal infection with *L. sigmodontis* leads to reduced granulocyte activation in $M3R^{-/-}$ mice 66

3.7 *In vitro* stimulation of bone marrow-derived neutrophils 68

3.8 Vascular permeability and whole blood *in vitro* assay 70

3.9 Migration kinetics during natural *L. sigmodontis* infection 71

4. Discussion 75

4.1 ChAt expression during natural *L. sigmodontis* infection 75

4.2 Influences of cholinergic signalling during *L. sigmodontis* infection in BALB/c mice 77

4.3 Lack of muscarinic type 3 receptor signalling during natural *L. sigmodontis* infection 79

4.4 Different infection routs of *L. sigmodontis* in $M3R^{-/-}$ mice 82

Complimentary projects 85

5. References 92

List of abbreviations 104

Publications in peer-reviewed journals 107

Conferences 109

Acknowledgements 110

1. Introduction

1.1 Parasites

Parasites are organisms that live at the expense and feed of another species (the host), either temporarily or continuously during their life cycle (1). The parasite exploits nutrients provided by the host. The host does not benefit from this relationship and during an antagonistic relationship like this, the host is often harmed in the progression. It is estimated that about 50% of all animals have at least a partial parasitic life style. They can live either internally in their host (endoparasites) such as parasitic helminths and protozoa, or externally (ectoparasites) such as blood-feeding arthropods.

Helminths are multicellular organisms that can be divided into the Platyhelminths (flatworms), which include trematodes (flukes) and cestodes (tapeworms) and the nematodes (roundworms) (2). Nematodes include the family of filariae. Human pathogenic filariae can cause tissue filariasis (e.g. *Onchocerca volvulus, Loa loa* and *Mansonella perstans)* and lymphatic filariasis (LF; e.g. *Brugia malayi, Brugia timori* and *Wucheria bancrofti)* (3). Infections with filariae have a wide range of disease expression, ranging from asymptomatic infections as in mansonellosis (*M. perstans*) to severe pathology and physical impairment as in case of onchocerciasis (*O. volvulus*) or LF (4).

1.2 Neglected tropical diseases

Neglected tropical diseases are poverty-associated tropical diseases that are prevalent worldwide with more than one billion people affected, but receive less attention. These include filarial infections such as onchocerciasis and LF. Due to the lack of global public awareness of these diseases, that mostly occur in rural areas of developing countries, they are referred to as "neglected tropical diseases" (5). Onchocerciasis and LF are prevalent in tropical and subtropical regions of the world, where they can cause stigmatising diseases. Approximately 21 million people in Sub-Saharan Africa, Yemen and Latin America are infected with *O. volvulus*, and about 114 million people with the filariae *M. perstans* (6, 7). Although *O. volvulus* infections tend to cause a rather mild dermatitis characterized by slight skin inflammation and high parasite loads, but infection can also lead to sever forms of skin pathology or even vision loss, if infected individuals possess a strong immune response that leads to the death of the filarial progeny, the microfilariae (MF) (8, 9). Onchocerciasis is transmitted to the human host via the bite of the *Simulium* (blackfly) vector. Then, L3 larvae

migrate through the subcutaneous tissue of the skin. After developing into adult worms and subcutaneous nodule formation, the females produce unsheathed MF that migrate through the skin and lymphatics until they are reabsorbed after another bite of the blackfly, where they develop into L3 larvae and the cycle restarts (10, 11).

In contrast, LF infections caused by *W. bancrofti* affect about 59 million people worldwide, while infections with *B. malayi* account for around 6 million infections (7). In LF, affected individuals suffer especially from lymphedema in the extremities or the scrotum (hydrocele) which can lead to elephantiasis. The symptoms impede the normal daily life of those affected and lead to social stigmatization (4). LF is transmitted via a blood meal by the mosquito vector of the *Mansonia*, *Aedes* and *Culex* genera (6, 12). In this case, the L3 migrate through the lymphatic vessels, and the developed adult worms produce MF, which subsequently migrate into the blood (6, 12). Here, the mosquitoes acquire the MF after another meal, too, where they develop into L3 larvae.

In order to reduce the incidence of LF and onchocerciasis, mass drug administration (MDA) was implemented. In recent years, LF and onchocerciasis have been treated annually with a combination of diethylcarbamazine (DEC) with albendazole or ivermectin (IVM) plus albendazole, respectively. Vector control programmes supported this. Nowadays, MDA includes a single dose triple therapy of IVM, DEC and albendazole for patients with LF in areas that are not co-endemic for onchocerciasis and/or loiasis. This treatment leads to a reduction of MF that lasts about two years, thus temporarily inhibiting the transmission (13, 14). In areas co-endemic for onchocerciasis, the WHO still recommends a combination of IVM and albendazole. However, individuals with high *Loa loa* MF loads have to be recognised and excluded from treatment to avoid sever adverse events due to rapid elimination of the MF. *L. loa* infections are characterized by an enormous accumulation of MF, which can lead to encephalitis if they are rapidly eliminated. Therefore, affected individuals can be treated with albendazole in advance to avoid sever adverse events of the therapy (15). Furthermore, dying MF in the eye of *Onchocerca*-infected individuals can cause blindness even in small numbers, which prevents the use of DEC in those patients (16). All of these drugs lead to the temporary elimination of MF in the skin and blood of the patients (17). However, the reduction of filariasis infections is impeded by the lack of macrofilaricidal substances as IVM, DEC and albendazole can only temporarily prevent the embryogenesis of filariae and thus limit their transmission (4, 18). Therefore, these drugs have to be administered annually for the reproductive life span of the adult worms. For onchocerciasis

this means a treatment period of 15 years and 5-8 years for LF patients. This long period challenges compliance of the patients. In addition, the amount of drugs and time needed to cover the whole treatment period presents a major challenge for the health care systems (4). Another complication is the treatment in co-endemic areas of Africa, where onchocerciasis and loiasis occur together as already mentioned. In addition, one must bear in mind that with the breadth and frequency of treatment, there were already suboptimal responses observed in areas that had several years of IVM MDA treatment due to developing drug resistance (12).

Interestingly, the mechanism of IVM is still not completely known. It is only known, that it hyperpolarizes glutamate-gated chloride channels, thus interrupts neuronal processing which leads to muscle paralysis of the parasite (4, 17, 19). DEC has a predominantly microfilaricidal effect, as it leads to temporary spastic paralysis due to the inactivation of calcium-dependent ion channels in the musculature of *B. malayi* (20, 21). Another drug target is the endosymbiotic *Wolbachia* bacterium, which can be found in almost all human pathogenic filariae except *L. loa* (22-24). Thus, *Wolbachia* are favourable target for treatment in co-endemic areas. *Wolbachia* are essential for filarial fecundity and survival. The dependency of filariae on the endosymbiont *Wolbachia* makes it possible to use antibiotics to eliminate the *Wolbachia* as anti-filarial treatment. They can be eliminated by doxycycline, which leads to a disrupted embryogenesis and killing of adult worms (18, 25-28). This effect was first tested in mouse models (29), using *L. sigmodontis* infection, and subsequently in humans suffering from onchocerciasis and LF (26, 28). The discovery of doxycycline therapy for filariasis is a huge advance, because it is the first safe macrofilaricidal compound and an already registered drug. However, there are disadvantages as doxycycline has to be given daily for 4-6 weeks and cannot be given to young children and pregnant or breast-feeding women (30, 31).

1.3 *L. sigmodontis* - an experimental mouse model to study filarial immune responses

Basic research to understand the immune response to human parasitic filariae such as *O. volvulus* and the associated search for a vaccine is challenging as rodents are not susceptible to *O. volvulus* (32). Thus, until the 1980s, studies investigated the immune responses using subcutaneous infections of primates with L3 larvae (10). *Brugia* species can infect rodents, but migration through the tissue and thus the complete life cycle does not occur. Finally, the rodent filarial nematode *L. sigmodontis*, which naturally infects cotton rats (*Sigmodon hispidus*), was discovered and the susceptibility of Mongolian gerbils (*Meriones unguiculatus*) and BALB/c mice was demonstrated (10, 33-35). Here, mice can be naturally

infected via the bite of the tropical rat mite (*Ornythyssus bacotii*) and the full developmental life cycle and migration of the filariae can be studied. This infection model allows to study the immune response during different developmental stages of *L. sigmodontis* (10, 36, 37) and it has been shown that there are many similarities in the immune response to *L. sigmodontis* in the mouse model and human filarial infections (34, 38). Therefore, this organism is particularly suitable to study the immune modulation of chronic filarial infections in order to test and identify possible drug candidates. For example, in *L. sigmodontis* infected mice, the filariae were first discovered to be dependent on the *Wolbachia* bacteria (39, 40). Furthermore, the influence of doxycycline on the survival and fertility of filariae was first shown in mice using the *L. sigmodontis* model (41) and then confirmed in humans (28).

The natural infection occurs through the blood meal of an infected tropical rat mite. The infective L3 larvae are transferred to the host and migrate through the skin. Over a period of 5 days, the L3 larvae migrate to the thoracic cavity, which is their preferred habitat in the host. Within their niche, the L3 molt into L4 larvae about 8 days post infection (dpi). Approximately after 30 dpi, the L4 larvae begin to develop into adult worms and reside in the thoracic cavity. Subsequently, the adult worms begin to reproduce and release their offspring, the MF (L1 larvae), about 50 dpi. The MF migrate into the blood of the host. If the host is bitten by a mite at this stage of infection, the mite ingests the MF with the blood meal. In the epithelium of the mite gut, the MF develop into L3 larvae via two molts and the cycle restarts (Fig.1) (42, 43). Susceptible BALB/c mice begin to eliminate adult worms at approximately 70 days. After 120 days, most animals have completely eliminated the worms. The semi-susceptible C57BL/6 mice, on the other hand, have eliminated most of the worms shortly after the development of adult worms around 40 dpi and therefore do not develop microfilaremia (44).

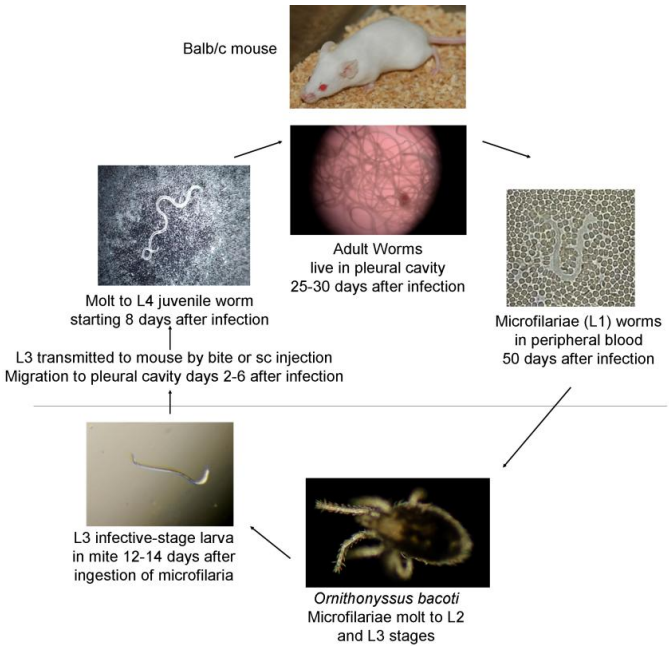

Figure 1: *Litomosoides sigmodontis* life cycle (42). The infective L3 larvae are transferred to the host through a blood meal of the mite *Ornithonyssus bacoti*. L3 larvae migrate into the thoracic cavity over a period of 5 days, where they moult into L4 larvae after about 8 days. The adult worms develop after about 25-30 days and start producing microfilaria (MF) after about 50 days, which migrate into the blood stream. There, MF are reabsorbed via another meal of the mites and develop into L2 larvae and after approx. 12-14 days into L3 larvae.

1.4 General immune response against pathogens

To successfully protect an individual against various diseases, the immune system must fulfil four important tasks. The first of these is the immunological recognition of the infection. Infectious pathogens are recognised by different cells of the immune system. This is done first by the innate immune system, with an immediate non-specific immune response. This is done by antigen-presenting cells such as dendritic cells (DC) and macrophages, which phagocytose the pathogen and present parts of it on their cell surface to activate other immune cells such as lymphocytes. Subsequently, the adaptive immune system is activated and supports the long-term defence. Then there are the immune effector functions. Here the complement system plays an important role, supporting the phagocytosis of pathogens through macrophages, DC and neutrophils which also initiate adaptive immune responses and thus, the destructive work of lymphocytes and the production of antibodies by plasma cells (45). Self-regulation of the immune response is the fourth important task so that the immune system does not turn these reactions against itself, as is e.g. the case in autoimmune diseases such as rheumatoid arthritis. Importantly, when the same pathogen infects the body again, the immune response is faster and stronger. The immunological memory serves this purpose. T and B lymphocytes establish memory cells in order to accelerate the adaptive immune response in the event of renewed contact; this phenomenon is also used for vaccinations.

1.5 Immune response against helminths

The immune response against helminths is very complex, as helminths themselves actively modulate the immune response of the host so that they can persist for months or years (46, 47). In general, helminths elicit a type 2-dominated immune response, which is characterised by the secretion of type 2 cytokines such as IL-4, IL-5 and IL-13 as well as the production of immunoglobulin E (IgE) antibodies (48-51). Another hallmark of helminth infection is eosinophilie (47, 52-54). Additionally, innate lymphoid type 2 cells (ILC2) and alternatively activated macrophages (AAMΦ) are associated with a type 2 immune response (55-57).

For filarial infection, the immune response differs when looking at the different developmental stages of the parasite. Using filarial mouse models, it was shown that at the beginning of the infection, L3 larvae penetrate the skin after the blood meal of an infected vector. The first line of defence within the skin leads to the recruitment of neutrophils (47, 58-60). Most of the L3 larvae (~80%) are already eliminated with the help of neutrophils, which were shown to degranulate and perform neutrophil extracellular traps (NETosis) (60, 61). The surviving L3 larvae migrate through the lymphatics and penetrate the lung to reach their desired destination, the thoracic cavity in case of *L. sigmodontis* (59). The L3 larvae trigger hereby mast cells to release CCL17, which leads to vasodilatation and facilitates larval migration (29, 62). Migrating larvae cause tissue damage, which leads to the production of thymic stromal lymphopoietin (TSLP), IL-25 and IL-33 by epithelial cells (63).

After about 5-8 days, the *L. sigmodontis* larvae reach the thoracic cavity, their habitat for a chronic infection (46, 59). One of the first cells in the thoracic cavity are ILC2, they are recruited by TSLP, IL-25 and IL-33. They are pivotal for the commencement and maintenance of the Th2 immune response by releasing IL-4 (64). Furthermore, they are main producers of IL-5 and IL-13, whereby they trigger eosinophil recruitment and development as well as further maintenance of the Th2 immune response (64-66). In addition, larval contact to DC leads to further cytokine release such as IL-4, IL-10 and TGF-ß (67-69). The cytokine IL-4 induces priming of naïve T cells to Th2 cells, while IL-10 and TGF-ß are crucial regulatory cytokines leading to the down-regulation of protective and inflammatory immune responses during helminth infection. As already mentioned, the cytokines IL-4, IL-5 and IL-13 are characteristic for a type 2 dominated immune response. While IL-13 alleviates larval tissue migration due to increased epithelial cell permeability, IL-5 and IL-9 promote infiltration of eosinophils and mast cells (70, 71). Granulocytes and mast cells are activated by binding IgE antibodies to the Fcε-receptor (FcεR). The binding of IgE to FcεR leads to the

release of proteins, that are present in granules of mast cells and eosinophils to control parasitic infection (62, 72, 73). The release of eosinophil-derived toxic proteins such as major basic protein (MBP) or eosinophil peroxidase (EPO) is crucial for adult worm elimination (74), as they are too large to be easily phagocytosed like smaller organisms such as bacteria. Furthermore, eosinophils do not only release toxic proteins in response to helminths but also form extracellular traps (EETosis) after contact with microfilariae and L3 larvae of *L. sigmodontis* (75). Here, DNA is released into the extracellular space and contains granular proteins such as eosinophil cationic protein (ECP) to capture the rapidly moving MF and larvae directly within the DNA nets. Similarly, neutrophils and NETosis are involved in the elimination of L3 larvae and in the clearance of adult worms (58, 76). Neutrophils do not only prime AAMΦ which enhance worm expulsion of the intestinal nematode *Nippostrongylus basiliensis* (77-80), but also form nodules around adult worms, thus controlling encapsulation and worm burden (81). Although, AAMΦ have no direct influence in worm killing of *L. sigmodontis*, they do possess important regulatory functions such as sustainment of type 2 responses and proliferation of T cells (77, 82, 83). However, type 1 immune responses can also have a positive impact on worm elimination. For example, IFN-γ has been shown to be important for the encapsulation of adult worms by neutrophils (81).

In the thoracic cavity, IL-4 primes $CD4^+$ T cells to Th2 cells, which produce more type 2 cytokines (66, 71, 84). $CD4^+$ T cells are crucial to control helminth infection, as it was shown that the depletion of $CD4^+$ T cells during *L. sigmodontis* infection causes higher numbers of MF and adult worms (85). Additionally, the absence of $CD4^+$ T cells results in reduced type 2 cytokine levels such as IL-4 and IL-5, which in turn limits the recruitment of eosinophils. In contrast, $CD8^+$ T cells do not seem to have an impact on worm burden following *L. sigmodontis* infection (86). Besides, B cell proliferation is induced by IL-4, IL-5 and IL-13, which initiate generation of antibody producing plasma cells. Initially, IgE is released in response to parasitic helminth infection to induce opsonisation (87). In the further course of the immune response, IL-4 leads to an antibody class switch from IgE to IgG1 in mice and IgG4 in humans (47, 88).

Furthermore, regulatory T cells (T regs) are essential in the immune response against parasites (83). Although, T regs limit inflammation and even control autoimmune responses, they are actively induced by helminths (89). In humans infected with *W. bancrofti* it was shown that lower levels of T regs were associated with pathology in comparison to asymptomatic patients (90). Similarly, in onchocerciasis it was shown that severe cases were associated with lower

levels of T regs (9). During infection with *L. sigmodontis*, T regs are induced accompanied by increased expression of inhibitory molecules such as CTLA-4. CTLA-4 as well as TGF-ß may contribute to the rather suppressive regulatory phenotype in helminths infection to promote survival of the parasite (91). Additionally, IL-10 like TGF-ß is involved in induction and function of T regs (88). Interestingly, over-expression of IL-10 by macrophages causes a resistant mouse strain to become susceptible to infection with the rodent filariae *L. sigmodontis* (92). The importance of IL-10 during chronic infection with *L. sigmodontis* was demonstrated by the fact that the susceptibility of C57Bl/6 IL-4 knock-out mice, which exhibited an increased number of adult worms, was abolished by a simultaneous depletion of the IL-4 and IL-10 genes (67).

In summary, the immune response against filariae is very complex and still not fully understood. Interestingly, helminths also actively influence the immune response of the host, which reveals some beneficial effects. They release different molecules called excretory/secretory (ES) products that aid them to evade the immune response and down-regulate chronic inflammation. One of those products is the filarial derived ES-62 (93-95). ES-62 possesses anti-inflammatory properties like inhibition of TNF release and prevented emergence of collagen-induced arthritis in mice (96). Furthermore, treatment with *L. sigmodontis* adult worm crude extract (LsAg) improved adipose tissue inflammation and glucose tolerance in obese mice (97). Additionally, Type 1 diabetes was prevented in non-obese diabetic mice by filarial infection (98). It was further demonstrated that filarial infection can protect against severe systemic bacterial infections like sepsis (99). As helminths down-regulate chronic inflammation it is under further investigation if they could be used for treatment of autoimmune diseases like inflammatory bowel disease (100-103), rheumatoid arthritis (104), type 1 diabetes (105-107) and allergies (108-110).

1.6 Neuro-immune interaction

For a long time the different physiological systems were studied in isolation from each other. However, it was shown that most physiological systems are interconnected and can affect each other. In particular, the immune system has long been considered independent of the other systems. However, it has been shown that the immune system does not work independently but interacts with the nervous system. This interaction may result from the release of immune factors like cytokines or chemokines by the nervous system or the production of neuro-mediators by immune cells (111, 112). The cooperation of the nervous and immune systems can take place via different roots: the hypothalamopituitary-adrenal

(HPA) axis, the sympathetic nervous system (SNS), the peripheral nervous system (PNS) and the parasympathetic vagal nerve. While the HPA axis and the SNS achieve an anti-inflammatory effect through the release of glucocoritcoids (113, 114), the release of calcitonin gene-related peptide (CGRP) and substance P from the PNS supports a pro-inflammatory immune response (114-116).

1.7 The cholinergic anti-inflammatory pathway

As already mentioned, there are four mechanisms by which the nervous system can control immune responses. These mechanisms are necessary to keep the body's immune system in balance. For example, a diminished inflammatory response would make a person more susceptible to infections or cancer, while an excessive inflammatory response may be directed against the body itself, as it is the case during autoimmune diseases (e.g. type 1 diabetes). Without control of the inflammatory response, a systemic inflammatory response can occur as pro-inflammatory mediators enter the circulation, which in severe cases can lead to multiple organ failure. One control mechanism is the cholinergic anti-inflammatory pathway (117, 118). Here, the vagal nerve can detect inflammatory processes via cytokine receptors at the afferent nerve fibres (Fig.2) (119). Upon pathogen contact, epithelial cells and immune cells release pro-inflammatory cytokines like TNF and IL-1ß (117, 120). As soon as an infection is detected, the brain instantly reacts and sends a signal through the efferent vagal nerve fibres through the celiac ganglion to the splenic nerve. The signal leads to a release of norepinephrine in the spleen. Norepinephrine induces the production of acetylcholine (ACh) in T lymphocytes (121). Once ACh is released into the extracellular space, it can affect other immune cells such as macrophages by dampening the pro-inflammatory cytokine release, but also T cells themselves in an autocrine manner to control inflammation (111, 117, 121).

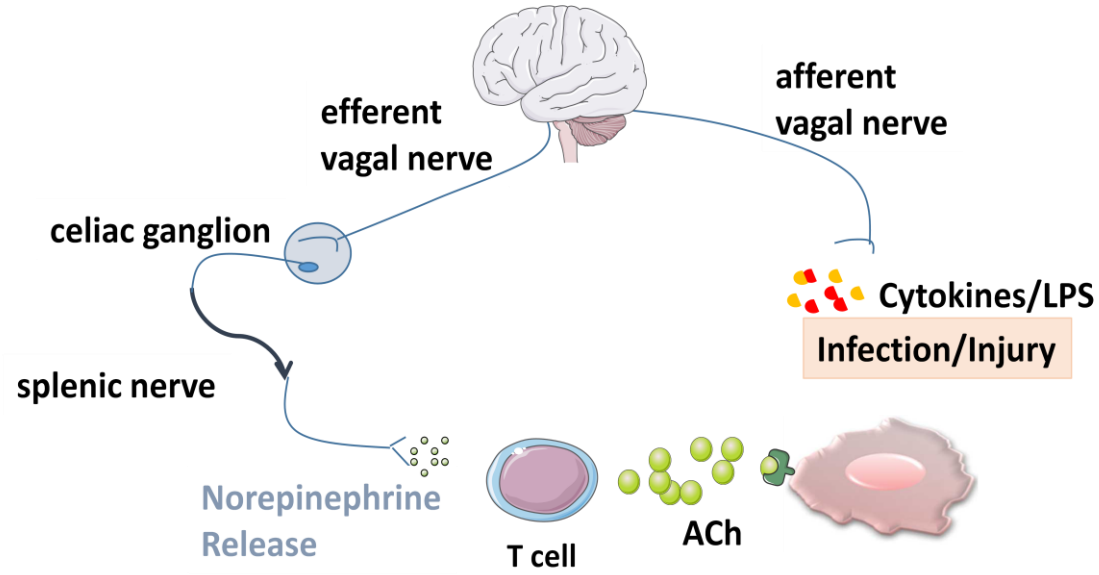

Figure 2: Cholinergic anti-inflammatory pathway (111). Inflammatory responses are detected by cytokine receptors on synaptic endings of afferent vagal nerve fibres. The brain can instantly transmit signals to the splenic nerve via the efferent vagal nerve fibres through the celiac ganglion. This leads to a release of norepinephrine in the spleen. Norepinephrine induces T cells to produce acetylcholine (ACh), which acts on the nicotinic ACh receptors (nAChR) on macrophages.

1.8 The neurotransmitter acetylcholine

ACh, like the catecholamines dopamine, norepinephrine and epinephrine, as well as serotonin, gamma-aminobutyric acid (GABA), glycine and glutamate, is probably one of the most important neurotransmitters. Various neuropeptides such as CGRP and substance P also play an important role as co-transmitters in synaptic modulation in the nervous system (122). The transmission of information in an organism and the control of various functions such as muscle movement, memory and the sleep-wake rhythm are regulated by neurotransmitters. An imbalance in the production or release of neurotransmitters due to malfunction or supply of central nervous substances such as nicotine or illicit drugs results in disturbances in physical and/or mental well-being. ACh is not only involved in muscle activity at motor endplates but also plays an important role in memory formation and other processes (123). ACh can bind to two different classes of receptors. These are nicotinic receptors (nAChR), which are ligand-gated ion channels, and metabotropic or muscarinic receptors (mAChR) (124, 125), that are G_q-coupled protein receptors and can be divided into 5 subtypes (M1, M2, M3, M4 and M5). While M1, M3 and M5 receptors have rather excitatory properties like the increase of excitability or stimulation of dopamine release from striatal synaptosomes (126, 127), the M2 and M4 receptors have inhibitory functions at cholinergic terminals acting in an antagonistic way (126, 128). The M3 receptor (m3AChR) is distributed throughout the central nervous system and in the periphery it is found in heart, lung, pancreas, smooth muscles, endocrine and exocrine glands (129-131).

As depicted below (Fig.3) nAChR can be located at both sides of the synapse (pre- and postsynaptic) and can either induce the release of neurotransmitters (132, 133) or increase excitation rate for signal transduction (134-136). Activation of nAChR at the presynaptic membrane leads to influx of Ca^{2+} ions either directly or indirectly via depolarization of potassium ions which induces release of neurotransmitters (137). ACh is synthesized from Acetyl-Coenzym A and choline by the enzyme choline acetlytransferase (ChAt) in the cytosol of presynaptic neurons (129). Upon activation, ACh is released to the synaptic cleft to act on excitatory or inhibitory mAChR on the postsynaptic membrane to induce e.g. muscle contraction or signal transduction (Fig.3).

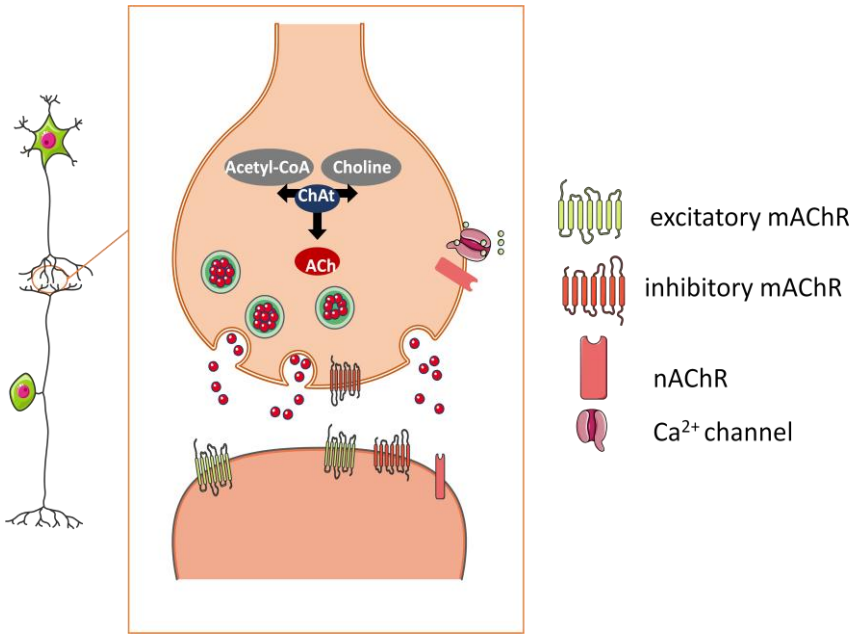

Figure 3: Acetylcholine synthesis and site of action of acetylcholine receptors (123). The enzyme cholineactelytransferase (ChAt) produces acetylcholine (ACh) through the molecules acetyl-Coenzym A (Acetyl-CoA) and choline. ACh is stowed in vesicles, transported to the presynaptic membrane and released into the synaptic cleft. ACh can now transmit the nerve signal by binding to nAChR and/or mAChR of the postsynaptic membrane of the next nerve cell. Binding to the receptors lead to opening of ion channels and a hyperpolarisation of the membrane.

However, ACh is not only found in the central nervous system but also in other tissues. As early as the 1970s, the amplification of T cell cytotoxicity via muscarinic receptor stimulation was discovered (138). Furthermore, ACh is not only produced and released by neurons, but also by several immune cells like $CD4^+$ T cells, B cells and ILC2s (139-141). ACh secreted by B cells independent of the nervous system can modulate the recruitment of neutrophils during endotoxemia (142). Interestingly, ACh has been found to play an important role in the immune response against helminths. On the one hand, antihelmintics already used against schistosomiasis interfere with ACh signalling, as it was shown that *Schistosoma* species also actively secrete acetylcholinesterases (AChE), an enzyme that breaks down ACh in Acetyl-

Coenzym A and Choline to stop ACh signalling (143, 144). The drugs on market are levamisole, monepantel and pyrantel, which interfere with the neuromuscular system of *Schistosoma species* (145, 146) leading to impaired worm development and muscle function (147). Additionally, *Schistosoma* and *Teania species* were found to secrete AChE themselves and thus might interfere with the immune modulation of the host (144).

AChE is bound to the tegument membrane on the outer surface of the parasite and when mice were immunized with a recombinant *Schistosoma japonicum* AChE, it led to maldevelopment and growth disturbances in male worms and higher incidence of immature eggs (143). In addition, *Taenia crassiceps* seems to modulate the immune response by active secretion of AChE and membrane bound AChE (148). In addition, patch clamp experiments have shown that AChEs of *Taenia* species are able to cleave ACh and thus might influence the neuronal signalling of the host (148). Most studies show that ACh produced by T cells signals through nAChRs, e.g. on macrophages to control inflammation by down-regulation of TNF release (149). However, the influence of mAChRs is also of interest. The lack of m3AChR leads to impaired mucus production and prolonged infection with *Citrobacter rodentium* despite an enhanced pro-inflammatory immune response (150). Furthermore, some studies suggest that m3AChR signalling induces a pro-inflammatory response in cigarette-smoke-induced lung inflammation (151, 152). Additionally, it was shown that m3AChR is an autoantigen in Sjögren`s syndrome, that is found at inflammatory regions in exocrine glands (153). There is also discussion of m3AChR being a potential target for colon cancer therapy as it was found to be involved in colorectal neoplasia (154, 155). Interestingly, it was shown that the absence of m3AChR during bacterial infection and infection with the intestinal helminth *N. brasiliensis* led to an impaired $CD4^+$ T cell response, lower Th1/Th17 cytokine release, reduced goblet cell expansion and endothelial permeability (156, 157). Furthermore, during *N. brasiliensis* infection, ILC2s release ACh affecting Th2 cytokine secretion and worm burden (140, 141). In addition, there are muscarinic receptor inhibitors on the market such as tiotropium, which is used as a bronchodilator for treatment of chronic obstructive lung disease (COPD) and helps to improve lung function (158, 159). Tiotropium has been shown to decrease neutrophil migration and reduce the cellular inflammatory response by inhibiting m3AChR (160). Another bronchodilator acting at mAChRs is aclidinum bromide (AB) which has a shorter half-life as tiotropium and similar effects on lung function in COPD patients (161). AB binds to all mAChRs, but the dissociation time from the m3AChR is the longest, making AB a selective inhibitor of the m3AChR (162). These findings further highlight the importance of neuro-immune interactions and should be further investigated.

1.9 Aim

According to the literature, the nervous and immune systems work closely together to eliminate and regulate infections. The nervous system can be directly or indirectly involved, e.g. through the release of neurotransmitters or peptides. Some immune cells can produce ACh themselves and most have nicotinic and muscarinic ACh receptors. Therefore, the production of ACh by various immune cell populations during natural infection with *L. sigmodontis* should be investigated. For this purpose development-specific time points were chosen, such as the arrival of the L3 larvae in the thoracic cavity (9 dpi), after development to L4 larvae (12-15 dpi), and the pre-patent (37 dpi) and patent (70 dpi) phases of the adult worms. Subsequently, the ACh signalling pathway should be disrupted using a muscarinic receptor inhibitor (AB) to determine the influence of the neurotransmitter during infection. The focus is especially on the type 3 muscarinic receptor, as little is known about muscarinic receptor signalling during inflammation. Most studies focus on ACh signalling through the α7nAChR especially on macrophages, which can control inflammation by down-regulation of pro-inflammatory cytokine release. Thus, the aim of this work was to investigate the influence of ACh signalling via m3AChR during infection with *L. sigmodontis*. To confirm the results of the cholinergic inhibitor experiments, m3AChR knockout ($M3R^{-/-}$) mice should be used and compared to BALB/c wild-type (WT) mice. The m3AChR was of special interest due to its distribution within the CNS, the lung, on immune cells and owing to the close proximity of *L. sigmodontis* residence (thoracic cavity) to the lung and its passage through it. The study was intended to investigate whether ACh plays a role in the immune response against *L. sigmodontis* during natural infection and to identify the essential protective mechanisms and their location, e.g. by circumventing the skin and lymphatic phase during L3 migration by intravenous infection. Furthermore, it was aimed to find out whether ACh already influences the cellular immune response in the skin during the initial infection and whether the signalling has an effect on the vascular permeability. These investigations will improve our knowledge about the interaction of the nervous system and the immune system and gain a better understanding of the immune response against helminths in order to find new drug targets.

2. Material and methods

2.1 Housing of animals

BALB/c WT mice and Mongolian gerbils were purchased from companies like Janvier and Charles River. M3R$^{-/-}$ mice were originally provided from Prof. Dr. William Horsnell (University of Cape Town) and bred in-house under adequate animal housing at the animal facility of the University Hospital Bonn (Institute of Medical Microbiology, Immunology and Parasitology). Chat Reporter mice were kept at the House of Experimental Therapy (HET) of the University Hospital Bonn. In both cases, animals were held under 12 hours photoperiod at room temperature ~21°C with ad libitum food and water access, according to the guideline of the European Union animal welfare. All proceedings and records were permitted by the Landesamt für Natur, Umwelt und Verbraucherschutze, Cologne, Germany.

2.2 Life cycle of *L. sigmodontis*

The tropical rat mite, *O. bacoti*, is bred in plastic basins covered in fine litter at 28°C inside an incubator with 80% air humidity to mimic natural environmental conditions. Three times a week mites were fed with fresh blood. In order to maintain the life cycle of *L. sigmodontis*, mites and cotton rats (*Sigmodon hidpidus*), the natural host, are required. Periodical analysis of MF load in the blood of the cotton rats was performed by taking 50 µL blood from the orbital vein to control the infection. Cotton rates sitting inside a metal cage were placed centrally onto basins filled with fine litter containing mites. Now, mites were able to fed on infectious blood of the cotton rats, containing MFs to fulfil the life cycle. After the blood meal saturated mites drop down to the litter. Subsequently, fine litter containing infectious mites was assembled in an Erlenmeyer flask covered with a synthetic polyamide gaze. These flasks were placed into basins filled with soap water and stored in the incubator at 28°C. The cotton rats are placed on top of fresh basins filled with soap water to get rid of any remaining mites. On the next day, cotton rats were placed into new cages with fresh litter. The MF develop inside the intermediate host into L3 larvae within 8-9 dpi. About 3-10 mites were analysed after 9 dpi to get an estimation of parasitemia to ensure proper infection for the experiments.

2.3 Experimental infection with *L. sigmodontis*

2.3.1 Natural infection

Mimicking a natural infection model, the litter with infectious rat mites from the Erlenmeyer flask gained from the maintenance of life cycle were placed into a plastic basin. Subsequently, mice were placed into metal cages on top of mites containing litter over night. On the next

day, the metal cages containing infected mice were transferred on top of the soap water containing plastic basin to get rid of mites that did not already drop down onto the litter. The old mite containing litter was frozen in a plastic bag at -20°C for two days to ensure the death of mites. One day later, mice were placed into plastic cages filled with fresh litter. For two more days the litter was refreshed and the old litter frozen at -20°C. Infected mice were housed in the animal facility until the experiment day.

2.3.2 Subcutaneous infection

Subcutaneous infection models are used to investigate the impact and function of the natural skin barrier. Therefore, Mongolian gerbils (Jirds) were naturally infected with *L. sigmodontis* as described previously. Gerbils stay infected for 5 days to ensure that infective L3 larvae migrate through the lymphatic vessels to the pleural cavity where the worms reside. After 5 days, gerbils were euthanized with an overdose of Isoflurane (Piramal Critical Care, West Drayton, UK). Afterwards, gerbils were cut open to expose the diaphragm in order to flush the pleural cavity with a total of 25 mL pre warmed RPMI medium (37°C; RPMI 1640, ThermoFischer Scientific) that was subsequently transferred into a petri dish (Greiner bio-one GmbH, Frickenhausen, Germany). L3 larvae were transferred into a new petri dish with fresh warm medium using a binocular. Subsequently, 40 L3 larvae were picked in a volume of 100 µL warm medium and transferred into a 1 mL syringe. For each mice a separate syringe was prepared and injected sub-cutaneously in the back of the neck (Fig.4).

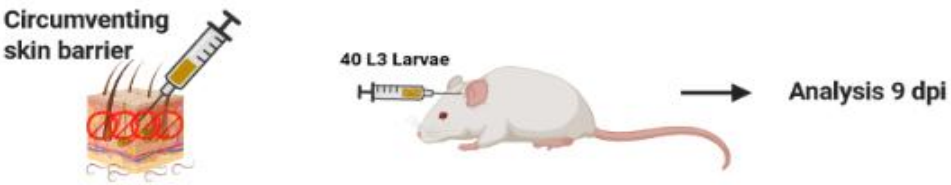

Figure 4: Subcutaneous infection model of *L. sigmodontis*. L3 larvae were isolated from the thoracic cavity of 5 day infected Mongolian gerbils. 40 L3 larvae within PBS or PBS only was injected subcutanously in the neck of the mice.

2.3.3 Intradermal infection

The first immune response at the site of infection when L3 larvae enter the host plays an important role and can be investigated by intradermal injection of a defined number of L3 larvae. To investigate this, mice were shaved at the right and left side of the hind legs. Two days later, mice were sedated with 2-3% Isoflurane and 1% oxygen supply. Subsequently, mice were injected intradermal with 10 L3 larvae in 10 µL PBS on the right hind leg and 10 µL PBS (PAA Laboratories GmbH Pasching, Austria) as control at the left hind leg (Fig.5). After three hours, mice were sacrificed through an overdose Isoflurane and the shaved

skin at the site of injection was cut out. The isolated skin was transferred into 2 mL Tube filled with 1.5 mL digestion medium (0.25 mg Liberase, 0.25 mg DNase/L in RPMI) and cut with scissors into small pieces. The skin suspension was incubated for 45 minutes at 37°C and shaken at 350 rpm.

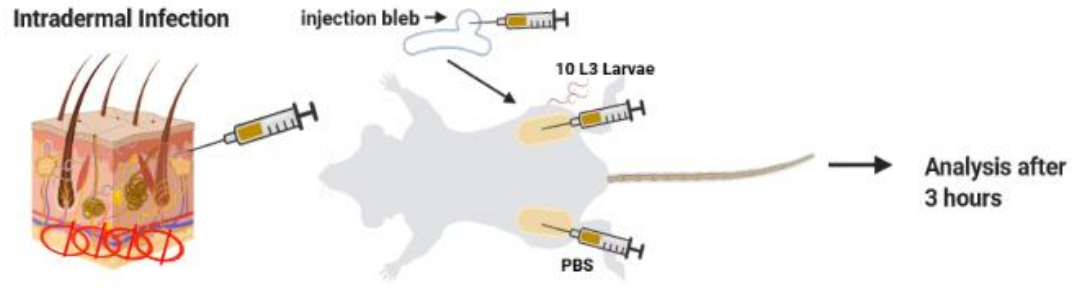

Figure 5: Experimental model of intradermal injection in mice. L3 larvae were isolated from the thoracic cavity of 5 day infected Mongolian gerbils. 10 L3 larvae within PBS or PBS only was injected intradermally.

2.3.4 Intravenous infection

Intravenous infection with *L. sigmodontis* L3 larvae was used to reveal effects of the lymphatic vessels on the migration of the larvae. Therefore, infective L3 larvae were isolated from infected gerbils as depicted in section 2.3.2. Afterwards, mice were placed under red light to ensure adequate filling of the veins to allow proper injection into the tail vein. For injection the mouse was immobilized in a mouse-constrainer and 40 L3 larvae were injected in a volume of 150 µL (Fig.6).

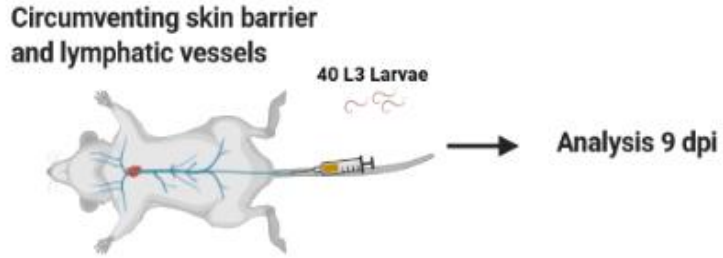

Figure 6: Experimental model of intravenous infection with *L. sigmodontis* L3 larvae. L3 larvae were isolated from the thoracic cavity of 5 day infected Mongolian gerbils. 40 L3 larvae within PBS or PBS only was injected into the tail vein.

2.4 *L. sigmodontis* adult worm extract (LsAg) preparation

For LsAg preparation Mongolian gerbils were infected naturally with *L. sigmodontis* (see 2.3.1) for at least 120 days. Adult worms were collected under sterile conditions with forceps from the thoracic cavity and transferred into a petri dish filled with ice-cold PBS. Washed worms were placed into a glass potter (Greiner bio-one GmbH, Frickenhausen, Germany) and filled with 5 mL ice cold PBS. Afterwards, worms were homogenized for about 15 minutes

on ice until no particles were visible anymore. The suspension was added to a 50 mL tube for centrifugation at 1,485 g for 10 minutes at 4°C. The supernatant containing the soluble extract was transferred to a fresh tube and protein concentration was determined by Bradford Assay.

2.5 Bradford assay

For determination of total protein concentrations within the LsAg a Bradfort assay (PAA, Pasching, Austria) was performed. First, a BSA standard series was prepared with PBS from 7.8 µg to 2000 µg/mL. The assay was performed in a 96 well flat bottom plate (Greiner bio-one, GmbH). 3 µL of antigen solution was added to the wells in triplicates in a serial dilution. Standards were applied as duplicates. Subsequently, without further incubation time 300 µL 1x Advanced Protein Assay was added and absorption was measured immediately at 590 nm. Final concentration of LsAg was adjusted to 1 mg/mL as working concentration and stored in aliquots at -80°C for later use.

2.6 General experimental *in vivo* set up

In general, 6 week-old mice were used. ChAt Reporter mice expressing the green fluorescence protein (eGFP) after synthesis of the enzyme ChAt, which is needed for production of ACh, were used to visualize ChAt production of different cell types during *L. sigmodontis* infection. In addition, $M3R^{-/-}$ mice on a BALB/c background were naturally infected and BALB/c WT mice were used as controls. For the experiments, mice were naturally infected with *L. sigmodontis*. Different infection time points were chosen to analyse parasitological and immunological parameters. Mice were euthanized after 7, 9, 12, 15, 37 or 72 days post infection. For the infection time point 72 dpi, MF load was analysed weekly starting at 50 dpi.

2.7 Analysis of microfilariae counts

A small portion of blood was drawn from the *vena fascialis* using lancets (Goldenrod). Blood was collected in an EDTA collection tube. Then, 50 µL were transferred into a 1.5 mL tube containing 1 mL red blood cell (RBC) lysis buffer (eBioscience, San Diego). After 5 minutes tubes were centrifuged at 400 g for 5 minutes (Eppendorf Centrifuge 5810R). The supernatant was discarded and the complete pellet was transferred to a microscope slide, enclosed with cover slips and MF were counted under the microscope using a 10x magnification.

2.8 Analysis of embryogenesis

Adult worms were isolated from the thoracic cavity of WT and $M3R^{-/-}$ mice at 70 dpi using PBS lavage. Five female adult worms per mouse were transferred individually into 1.5 mL

tubes. Subsequently, 1mL of 70% ethanol was added to fix the worms. Later, the individual worms were homogenised in 80µL PBS and 20 µL Hinkelmann solution (0.5 % eosin Y, 0.5 % phenol, 0.185 % formaldehyde in distilled water). Embryonic stages were counted in 10 µL under the microscope (10 x magnification).

2.9 Plasma isolation

Before anaesthesia, blood was collected from the *vena fascialis* and added to EDTA tubes. Blood was centrifuged at 6000 g for 5 minutes at room temperature (RT). After centrifugation corpuscular portions were located at the bottom of the tube. The upper phase, the plasma was transferred into 96 deep well plates (Greiner bio-one, GmbH) and stored at -20°C.

2.10 Isolation of spleen cells

Mice were euthanized with an overdose of Isoflurane. The spleen was removed after opening the abdomen and put into a 15 mL tube containing 2 mL ice-cold RPMI medium. Then, the spleen was transferred onto a 70 µm cell strainer on top of a 15 mL tube. Using a plunger of a 10 mL syringe the spleen was minced and washed with 8 mL RPMI medium to generate a single spleen cell suspension. The single cell suspension was centrifuged for 8 minutes at 400 g and 4°C. Subsequently, the supernatant was discarded and 1 mL of RBC lysis buffer was added to the cell pellet for 5 minutes at RT. The lysis reaction was stopped by adding 5 mL of RPMI 1640 medium (ThermoFischer Scientific, Germany). Afterwards, the single cell suspension was centrifuged again under same conditions. The supernatant was discarded and cell pellet was resuspended with 10 mL cell culture medium (RPMI with 10 % fetal calve serum, 1 % L-glutamine, 1 % penicillin/streptavidin (all, ThermoFischer Scientific)), counted with CASYton and adjusted to 1 x 10^7 cells/mL. Cells were now ready for flow cytometry preparation or fluorescence activated cell sorting to isolate macrophages for PCR analysis to determine ChAt expression. Macrophages were sorted as $CD11b^+F4/80^+$ cells.

2.11 Isolation of thoracic cavity cells

The abdomen of mice were opened carefully to expose the diaphragm. A whole was incised into the diaphragm to flush the thoracic cavity with 1 mL ice-cold PBS but with a total of 5 mL to isolate pleural cavity cells. The gained pleural cavity cell suspension was transferred into a 15 mL tube with cell separation filters (70 µm; Miltenyi Biotec) on it to hold back residing worms there. Isolated worms were placed into PBS of a 6 well plate for further examination of length and numbers. Cell suspension of the first mL of thoracic cavity lavage was transferred into a separate tube and centrifuged at 400 g for 8 minutes at 4°C. The

supernatant was stored at -20°C for later cytokine and chemokine analysis and the cell pellet was transferred to the remaining cell suspension. The cell suspension was centrifuged under the same conditions as the first mL. The supernatant was discarded and one mL of RBC lysis reagent was applied to the cell pellet for 5 minutes. Afterwards, the thoracic cavity cells were washed with ice-cold PBS and centrifuged again to get rid of RBC lysis solution. The cells were counted using CASYton and adjusted to 1 x 10^7 cells/mL. Cells were further used for flow cytometry and an *in vitro* cell culture was performed for 72 hours.

2.12 Bronchio-alveolar cell isolation

The skin of the throat was opened carefully, the endothelium surrounding the trachea and salivary glands were removed to expose the trachea. An indwelling venous cannula (20G; Braun, Deutschland) was inserted into the trachea to rinse the lungs with 1 mL ice-cold PBS using a 1 mL syringe (Braun). The bronchioles were flushed with 5 mL PBS in total. The first mL of bronchio-alveolar lavage (BAL) was used for cytokine analysis and stored at -20°C. Isolated cells were investigated by flow cytometry.

2.13 Lung cell isolation

After the BAL, the lung was exposed by opening the rib cage. The lung was isolated and placed into a petri dish filled with PBS for washing. Then, the lung was cut into two pieces. The terminal bronchioles from the left part of the lung were placed into a 1.5 mL tube, directly given in liquid N_2 and frozen at -80°C for further cytokine analysis. The rest of the lung was transferred into a 15 mL tube with 5 mL digestion buffer (RPMI medium with 0.5 mg/ml collagenase (Roche, Mannheim), minced with scissors into small pieces and incubated for 45 minutes at 37°C and 200 rpm. The reaction was stopped by adding 1 mL of heat-inactivated fetal bovine serum (FBS). A single cell suspension was performed using a filter (70 µm) and a plunger of a 10 mL syringe. Then, the cell suspension was centrifuged at 400 g for 5 minutes at 4°C. The supernatant was removed and 1 mL of RBC lysis buffer was added for 5 minutes at RT. The reaction was stopped by adding 10 mL of FACS buffer (1x PBS, 1.5 % BSA and 2mM EDTA) and centrifuged under same conditions. Afterwards, supernatant was discarded and the cell pellet was resuspended in 5 mL cell culture medium (RPMI with 10 % fetal calve serum, 1 % L-glutamine, 1 % Penicillin/Streptavidin), counted with CASYton and adjusted to 1 x 10^7 cells/mL.

2.14 Cell staining for flow cytometry

Flow cytometric analysis is used to investigate the impact of ACh on different cell populations during *L. sigmodontis* infection. Here, cells can be distinguished via granularity (forward scatter (FWS)) and size (sideward scatter (SSC)). Additionally, cells can be characterised using fluorescence coupled antibodies for cell surface or intracellular markers. Thus, single cell suspensions of BAL, thoracic cavity lavage, spleen and lung were prepared for flow cytometric analysis. Four different staining sets were performed (Table1-4). Given that BAL yielded a lower number of cells only staining 4, a general staining for surface markers of myeloid and lymphocytic cells, was used. Spleen, lung and thoracic cavity cells provided enough cells to complete all 4 staining sets. Staining 1 to 3 were intracellular stainings to investigate cell populations of innate lymphoid cells (ILCs). Firstly, 5 x 10^6 cells of each sample was added into a 15 mL tube. The samples were centrifuged for 5 minutes at 400 g and 4°C. Afterwards 200 µL Fix/Perm buffer (ThermoFischer Scientific) was added to each cell pellet and incubated for 3 hours at 4°C (stain 1-3). Then, samples were washed by two centrifugation steps with FACS buffer (PBS/1% BSA, 2 mM EDTA) and incubated in Fc-blocking buffer (PBS/1% BSA + rat IgG (1µg/mL; Sigma, St. Louis, USA)) at 4°C over night. The following day, samples were centrifuged at 400 g for 5 min, cell pellets were resuspended in Perm buffer (ThermoFischer Scientific) for 20 min at RT. After that, 50 µL of each staining master mix was applied for 45 min at 4°C in the dark. In the end, the staining mix was removed by a washing step with FACS buffer. Cell pellets were resuspended with MACS buffer (Milteny Biotec) and were ready for measurement using the CytoFLEX (Beckman Coulter). Staining was performed similarly without permeabilisation step as now intracellular antibodies were used. Cells were analysed as depicted in the gating strategies (Fig.6-9) using FlowJo software V10.

Table 1: Intracellular staining scheme for ILC 1 cells

Stain 1 ILC1s	**lung, pleura, spleen**	
Dye	Antigen	Final Dilution
FITC	CD49b	150
PerCP Cy5.5.	CD45	150
PE	CD49a	200
PE-Cy7	NKp46	200
APC	T-bet	150
Al700	TCRb	200
BV421	Lineage	200

Table 2: Intracellular staining scheme for ILC 2 cells.

Stain 2 ILC2s	**lung, pleura, spleen**	
Dye	Antigen	Final Dilution
FITC/Al488	CD45	150
PE	CD90.2	200
PE-Cy7	GATA-3	200
APC	IL-33R	200
Al700	TCRb	200
BV421	Lineage	200
BV510	Sca-1	300

Table 3: Intracellular staining scheme for ILC 3 cells.

Stain 3 ILC3s	**lung, pleura, spleen**	
Dye	Antigen	Final Dilution
PerCP Cy5.5.	CD45	150
PE	RORgt	200
PE-Cy7	NKp46	200
APC	T-bet	150
Al700	TCRb	200
BV421	Lineage	200

Table 4: Extracellular staining scheme for myeloid cells and lymphocytes.

Stain 4 **myeloid cells and lymphocytes**	**lung, pleura, spleen, BAL**	
Dye	Antigen	Dilution
Al488	CD3	200
PE	Siglec-F	200
PerCp-Cy5.5	CD8	200
PE-Cy7	I-Ab	200
APC	CD19	200
APC-Cy7	Ly6C	200
Al700	CD4	200
BV421	Ly6G	200
BV510	CD11b	200
BV605 FACS	CD11c	200

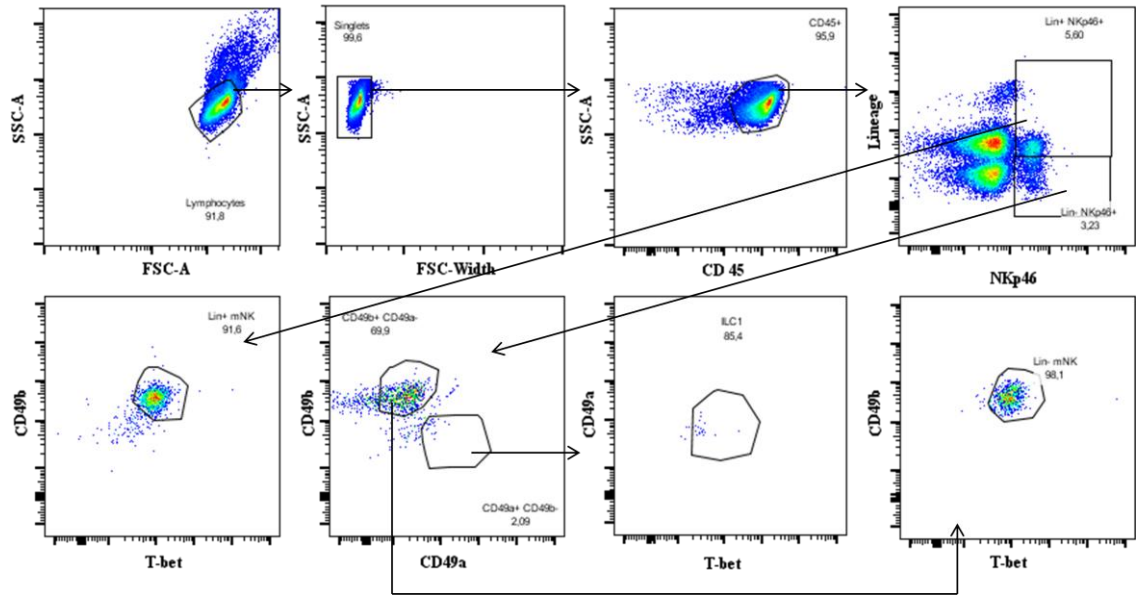

Figure 6: Gating strategy for innate lymphoid type 1 cells. Gating strategy for ILC1 cells in all experiments using thoracic cavity lavage, spleen and the right lobe of the lung of BALB/c and M3R$^{-/-}$ mice. ILC1 were gated as CD45^{+} Lin^{-} CD49a^{+} CD49b^{-} T-bet^{+}, Lin^{+}mNK cells as CD45^{+} Lin^{-} CD49a^{-} CD49b^{+} T-bet^{+} and Lin^{+}mNK cells as CD45^{+} Lin^{+} CD49b^{+} T-bet^{+}.

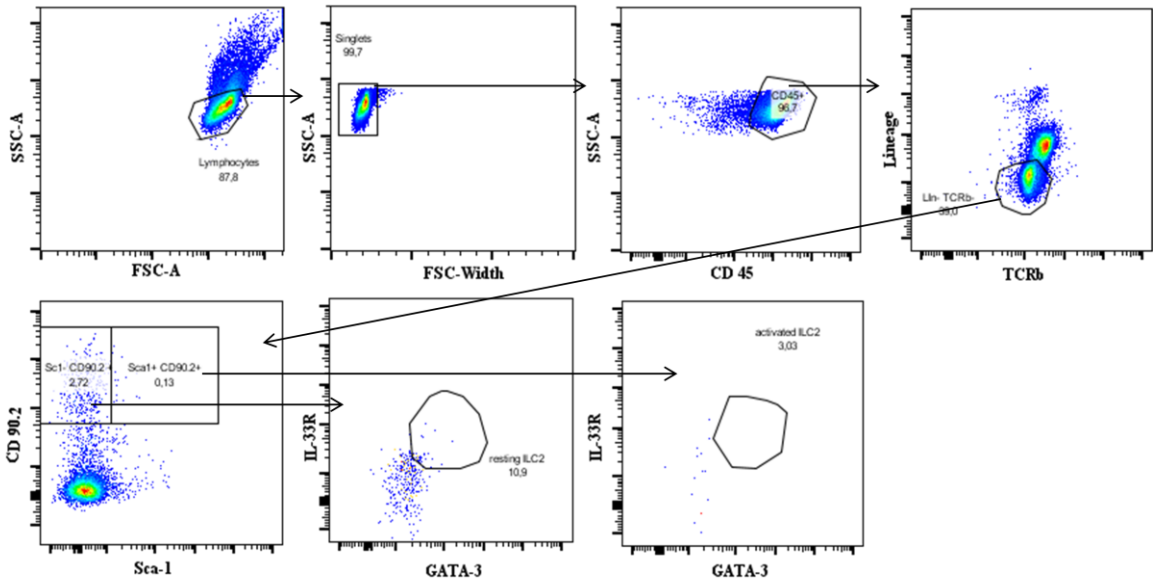

Figure 7: Gating strategy of innate lymphoid type 2 cells. Gating strategy for ILC2 cells in all experiments using thoracic cavity lavage, spleen and the right lobe of the lung of BALB/c and M3R$^{-/-}$ mice. Resting ILC2 were gated as CD45^{+} Lin^{+} TCRb^{+}CD90.2^{+}Sca-1^{-} GATA-3^{+}IL-33-R^{+} and activated ILC2 as CD45^{+} Lin^{+} TCRb^{+}CD90.2^{+}Sca-1^{+}GATA-3^{+}IL-33-R^{+}. Activated and resting ILC2 were added and given as total ILC2.

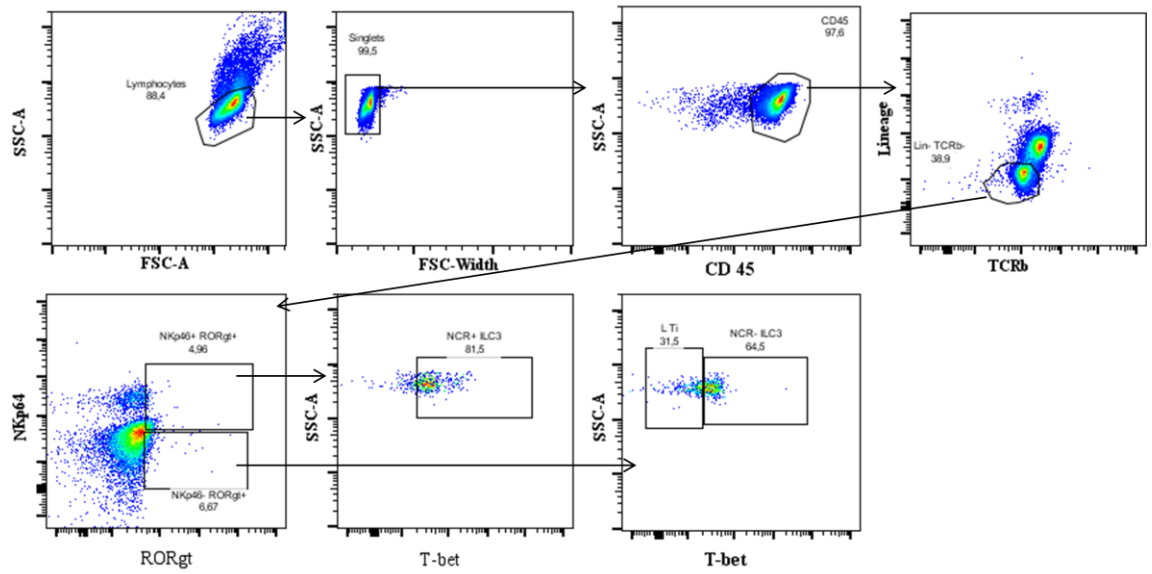

Figure 8: Gating strategy of innate lymphoid type 3 cells. Gating strategy for ILC3 cells in all experiments using thoracic cavity lavage, spleen and the right lobe of the lung of BALB/c and M3R$^{-/-}$ mice. Lymphoid tissue inducer cells (L Ti) were gated as Lin$^-$ TCRb$^-$ NKp46$^-$ RORgt$^+$ T-bet$^-$, NCR$^-$ ILC3 as Lin$^-$ TCRb$^-$ NKp46$^-$ RORgt$^+$ T-bet$^+$ and NCR$^+$ ILC3 as Lin$^-$ TCRb$^-$ NKp46$^+$ RORgt$^+$ T-bet$^+$.

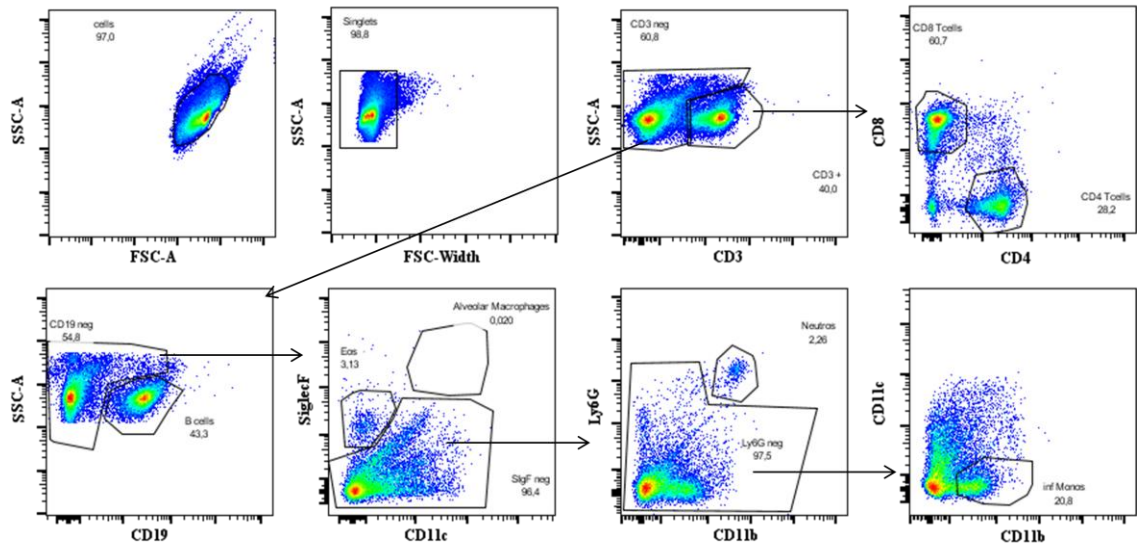

Figure 9: Gating strategy of myeloid and lymphoid cell populations. Gating strategy for myeloid (macrophages, eosinophils and neutrophils) and lymphoid (CD4$^+$, CD8$^+$ T cells and B cells) cells in all experiments using bronchio-alveolar lavage (BAL), thoracic cavity lavage (TC), spleen and the right lobe of the lung of BALB/c and M3R$^{-/-}$ mice. Alveolar Macrophages in the BAL and lung were gated as SiglecF$^+$ CD11c$^+$, macrophages in TC and spleen were gated as CD3$^-$ SiglecF$^{+/-}$ CD11c$^-$ Ly6G$^-$ CD11b$^+$, eosinophils as CD3$^-$ SiglecF$^+$ CD11c$^-$ and neutrophils as CD3$^-$ CD11b$^+$ Ly6G$^+$. T lymphocytes were gated as CD3$^+$ CD4$^+$ and CD3$^+$ CD8$^+$ and B cells as CD3$^-$ CD19$^+$.

2.16 Filarial analysis

Filariae were isolated from the thoracic cavity and added to a 6 well plate with PBS. Then, filariae were separated for counting and the length was measured with a ruler. If the worms were not already at an adult stage, gender was confirmed using light microscopy. To assess

the embryogenesis, five female worms from each mouse were isolated at day 72 post infection and individually transferred into a 1.5 mL tube and 1 mL 4 % formalin was added for fixation. One day later, formalin was exchanged with 1 mL 70 % ethanol. Each worm was homogenized in 80 µL PBS and 20 µL Hinkelman solution (0.5 % eosin Y, 0.5 % phenol, 0.185 % formaldehyde) by using a mortar. The different embryonic stages (egg, morula, pretzel, stretched MF) were counted using a light microscope (10x magnification) in 10 µL of the suspension.

2.17 Enzyme-linked immunosorbent assay (ELISA)

The first millilitres of BAL and thoracic cavity lavage were measured by ELISA to quantify cytokine and chemokine concentrations. Therefore, cytokines were measured according to the manufacturers protocols using Ready-Set-Go ELISA kits (Thermo Fischer Scientific; IL-4, IL-5, IL-6, IL-13, IFN-y, TNF, IL-1ß) or Dou Sets (R&D systems: Eotaxin 1,Eotaxin 2, CXCL-1, CXCL-2, CXCL-5, elastase, RANTES, Granzyme B). The primary antibody was diluted with coating buffer (1:10 dilution with distilled water, Thermo Fisher) or PBS (R&D system) and applied to 96 well ELISA plates (Greiner Bio-One) over night at 4°C. On the next day, coated ELISA plates were washed three times with washing buffer (PBS/0.05 % Tween (Sigma-Aldrich)). Afterwards ELISA plates were blocked with 1x Assay Diluent (Thermo Fisher) or PBS with 1 % BSA (R&D) for two hours at RT. Subsequently, ELISA plates were washed again and samples were applied in duplicates as well as a serial dilution of supplied standards over night at 4°C or for 3 hours at RT. The following day, plates were washed three times and the secondary antibody diluted in 1x Assay diluent (Thermo Fisher) or PBS/1% BSA (R&D) was applied for 1 hour at RT. After three washing steps the enzyme avidin peroxidase (Thermo Fisher) or horseredish peroxidase (R&D) was added for 45 minutes at RT. Plates were washed again for three times. Next, tetramethylene benzidine (TMB) was added for a maximum of 15 minutes or until the colour change occurred. The reaction was stopped by adding 1 M H_2SO_4 (Merck). The optical density was measured at 450 nm and 650 nm using SpectraMax pc plate reader (Molecular Devices, Ismaning, Germany).

2.18 RNA isolation and detection of ChAt expression by PCR analysis

Macrophages isolated via fluorescence activated cell sorting were transferred in 1 mL Trizol (Biorad) and lysed by pipetting up and down. Then, 200 µL chloroform was added to the 1.5 mL tube was inverted for 15 seconds. After an incubation time of two to three minutes at room temperature (RT) the sample was centrifuged at 12,000 g for 15 minutes at 4°C. The

upper aqueous phase was transferred into a new 1.5 mL tube and 500 µL of 100 % Isopropanol (Invitrogen) was added and incubated for 10 minutes at RT. After another centrifugation step at 12,000 g for 15 minutes at 4°C, the supernatant was removed and 1 mL 75% ethanol was added. The samples were subsequently centrifuged at 7,500 g for 5 minutes at 4°C. The supernatant was discarded and the pellet was air dried for 5 - 10 minutes at 37°C. Then, the pellet was resuspended in 20 µL RNase-free water (Qiagen). Afterwards, potential remaining genomic DNA was removed according to the manufacturers protocol using the DNAfree kit (Qiagen). cDNA synthesis was performed with the First-Strand-Sythesis Kit (Qiagen) according to the manufacturers protocol. Then ChAt expression was determined by PCR with ChAt Primers (Qiagen). The PCR program possessed three cycles, at the first cycle samples were heated to 95°C for15 minutes, followed by 35 repetitions of the second cycle containing three steps (95°C for 15 seconds (sec), 58°C for 30 sec and 72°C for 5 minutes). In the end samples were heated to 72°C for 5 minutes. Subsequently, samples were transferred to a 2 % agarose gel (Merck) for detection.

2.19 Isolation of bone marrow-derived neutrophils

Bone marrow-derived (bmd) neutrophils were isolated using magnetic activated cell sorting (MACS). Characteristic cell surface markers like LyG6 for neutrophils are magnetically labelled and used for specific isolation of cell populations using a magnetic field. Therefore, BALB/c WT and $M3R^{-/-}$ mice were euthanized. Flesh from the bones (tibia, femur) was removed using scissors and paper towels. Isolated bones were placed into a petri dish with cold PBS. Under sterile conditions the far end of the bones were cut. With a 10 mL syringe and 25 gauge needle the bone marrow was flushed out with cell culture medium. Bone marrow and cells were filtered through a cell strainer (70 µm) in a 50 mL tube. The cell suspension was centrifuged at 400 g for 8 min at 4°C. The supernatant was discarded and 1 mL of RBC lysis buffer was added for 5 min. The reaction was stopped with 9 mL cell culture medium and centrifuged. The cells were resuspended in 10 mL MACS buffer and counted via the CASYton. Afterwards,10 µL of anti-Ly6G MicroBeads UltraPure (Miltenyi Biotec) were added per 10^7 cells and 90 µL MACS Buffer for 15 min at 4°C. Subsequently, cells were washed by adding 3 mL MACS buffer and centrifuged. The cell pellet was resuspended in 1 mL MACS buffer. Then, MACS MS columns were prepared according to the manufacturer`s protocol by rinsing with MACS buffer. Samples were applied to the columns and the flow through was collected. Columns were washed three times with MACS buffer. In the end, columns were removed from the magnetic field and immediately flushed

out with 1 mL MACS buffer by firmly pushing the plunger into the column to isolate magnetically labelled neutrophils. Purified neutrophils were counted with the CASYton and purity was checked via flow cytometry using CD11b and anti-Ly6G antibodies (>90%).

2.20 *In vitro* activation assay and co-culture

An *in vitro* analysis of the activation status of bone marrow-derived neutrophils and their impact on L3 larval activity was performed. Therefore, L3 larvae were isolated from infected gerbils (5 dpi) via thoracic cavity lavage with pre-warmed RPMI medium including 1 % L-glutamin and 1 % penicillin/streptavidin as described in section 2.3.2. For the co-culture 10 L3 larvae were placed in 50 µL cell culture medium per well until neutrophils were added. Samples were prepared as triplicates and L3 larvae in 200 µL cell culture medium alone served as control. Subsequently, neutrophils were isolate, adjusted to 2x 10^5 cells in 150 µL and added to the prepared L3 larvae in a 96 well flat bottom plate for up to 4 days at 37°C and 5 % CO_2. Each day the motility of the Larvae was determined by using a score from 0 to 4 (0 = no movement; 1 = only movements at the tips of L3; 2 = non-continuous movement; 3 = continuous, slower movement; 4= continuous, fast movement). In addition, a second plate mirroring the motility assay was prepared but this time using RPMI medium (RPMI/1 % L-glutamine, 1 % penicillin/streptavidin). Furthermore, a third plate was set up with additional stimuli like LPS (100 ng/mL), PMA (50 ng/mL), zymosan (500 µg/mL) and LsAg (25 µg/mL). The stimulation was done in triplicates. Additionally, all stimuli were tested in combination with DNase (60 U/mL) a control for the DNA release after 6 hours of stimulation at 37°C and 5 % CO_2. After 6 h cell culture supernatant was collected for DNA quantification and cells were used for flow cytometric analysis to investigate expression of activation markers (CD54, CD86 and MHCII).

2.21 Whole blood activation assay

Whole blood (200µL per animal) was collected from the animals via the fascialis vein using a lancet. The blood from five animals was pooled and centrifuged at 400 g for 5 min to remove the plasma. Subsequently, cells were washed with RPMI medium and centrifuged under the same conditions. The supernatant was discarded, cells were resuspended to the original volume and diluted 1:2 with RPMI medium. Then, 200 µL of the cell suspension was added per well in a 96 well plate. The cells were then stimulated with LsAg (0.2, 2 and 20µg/mL) and anti-FcεR (1.6, 6.25 and 25 µg/mL). Ionomycin (1 µg/mL) served as positive control, while one condition was not stimulated to provide a negative control. Cells were stimulated for 45 min at 37°C 5% CO_2. After the stimulation, Golgi Stop was added to all conditions for

two hours. Afterwards, cells were washed with PBS and analysed by flow cytometry. Basophils were gated as $CD4^{-}$ $B220^{+}$ IgE^{+} cells.

2.22 DNA quantification

DNA quantification was performed using the Quant-iT dsDNA Assay Kit (Thermo Fischer). Prior assay performance and directly after the stimulation was finished, micrococal nuclease (5 U/well) was added to the samples for 15 min in the incubator to loosen DNA traps attached to the bottom of the plate. The reaction was stopped by adding 1 mM EDTA. The cell culture plates were centrifuged at 400 g for 5 min. The supernatant was stored at -20°C and/or directly used for DNA quantification. Provided standards and samples were applied as duplicates. The Assay reagent was prepared and added to samples and standards and absorption was measured at 485/535 nm via the Tecan infinite M plex fluorescence reader.

2.23 Vascular permeability assay

To assess the vascular permeability, mice were anesthetized with an intraperitoneal injection of Ketanest® (100 mg/kg body weight) and Rompun® (16 mg/kg body weight) with a volume of 150 µL. During anaesthesia mice were kept warm using a red light. Then, mice were injected intra-cutaneously with 10 µg/µL LsAg in the left ear and 10 µL PBS in the right ear. hree minutes later 30 mg kg^{-1} Evens Blue diluted in 0.9 % sodium chloride (e.g. 19 g/mice: 0.57 mg/200 µL) was injected intravenously in the tail vein of the sedated mice. After 10 minutes, mice were euthanized and the ears of the mice were cut. The ears were transferred into 2 mL tubes filled with 500 µL >99 % formamide (Sigma Aldrich). The ears in solution were incubated at 56°C for 48 hours at 350 rpm. The leakage of Evens Blue was measured at 620 nm (Spectramax 240 pc, Molecular Devices). Using a serial dilution of Evens Blue as standard, the concentration of the leakage was determined.

2.24 Statistical analysis

Statistical analysis and organisation of graphs was performed using GraphPad Prism software version 9 (GraphPad Software, Inc., La Jolla, USA). The Microplate Data Acquisition and Analysis Software from Molecular Devices, Synnvale, USA, was used to analyse ELISA and Bradford measurements with SoftMax Pro. The analysis and gating procedure of flow cytometry data was performed with the FlowJo V10.2 software, FlowJo LLC, Ashland, Oregon.

3. Results

3.1 Expression of choline acetyltransferase in immune cells during *L. sigmodontis* infection

In order to investigate the interaction of ACh signalling and the immune system during helminth infection, the model organism *L. sigmodontis* was used. At first, the ability of immune cells to express ChAt was analysed via flow cytometry using B6.Cg-Tg(RP23-268L19-EGFP)2Mik/J mice (ChAt reporter mice). ChAt is the enzyme needed to generate ACh. The ChAt reporter mice are transgenic mice, wherein the endogenous ChAt transcriptional regulatory elements direct the expression of eGFP during development as well as in the adult mouse. These mice enable the fluorescent visualization of cells producing ACh via flow cytometry. ChAt reporter mice were naturally infected by the bite of the rat mite *O. bacoti* and the immune cell populations were analysed by flow cytometry in naïve mice, at day 5, when L3 larvae infiltrate the thoracic cavity, where the worms reside, and 35 dpi after the moult into adult worms. Myeloid and lymphoid cells at the site of infection (thoracic cavity) and in the spleen showed a certain baseline expression of ChAt in naïve mice (Fig.10,11). *L. sigmodontis* infection led to an infiltration of immune cells to the thoracic cavity. Especially at 35 dpi after the moult into adult worms, there was an increase of macrophage (naïve = 3.9 x 10^5 cells (arithmetic mean); d5 = 3.8 x 10^5 cells; d35 = 9.4 x 10^6 cells), neutrophil (naïve = 2.8 x 10^4 cells; d5 = 2.7 x 10^4 cells; d35 = 6.9 x 10^5 cells) and eosinophil (naïve = 36.0 x 10^3 cells; d5 = 6.6 x 10^3 cells; d35 = 3.2 x 10^6 cells) cell numbers and, $CD4^+$ and $CD8^+$ T cells as well as B cells in the thoracic cavity (Fig.10A,B). Although, macrophages showed the highest baseline expression of ChAt (naïve = ~737 MFI; Fig. 10C), their ChAt expression strongly varied among mice at 35 dpi. In contrast, ChAt expression in neutrophils was significantly up-regulated in infected animals at 35 dpi compared to 5 day infected mice ($p = 0.0341$; naïve = ~219 MFI; d35 = ~561 MFI; Fig.10B). Whereas ChAt expression of eosinophils in the thoracic cavity was significantly down-regulated in 35 day-infected animals compared to naïve mice ($p = 0.0089$; naïve = 409 MFI; d5= 344 MFI; d35 = 138 MFI; Fig.10C). *L. sigmodontis* infection leads to significantly increased numbers of $CD4^+$ and $CD8^+$ T cells as well as B cells in the thoracic cavity of 35d-infected mice compared to naïve and 5 day-infected mice (Fig.10C). Interestingly, $CD4^+$ T cells of 5 day-infected mice showed a significantly higher ChAt expression compared to naïve mice ($p = 0.0024$; naïve = ~141 MFI d5 = ~560 MFI; d35 = ~130 MFI). In contrast, at 35 dpi ChAt expression of $CD4^+$ T cells was significantly

decreased compared to 5 dpi ($p < 0.0001$; Fig.10D). In addition, ChAt expression of $CD8^+$ T cells increased with the course of infection (naive = ~130 MFI; d5 = ~243 MFI; d35 = ~354 MFI; Fig. 10D) in the thoracic cavity, accompanied by increasing ChAt expression of B cells (naïve = ~290 MFI; d5 = ~310 MFI; d35 = ~411 MFI; Fig.10D).

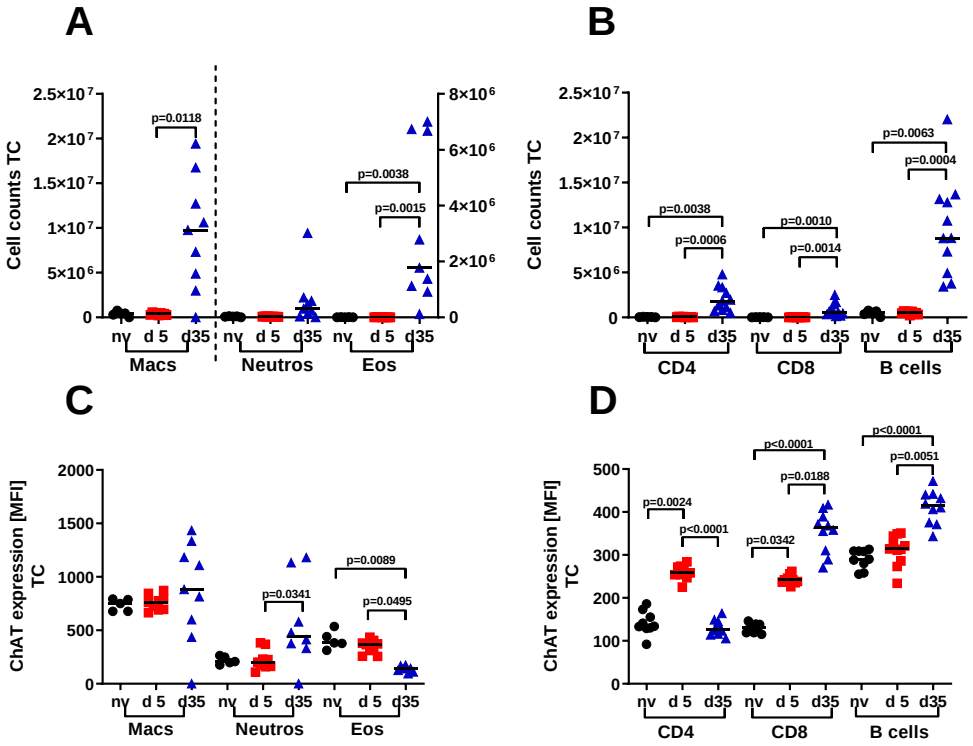

Figure 10. Cellular composition in the thoracic cavity and ChAt expression in myeloid and lymphoid cells during natural *L. sigmodontis* infection. ChAt expression and cellular influx after 5 (d5) and 35 days (35d) of natural *L. sigmodontis* infection in ChAt reporter mice compared to non-infected (naïve) mice. Total cell numbers of macrophages (Macs), neutrophils (Neutros), eosinophils (Eos) (A) as well as $CD4^+$ and $CD8^+$ T and B cells (B) cells in the thoracic cavity (TC) and corresponding ChAt expression (C,D). Statistical significance was analysed by Kruskal Wallis and Dunn's post hoc test ****p<0.0001. Data represented is one of two independent experiments with n=5 naïve mice and 8 infected mice.

L. sigmodontis infection led to an increased number of macrophages in the spleen at 35 dpi (naïve = ~2.63 x 10^6 cells; d5 = ~2.56 x 10^6 cells; d35 = ~6.96 x 10^6 cells; Fig.11A). In contrast, neutrophils significantly decreased at 35 dpi compared to 5 day-infected mice (naïve = ~3.28 x 10^6 cells; d5 = ~5.56 x 10^6 cells; d35 = ~2.19 x 10^6 cells, Fig.11A). Eosinophils showed no differences in spleen cell numbers of naïve and infected mice (naïve = ~5.82 x 10^5 cells; d5 = ~1.42 x 10^6 cells; d35 = ~8.23 x 10^5 cells, Fig.11A). However, ChAt expression was significantly decreased in the course of infection in case of both, eosinophils (naïve =199 MFI; d5 =145 MFI; d35 =71 MFI; Fig.11C) and neutrophils (naïve = 96 MFI; d5 = 75 MFI; d35 = 0 MFI). Regarding lymphoid cell populations in the spleen, it was observed that $CD4^+$ T cell numbers decreased (naïve = 1.429 x 10^7 cells;

d5 = 1.062 x 10^7 cells; d35 = 8.453 x 10^6 cells, Fig.11B) during infection but possessed a higher ChAt expression (naïve = 77 MFI; d5 = 113 MFI; d35 = 172 MFI, Fig.11D). In contrast, $CD8^+$ T cell populations increased in the spleen from 5 to 35 dpi (naïve = 3.22 x 10^5 cells; d5 = 2.414 x 10^5 cells; d35 = 6.071 x 10^6 cells; Fig.11B) but did not show statistical significant differences in their mean ChAt expression (naïve = 166 MFI; d5 = 185 MFI; d35 = 187 MFI, Fig.11D). B cell numbers increased significantly in the spleen of 35 day-infected mice compared to naive mice (naïve = ~2,136 x 10^7 cells ; d35= ~3,387 x 10^7 cells), whereas ChAt expression was decreased (naïve = 264 MFI; d5 = 286 MFI; d35 = 186 MFI; Fig.11D).

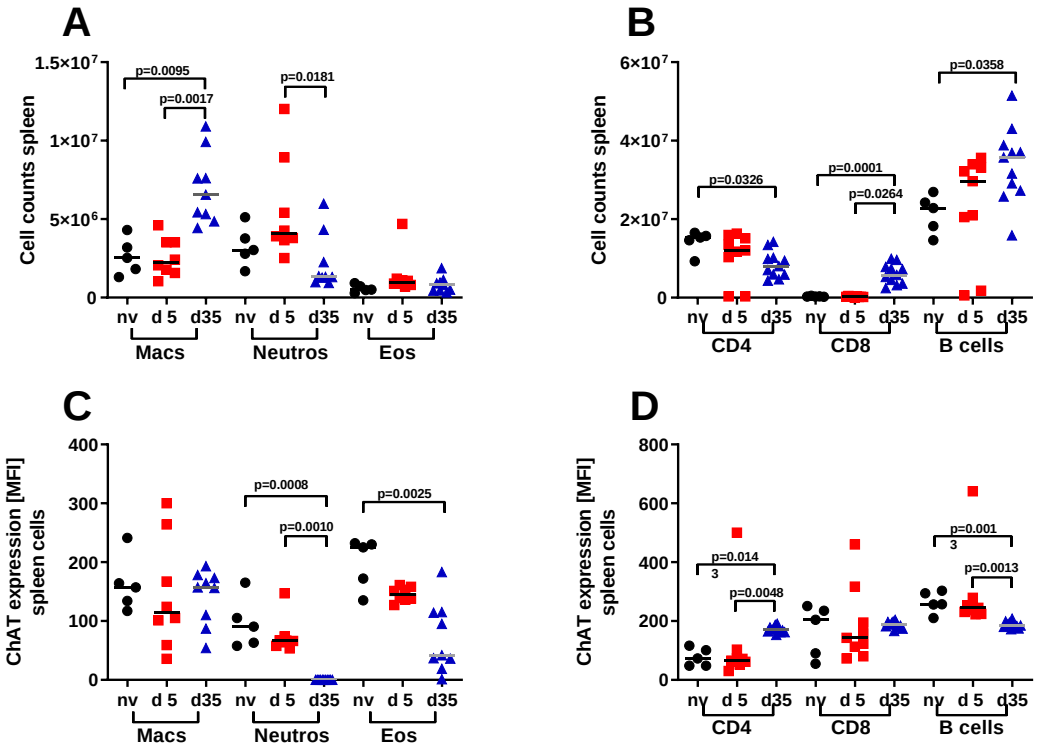

Figure 11. Cellular composition of spleen and ChAt expression in myeloid and lymphoid cells during natural *L. sigmodontis* infection. ChAt expression and cellular influx at 5 (d5) and 35 days (d35) of natural *L. sigmodontis* infection in ChAt reporter mice compared to non-infected (naïve) mice. Total cell numbers of macrophages (Macs), neutrophils (Neutros) and eosinophils (Eos) (A) as well as cell numbers of $CD4^+$ T cells (CD4), $CD8^+$ T cells (CD8) and B cells (B) in the spleen and corresponding ChAt expression (C,D). Statistical significance was analysed by Kruskal Wallis and Dunn's post hoc test. Data represented is one of two independent experiments with n=5 naïve mice and 8 infected mice.

In order to confirm if the measured ChAt expression in macrophages by flow cytometry, a PCR analysis was performed. Therefore, macrophages were sorted as $F4/80^+$ cells using magnetic activated cell sorting. The cDNA was generated from RNA of isolated macrophages of spleens from 35 day-infected mice. PCR was performed using ChAt specific primers and the PCR product was visualized using a 2% agarose gel. The ChAt PCR product had a size of

165 base pairs (bp). Fig. 12 shows that the PCR confirmed the ChAt expression for almost all samples indicated by obtained bands at ~165 bp compared to the 100 bp ladder control.

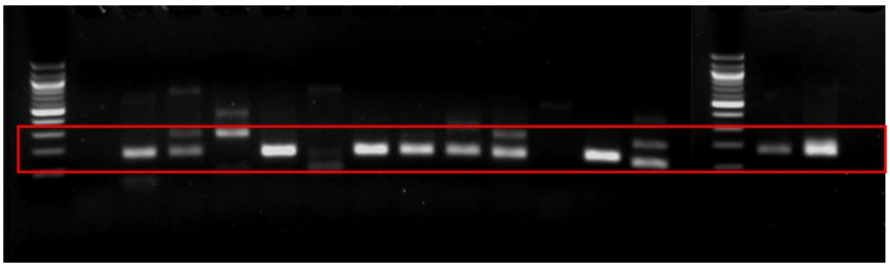

Figure 12. Confirmation of ChAt expression in macrophages during natural *L. sigmodontis* infection. 2% agarose gel showing ChAt expression from a PCR run from sorted macrophages of spleen cells after 35 days post infection. The detected band at 165 base pairs (bp) shows that macrophages in the spleen express choline acetlytransferase (ChAt) during infection and it is therefore of importance in the infection process.

3.2 Influences of cholinergic signalling during *L. sigmodontis* infection in BALB/c mice

3.2.1 Cholinergic inhibition with aclidinium bromide increases the worm burden following natural *L. sigmodontis* infection

Due to the observations of altered ChAt expression in immune cells during *L. sigmodontis* infection, we investigated the impact of cholinergic signalling during *L. sigmodontis* infection in BALB/c mice using the muscarinic receptor inhibitor AB, that primarily targets the m3AChR (162). BALB/c WT mice were treated intranasally with AB to inhibit cholinergic signalling or with PBS/10% DMSO as vehicle control prior natural infection with *L. sigmodontis.* In order to account for the migration time L3 larvae need to enter the thoracic cavity, mice were also treated the following four days daily, as AB has a short half-life. The worm recovery was analysed at 9 dpi, a time point most larvae have reached the thoracic cavity (37, 42). Mice that were treated with AB had a higher worm recovery compared to the vehicle (VEH) group (VEH = ~3.8 worms; AB = ~8 worms; $p = 0.0233$; Fig.13A). The infection led to increased cell numbers in the BAL in both vehicle and AB-treated mice (naïve = ~9.505×10^5 cells; VEH Ls = ~4.612×10^6 cells; AB Ls = ~5.702×10^6 cells; Fig.13B), with by trend higher numbers in the mice treated with the inhibitor. The same trend was observed when cellular infiltration to the thoracic cavity was assessed. Total immune cell numbers increased in infected mice treated with AB (AB Ls) compared to infected vehicle mice (VEH Ls) and naïve mice (naïve = 1.725×10^6 cells; VEH Ls = 4.61×10^6 cells; AB Ls = 5.702×10^6 cells; Fig.13C). In accordance with the higher cell numbers in the infected mouse groups, the individual numbers of neutrophils (naïve = ~8.922×10^3 cells;

VEH Ls = ~1.115x10^5 cells; AB Ls = ~1.709 x 10^5 cells) and eosinophils (naïve = ~9.535 x 10^3 cells; VEH Ls = ~5.593 x 10^5 cells; AB Ls = ~6.667 x 10^5 cells) within the thoracic cavity were also elevated (Fig.13D, E). Thus, lack of cholinergic signalling increased worm recovery in naturally infected BALB/c mice and was associated by trend with increased cell numbers.

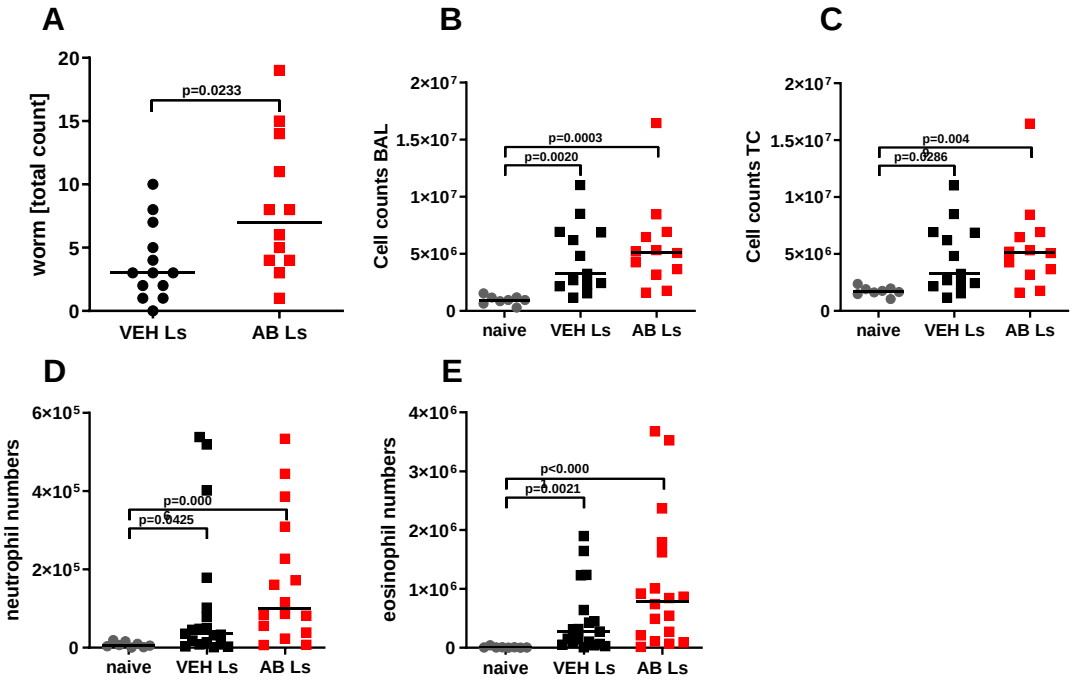

Figure 13. Cholinergic inhibition increased worm recovery after natural *L. sigmodontis* infection in BALB/c mice. Worm burden at 9 days post natural *L. sigmodontis* infection in BALB/c WT mice treated with either 10%DMSO/PBS or aclidiniumbromide (AB) for 5 days (A). Total cell counts of bronchio-alveolar fluid (BAL; B) thoracic cavity lavage (TC; C) and total numbers of neutrophils (D) and eosinophils (E) within the thoracic cavity. Statistical significance was analysed by two-tailed non-parametric Mann-Whitney-U-test or Kruskal-Wallis with Dunns` post hoc test; *p<0.05, **p<0.01. Data represented is pooled data of two independent experiments (n=12;13).

3.2.2 Intravenous infection with *L. sigmodontis* abolishes the higher worm recovery

Lack of cholinergic signalling resulted in an increased worm recovery in AB-treated mice compared to vehicle controls, but neutrophil and eosinophil numbers, which are associated with protective immune responses against L3 (58, 163), showed no significant differences. Therefore, mice were infected intravenously with a defined number of L3 larvae (40) to circumvent the skin barrier and the lymphatic system. The skin barrier is the first obstacle L3 larvae have to overcome to infiltrate the host. Interestingly, the stronger worm recovery in mice treated with AB is abolished upon intravenous infection, as the worm burden of vehicle control mice and AB-treated mice were comparable (VEH = ~4.1 worms; AB = ~5 worms; Fig.14A). Cell numbers of BAL fluid (VEH = 4.879x10^5 cells; AB = 5.422x10^5 cells;

Fig.14B), thoracic cavity (VEH = 1.282x10^6 cells; AB = 1.734x10^6 cells, Fig.14C) and spleen (ctrl = 5.023x10^7 cells; AB = 4.546x10^7 cells, Fig.14D) did not reveal any statistical significant differences between both groups after intravenous infection. In addition, the cellular composition of the thoracic cavity was examined and showed no statistical significant differences in numbers of myeloid cells like macrophages, neutrophils and eosinophils. $CD4^+$ and $CD8^+$ T cell as well as B cell numbers did not show statistical significant differences between both groups (Fig.14E).

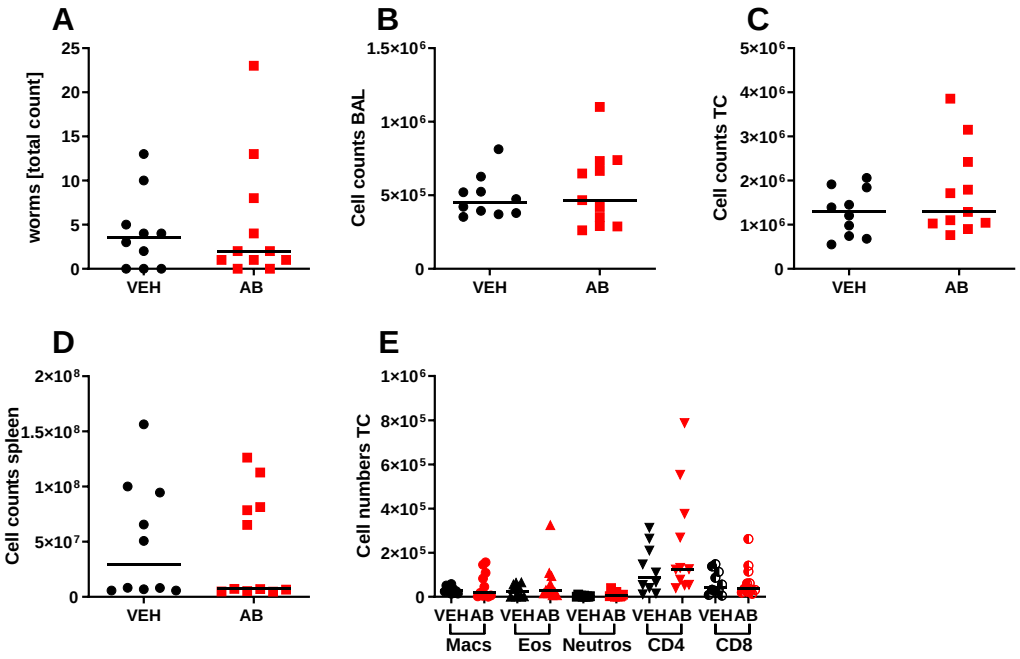

Figure 14: Intravenous infection abolished higher worm recovery during cholinergic inhibition. Total worm counts at 9 days post intravenous infection with 40 L3 Larvae in mice treated either with AB or PBS as vehicle (VEH) control (A). Total cell numbers of BAL (B), thoracic cavity (C) and spleen (D), as well as cellular composition of major cell populations (Macs= macrophages; Eos=eosinophils; Neutros= neutrophils; CD4= $CD4^+$ T cells; CD8= $CD8^+$ T cells) within the thoracic cavity (E). Results are shown as median. Data represented is pooled data of two independent experiments with n=5 (A-E). Statistical analysis was done using two-tailed non-parametric Mann-Whitney-U-test.

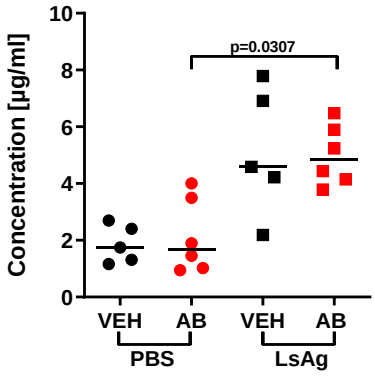

Figure 15: *.L. sigmodontis* crude extract increased vascular permeability independent of cholinergic inhibition. Vascular permeability was determined by Evans blue leakage after PBS and LsAg injection in the ears of mice treated with AB or vehicle. Results are shown as median. Data represented is one experiment of two independent experiments with n=5-6. Statistical analysis was done using Kruskal-Wallis and Dunn`s post hoc test.

As circumvention of skin barrier and lymphatic system resulted in a similar worm burden of PBS and AB treated mice, either local immune response within the skin or the migration through the lymphatic vessels might be responsible for the higher worm recovery in naturally infected animals. Therefore, the vascular permeability was analysed (164), as it was already shown that an enhanced vascular permeability facilitates larval migration (62). Here, the ability of Evans blue to bind albumin is used to investigate membrane integrity, as albumin is not able to penetrate endothelial membranes under physiological conditions. The vascular permeability assay analyses the leakage of albumin in the surrounding tissue by measuring optical density of Evans blue. Intradermal PBS injection into the ear of the mice treated with AB or PBS showed a comparable leakage of Evans blue (VEH = ~1.863 µg/mL; AB = ~2.135 µg/mL; Fig.15). However, LsAg injection significantly increased the leakage of Evens blue in mice treated with AB compared to PBS treated control mice (VEH LsAg = ~5.136 µg/mL; AB LsAg = ~4.998 µg/mL, Fig.15). However, there was no difference in vascular permeability after LsAg treatment in mice treated with or without AB.

In summary, intravenous infection re-establishes a comparable worm burden in AB-treated mice and VEH controls, indicating that immune responses within the skin or during the migration of the L3 larvae to the thoracic cavity are responsible for the increased worm burden observed in AB-treated mice. Cellular composition of the thoracic cavity and total immune cell numbers of BAL, thoracic cavity and spleen showed no statistical significant differences between both infected groups. As the vascular permeability was not affected by cholinergic signalling, impaired immune responses within the skin may lead to the observed increased worm burden in AB-treated mice.

3.2.3 Cholinergic inhibition with aclidinium bromide during intradermal *L. sigmodontis* infection

As the vascular permeability and immune cell analysis during *L. sigmodontis* infection showed no differences in mice treated with AB and vehicle, we suggested that the local immune response within the skin might be affected. The skin is the first obstacle L3 larvae have to overcome. Therefore mice were infected intradermally with 10 L3 larvae at the upper hind leg regions to analyse the local immune response within the skin after 3 hours. Mice treated with AB possessed higher frequencies of eosinophils within the skin after PBS (ctrl = 0.453 %; AB = 0.827 %) and L3 (ctrl = 0.458 %; AB = 1.426 %) injection. However, L3 injection did not further increase eosinophil frequencies (Fig.16A). In addition, activation of eosinophils was measured by expression of MHCII, which was neither altered after L3 injection nor after AB treatment (Fig.16B). Frequencies of neutrophils were comparable after PBS injection in both groups (Fig.16C). L3 injection led to significantly increased frequencies of neutrophils compared to PBS controls (vehicle PBS = 1.789 %; vehicle L3 = ~3.765 %). Similarly, mice treated with AB possessed significantly higher frequencies of neutrophils after L3 injection compared to their corresponding PBS control and showed an even stronger increase than the vehicle-treated mice (AB PBS = 1.366 %; AB L3 = ~4.881 %; Fig.16C). Nevertheless, neutrophil activation was reduced upon L3 injection in both vehicle and AB treated mice. Activation was measured using mean fluorescence intensity of MHCII, CD86 and CD54 expression. All three expression markers were reduced upon intradermal L3 injection in vehicle mice and AB-treated mice compared to their PBS controls (Fig.16D-F). However, only in AB treated mice the reduced activation of neutrophils was statistically significant.

In summary, we observed that mice treated with AB showed a higher susceptibility for *L. sigmodontis* infection that was accompanied by a slightly higher infiltration of immune cells into the thoracic cavity and BAL. The higher worm recovery was not associated by altered vascular permeability, although the intravenous infection abolished the higher worm recovery. However, local immune response within the skin after intradermal infection revealed a reduced neutrophil activation (MHCII, CD86, CD54) in AB-treated mice compared to control mice.

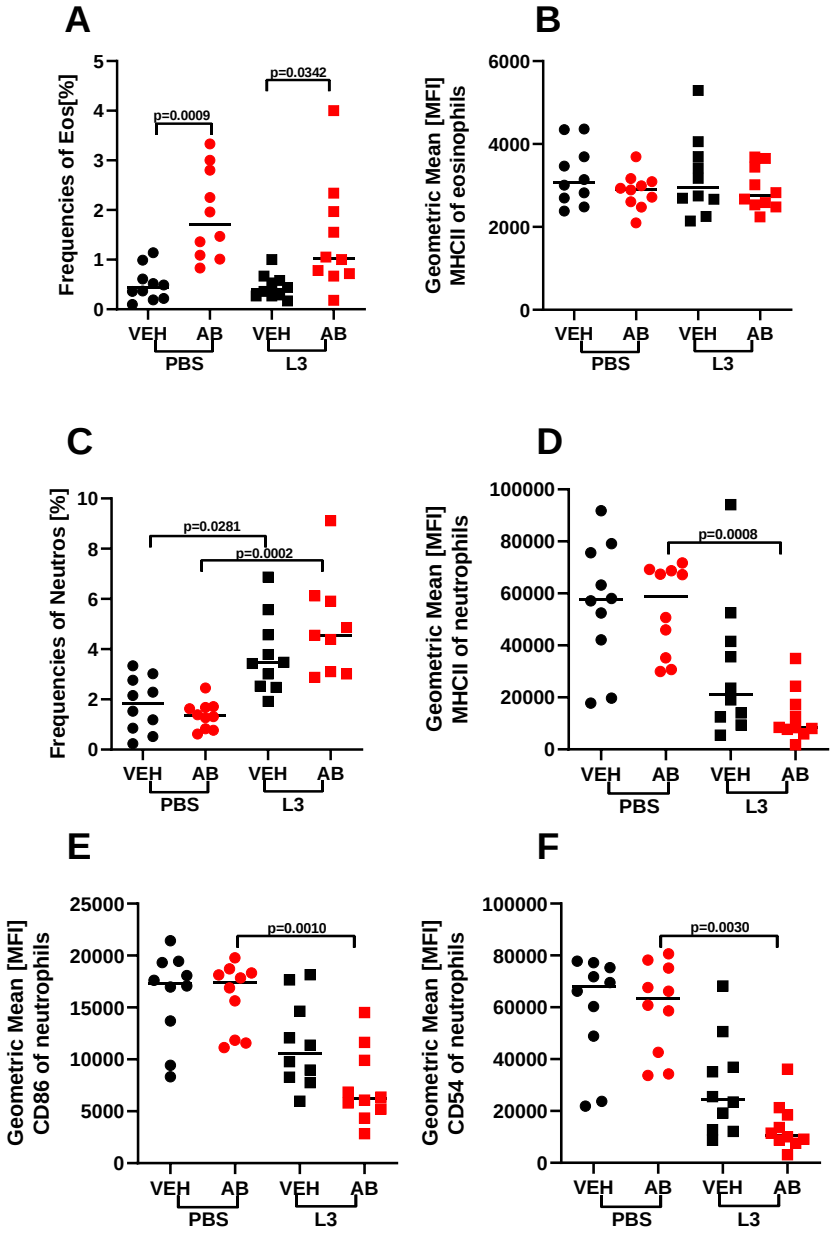

Figure 16. Cholinergic inhibition led to a reduced neutrophil activation after intradermal L3 injection. Frequency of eosinophils (Eos; A) and neutrophils (Neutros; C), as well as their respective MHCII (B, D) expression. Additionally, CD86 and CD54 expression of neutrophils is displayed (E,F) in WT mice treated with PBS or AB 3h post intradermal *L. sigmodontis* infection. Results are shown as median. Data represented is one of two experiments with n=10. Statistical analysis is performed using Kruskal Wallis and Dunn`s post hoc test.

3.3 Lack of muscarinic type 3 receptor signalling during *L. sigmodontis* infection

3.3.1 Lack of M3R leads to a delayed but higher worm recovery after natural *L. sigmodontis* infection

As cholinergic inhibition using AB may not exclusively inhibit signalling through the m3AChR, $M3R^{-/-}$ mice on a BALB/c background were used to exclusively investigate the mechanism of ACh signalling through the m3AChR. BALB/c WT mice were used as control

group. Following natural *L. sigmodontis* infection L3 larvae reach the thoracic cavity after about 5 days (43). Around day 8 L3 larvae develop into L4 larvae. Therefore, 9 dpi was the first time point to be analysed to determine if all L3 larvae reached the thoracic cavity. The second time point was at 15 dpi when the larvae should have completed the moult into L4 larvae. Thirdly, worm burden was analysed at 37 dpi when most worms developed to adults but did not yet produce MF (prepatent infection). The last time point covered the chronic infection stage at 70 dpi, at this time female worms already produced MF (patent infection). The worms were isolated and counted by flushing the thoracic cavity with PBS.

Unexpectedly, at 9 dpi $M3R^{-/-}$ mice revealed a significantly lower worm burden compared to WT mice ($p = 0.0008$; WT = ~30 worms; KO = ~9 worms; Fig.17A). However, $M3R^{-/-}$ mice showed a higher worm recovery compared to WT mice at 15 and 37 dpi (Fig.17B,C), which is in accordance with the observations in mice treated with the muscarinic inhibitor AB. At 15 dpi, the $M3R^{-/-}$ mice showed a higher worm burden compared to the control mice ($p = 0.0033$; WT = ~23 worms; KO = ~37 worms; Fig.17B) and the difference in worm burden was maintained at 37 dpi ($p = 0.0086$; WT = ~18 worms; KO = ~45 worms; Fig.17C). Additionally, the worm length and development was investigated. The adult worms revealed a mean length of 15 mm for the male worms in both WT and $M3R^{-/-}$ mice (Fig.17D). In contrast, female worms were significantly shorter in $M3R^{-/-}$ mice ($p = 0.0002$; WT = 47.9 mm; KO = 29.35 mm; Fig.17D). Interestingly, during the course of infection, $M3R^{-/-}$ mice seem to have a stronger clearance of the worms in the thoracic cavity, resulting in a comparable worm burden in both groups at 70 dpi (WT = ~18 worms; KO = ~14 worms; Fig.17E). Along with the reduction of worm numbers, the female worms also displayed an increase in length in the $M3R^{-/-}$ mice so that there was no statistical significant difference in length anymore between WT and $M3R^{-/-}$ mice (WT = 61.7 mm; KO = 57.5 mm; Fig.17D).

In summary, it was observed that during natural infection, mice lacking the type 3 muscarinic receptor showed a delayed migration of L3 larvae to the thoracic cavity. However, starting at 15 dpi the worm recovery was significantly higher in the $M3R^{-/-}$ compared to WT mice. In the end, worm clearance was enhanced leading to a similar worm burden in both groups at 70 dpi.

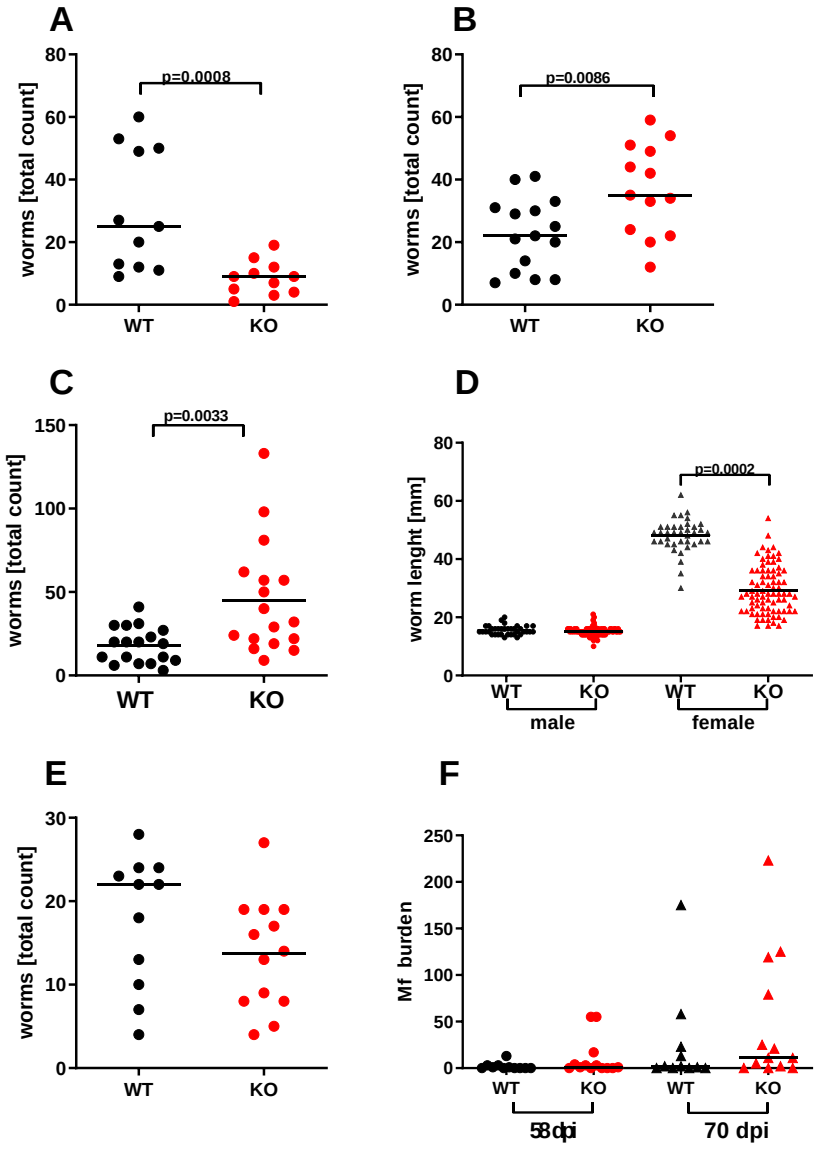

Figure 17: Delayed migration but increased worm burden following 15 days of natural *L. sigmodontis* infection in M3R$^{-/-}$ mice. Total worm burden after 9 , 15 , 37 and 70dpi (A, B, C, E) . Worm length after 37 dpi (D) and microfilarial load (MF) (F) at 58 and 70 dpi. Data represented is pooled data from two to three independent experiments per infection time point. Statistical significance was analysed by two-tailed non-parametric Mann-Whitney-U-test. *p<0.05, **p<0.01.

After the filariae develop into adults, they start to produce their progeny (MF). The MF are released in the blood stream at around day 50 of infection. Blood was taken from infected animals at two different time points, 58 and 70 dpi, to count the offspring. At 58 dpi both WT and M3R$^{-/-}$ mice possessed microfilariae, with no significant differences (Fig.17F). Five out of 11 WT animals possessed MF and 6 out of 13 M3R$^{-/-}$ mice were MF^{+}. On day 70, the number of MF^{+} animals in both groups increased to 7 MF^{+} of the WT animals and 10 MF^{+} among the M3R$^{-/-}$ mice. MF numbers increased within those two weeks in both groups, showing by trend higher numbers in M3R$^{-/-}$ mice compared to WT mice, but this did not reach statistical significance (WT = ~25 MF/50 µL blood; KO = ~48 MF/50 µL blood; Fig.17F).

The length of male and female adult worms isolated from the thoracic cavity of WT and M3R$^{-/-}$ mice were comparable at 70 dpi (Fig.18A). Additionally, the embryonic stages of the individual female worms were investigated at 70 dpi. The different developmental stages of the worms like eggs, morulae, pretzel and the stretched MF were counted. The numbers of eggs and morulae were by trend higher in the WT mice compared to the M3R$^{-/-}$ mice but were not statistically significant (Fig.18B). The amount of pretzel stages and stretched Mf were higher in the WT mice and only present in small numbers in the M3R$^{-/-}$ mice. However, in the repeat experiment the embryogenesis showed higher numbers of eggs, morulae, pretzel and stretched MF in M3R$^{-/-}$ mice compared to WT mice (data not shown), exactly the other way around, indicating no differences in embryogenesis between WT mice and M3R$^{-/-}$ mice.

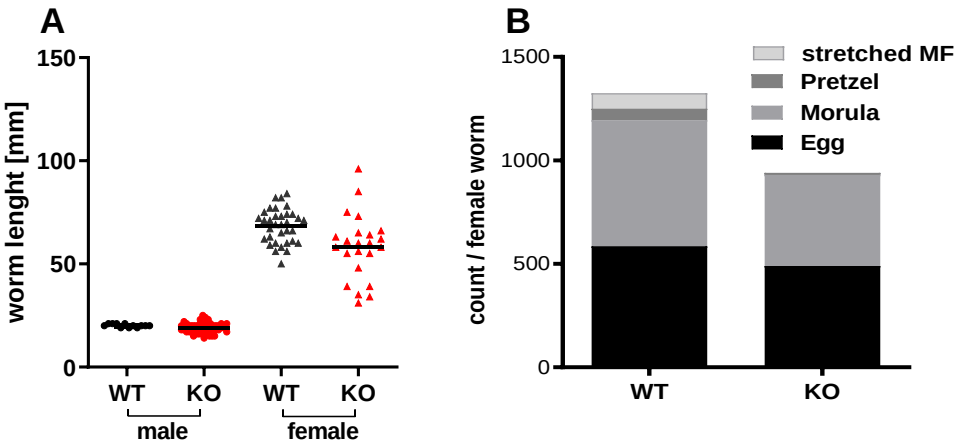

Figure 18: **Worm length and embryogenesis in WT and M3R$^{-/-}$ mice.** Worm length (A) and embryogenesis (B) in WT and M3R$^{-/-}$ mice at day 70 of natural infection with *L. sigmodontis*. Different stages of embryogenesis were counted in WT and M3R$^{-/-}$ mice in 5 individual female worms per mouse after 70 dpi. (A) Data represented is one of two independent experiments. Statistical significance was analysed by Kruskal Wallis and Dunn's post hoc test.

3.3.2 Cellular recruitment to different body compartments at 9 days post natural *L. sigmodontis* infection

The general migration time of infectious L3 Larvae to the thoracic cavity after natural *L. sigmodontis* infection takes about 5 days (43). After ~8 days L3 larvae start do develop into L4 larvae. Therefore, the first time point analysed for these experiment was 9 dpi to be sure that all L3 larvae did reach the thoracic cavity. The worms were isolated and counted by flushing the thoracic cavity with PBS. With this technique, immune cells were washed out as well and investigated using flow cytometry. Afterwards, the lung was flushed with PBS to isolate immune cells within the lung (BAL and lung). Then, the spleen was isolated to analyze

the systemic immune response. All cells were counted and cell populations were analysed by flow cytometry. Total cell counts of BAL revealed no differences between WT and M3R$^{-/-}$ mice at 9 dpi (WT = ~1.127 x 10^6 cells; KO = ~1.213 x 10^6 cells; Fig.19). In contrast, in the thoracic cavity (WT = ~1.247 x 10^7 cells; KO = ~0.611 x 10^6 cells) and spleen, cell counts were lower in the M3R$^{-/-}$ mice compared to WT mice (WT = ~1.470 x 10^8 cells; KO = ~1.335 x 10^8 cells, Fig.19B,C). Similarly, cell numbers in the lungs were significantly lower in M3R$^{-/-}$ mice compared to WT mice (WT = ~7.406 x 10^7 cells; KO = ~4.656 x 10^7 cells, Fig.19D).

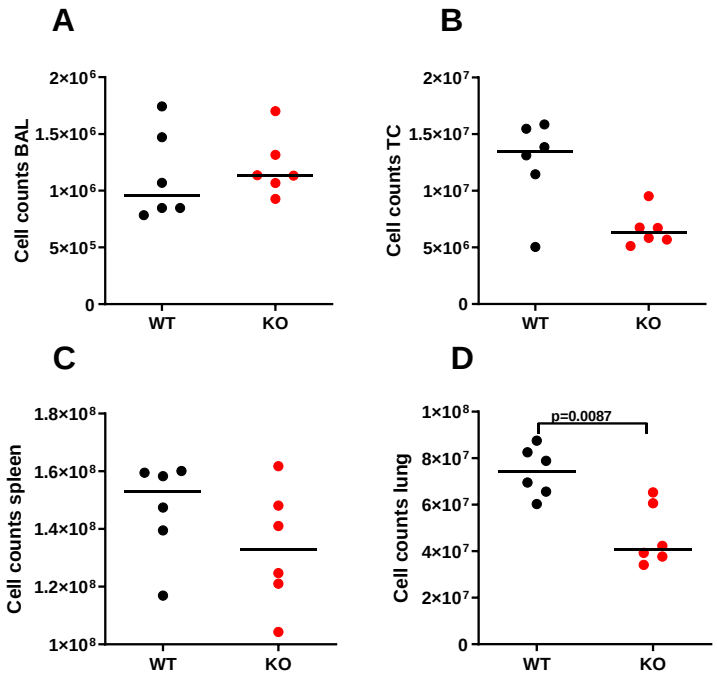

Figure 19: Comparison of total cell counts in different body compartments in BALB/c and M3R$^{-/-}$ mice after 9 dpi. Total cell counts of bronchio-alveolar fluid (BAL) (A), thoracic cavity (TC) (B), spleen (C) and lung cells (D) following natural infection 9 dpi. Statistical significance was analysed by two-tailed non-parametric Mann-Whitney-U-test. Data represented is one experiment representative of 2 of 3 experiments with 6 mice per group.

Cellular composition of the bronchio-alveolar fluid mainly consisted of alveolar macrophages after 9 dpi (WT = ~9.42 x 10^5 cells ; KO = ~9.02 x 10^5 cells; Fig.20A). Eosinophil constituted less than 5 % in both WT and M3R$^{-/-}$ mice. M3R$^{-/-}$ mice revealed slightly higher numbers of eosinophils compared to WT mice (WT = ~4.95 x 10^4 cells; KO = ~1.39 x 10^4 cells, Fig.20A), but this difference was not confirmed in the repeat experiments. Neutrophils did not show any differences in their numbers in both groups (WT = ~1.87 x 10^3 cells; KO = ~1.33 x 10^3 cells, Fig.20A). Lymphoid cells like B cells, CD4$^+$ and CD8$^+$ T cells were each lower than 1 %, with increased B cell numbers in the knockout mice (WT = ~2.05 x 10^3 cells;

KO = ~7.28 x 10^3 cells; Fig.20B) that did not reach statistical significance, but the trend was verified in repeat experiments.

In the thoracic cavity, the cellular composition looked quite different. Here, the eosinophils contributed more than 20 % of the total cells and WT mice showed increased numbers compared to $M3R^{-/-}$ mice, which was confirmed in the repeat experiments (WT = ~3.67 x 10^6 cells; KO = ~1.43 x 10^6 cells; Fig.20C). Neutrophil cell numbers were decreased in the knockout mice as well at 9 dpi in contrast to WT mice (WT = ~1.07 x 10^5 cells; KO = ~5.41 x 10^4 cells, Fig.20C). Although this trend did not reach statistical significance, it was also observed in the repeat experiments. Macrophages (WT = ~6.19 x 10^5 cells; KO = ~5.64 x 10^5 cells) were present in equal frequencies in both mouse groups after 9 dpi (Fig.20C). In contrast, $CD4^+$ and $CD8^+$ T cells were significantly reduced ($CD4^+$: WT = ~1.12 x 10^6 cells; KO = ~2.74 x 10^6 cells; $CD8^+$: WT = ~6.28 x 10^5 cells; KO = ~7.27 x 10^4 cells) while B cells were present in equal numbers in $M3R^{-/-}$ and WT mice (WT = ~2.29 x 10^6 cells; KO = ~2.36 x 10^6 cells, Fig.20D). Regarding the systemic immune response within the spleen, myeloid and lymphoid cell numbers did not show any statistically significant differences between WT and $M3R^{-/-}$ mice at 9 dpi (Fig.20E,F). However, there was by trend a reduction in $CD4^+$ and $CD8^+$ T cells as well as B cells in the spleen of $M3R^{-/-}$ mice compared to WT mice in all experiments.

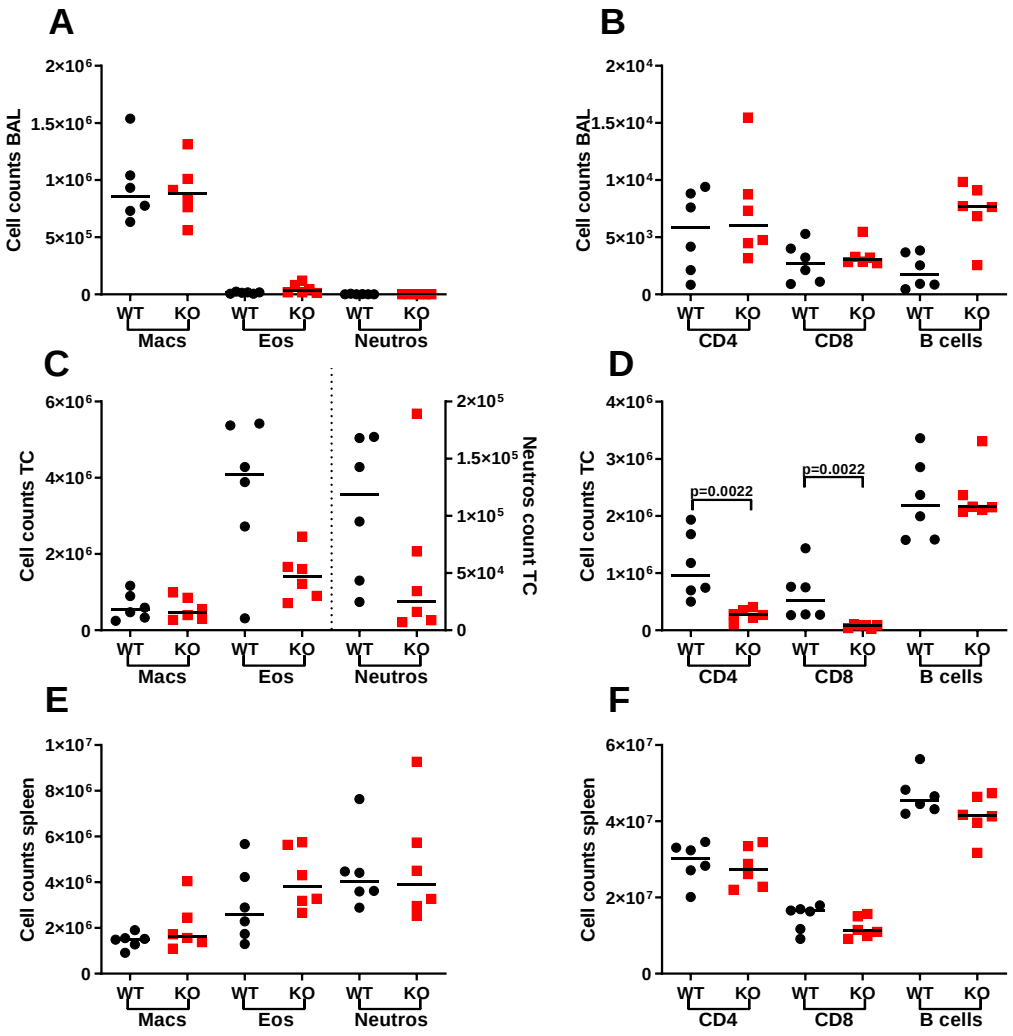

Figure 20: Comparison of the cellular composition and cell frequencies following L3 migration in BALB/c and M3R$^{-/-}$ mice at 9 dpi. Cell numbers of macrophages (Macs), neutrophils (Neutros), eosinophils (Eos)(A, C and E), CD4^{+} T cells (CD4), CD8^{+} T cells (CD8) and B cells (B, D and F) within the bronchio-alveolar fluid (BAL; A,B), thoracic cavity (TC; C,D) as well as the cellular composition of the spleen (E, F) following L3 migration 9 dpi. Statistical significance was analysed by two-tailed non-parametric Mann-Whitney-U-test. *p<0.05, **p<0.01. Data represented is one representative experiment out of 2 experiments with 6 mice per group.

Additionally, cytokine levels were measured within the thoracic cavity where the worms reside during infection. Cytokine levels were measured in the first mL that was used to flush the thoracic cavity. As neutrophil proportions were quite low in the beginning of the infection CXCL-5 a chemokine for neutrophil attraction was analysed. M3R$^{-/-}$ mice showed significantly higher levels of CXCL-5 compared to WT mice (WT = ~45.15 pg/µL; KO = ~69.28 pg/µL; Fig.21A). Elastase and MPO are enzymes in neutrophils that are responsible for regulation and termination of inflammatory processes. There were no differences in elastase levels between both mouse groups during infection (WT = ~73.12 pg/µL; KO = ~68.91 pg/µL, Fig.21B). However, MPO was significantly lower in the thoracic cavity of knock-out mice compared to WT mice (WT = ~191 pg/µL; KO = ~16.21 pg/µL, Fig.21C).

Furthermore, IL-5 which is responsible for eosinophil activation and B cell proliferation, showed significantly higher levels in M3R$^{-/-}$ mice (WT= ~13.47 pg/µL; KO= ~27.68 pg/µL, Fig.21D).

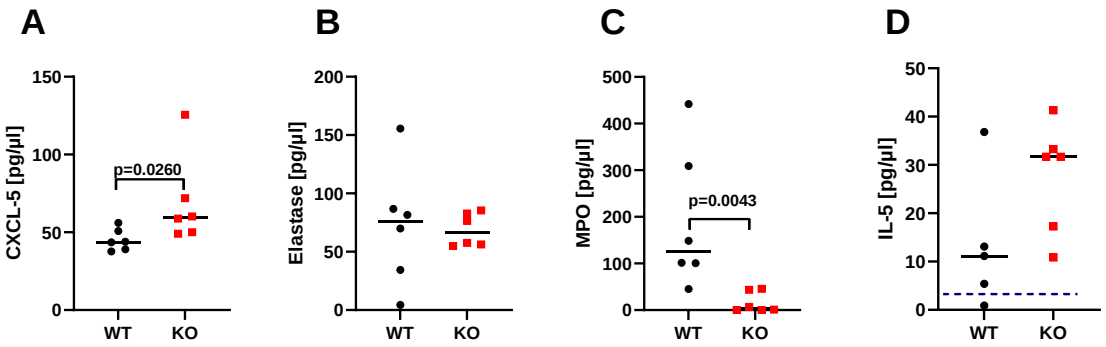

Figure 21: Cytokine release within the thoracic cavity of BALB/c and M3R$^{-/-}$ mice after 9 days post infection. CXCL-5 (A), elastase (B), MPO (C) and IL-5 (D) concentration in the thoracic cavity following *L. sigmodontis* infection 9 dpi. Statistical significance was analysed by two-tailed non-parametric Mann-Whitney-U-test. Data represented is one representative experiment out of two experiments with 6 mice per group.

To summarize, with regard to the total cell counts of the different body compartments the most prominent differences observed at 9 dpi on the cellular level was the reduction of CD4^{+} T cells and CD8^{+} T cells in the thoracic cavity of M3R$^{-/-}$ mice compared to WT mice, which might be due to the lower worm burden. Additionally, despite the lower numbers of eosinophils, higher levels of IL-5 was detected within the thoracic cavity of M3R$^{-/-}$ mice. One cause could be a delayed recruitment of the eosinophils due to the lower worm burden at the beginning of the infection in the M3R$^{-/-}$ animals compared to the WT animals. Thus, the IL-5 secretion in the WT mice could already been down-regulated, as sufficient eosinophils were already recruited. Furthermore, the lower levels of MPO might be due to the reduced numbers of neutrophils in the thoracic cavity of M3R$^{-/-}$ mice compared to WT controls.

3.3.3 Cellular composition in different body compartments at 15 days of natural *L. sigmodontis* infection

Secondly, parasitological and immunological parameters were investigated 15 days after natural infection. All larvae should have reached the L4 stage by that time-point but not yet developed to adult worms (42). Although the worm burden was higher in the M3R$^{-/-}$ mice at 15 dpi compared to the WT mice, the cell counts of BAL (WT = ~1.13 x 10^6 cells; KO = ~1.01 x 10^6 cells), thoracic cavity (WT = ~6.73 x 10^6 cells; KO = ~6.63 x 10^6 cells) and spleen (WT = ~1.47 x 10^7 cells; KO = ~2.00 x 10^7 cells) did not show any differences (Fig.22). Only lung cell numbers were significantly lower in M3R$^{-/-}$ mice (WT = ~1.87 x 10^7 cells;

KO = ~1.25 x 10^7 cells, Fig.22D), which might be due to the smaller size of the organ itself in the M3R$^{-/-}$ mice compared to WT mice.

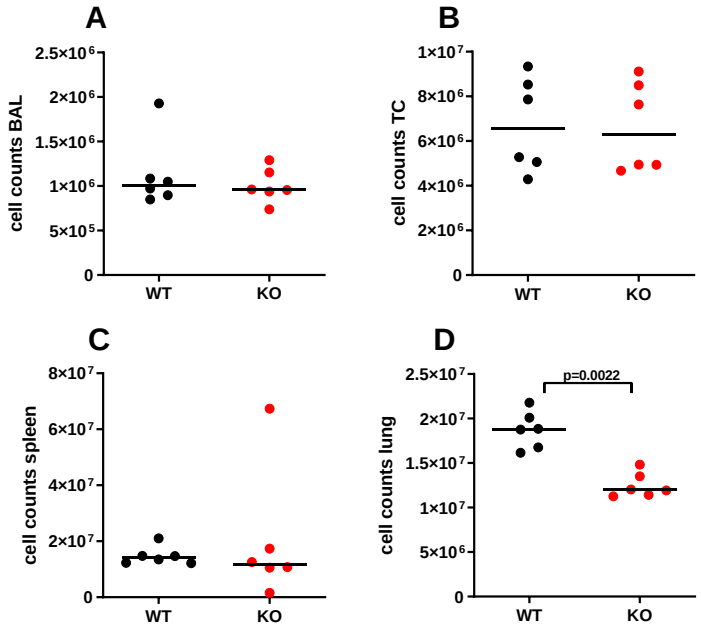

Figure 22: Comparison of total cell counts in different body compartments in BALB/c and M3R$^{-/-}$ mice after 15 dpi. Total cell counts of bronchio-alveolar fluid (BAL) (A), thoracic cavity (TC) (B), spleen (C) and lung cells (D) following *L. sigmodontis* infection 15 dpi. Statistical significance was analysed by two-tailed non-parametric Mann-Whitney-U-test. *p<0.05, **p<0.01. Data represented is one experiment with 6 mice per group representative of 2 out of 3 experiments.

At 15 dpi, the BAL mainly consisted of alveolar macrophages and did not show differences in macrophages, eosinophils and neutrophils between WT and M3R$^{-/-}$ mice (Fig.23A). Lymphoid cell numbers slightly increased compared to the first infection time point at 9 dpi. CD4$^+$ (WT = ~1.22 x 10^4 cells; KO = ~1.54 x 10^4 cells) and CD8$^+$ T cells (WT = ~1.21 x 10^3 cells; KO = ~2.93 x 10^3 cells) as well as B cells (WT = ~5.44 x 10^3 cells; KO = ~1.04 x 10^4 cells; Fig.23B) were elevated by trend in the M3R$^{-/-}$ mice but this did not reach statistical significance and was not confirmed in the repeat experiments (data not shown). Myeloid cell numbers within the thoracic cavity did not reveal any differences in WT and M3R$^{-/-}$ mice (Fig.23C). Similar to the first infection time point, CD4$^+$ (WT = ~2.79 x 10^5 cells; KO = ~1.22 x 10^5 cells) and CD8$^+$ T cells (WT = ~8.75 x 10^4 cells; KO = ~2.29 x 10^4 cells) were significantly reduced in the thoracic cavity of mice that lack type 3 muscarinic receptor compared to WT mice (Fig.23D). B cells were present at equal numbers in both mouse groups (WT = ~3.27 x 10^6 cells; KO = ~2.93 x 10^6 cells, Fig.23D).

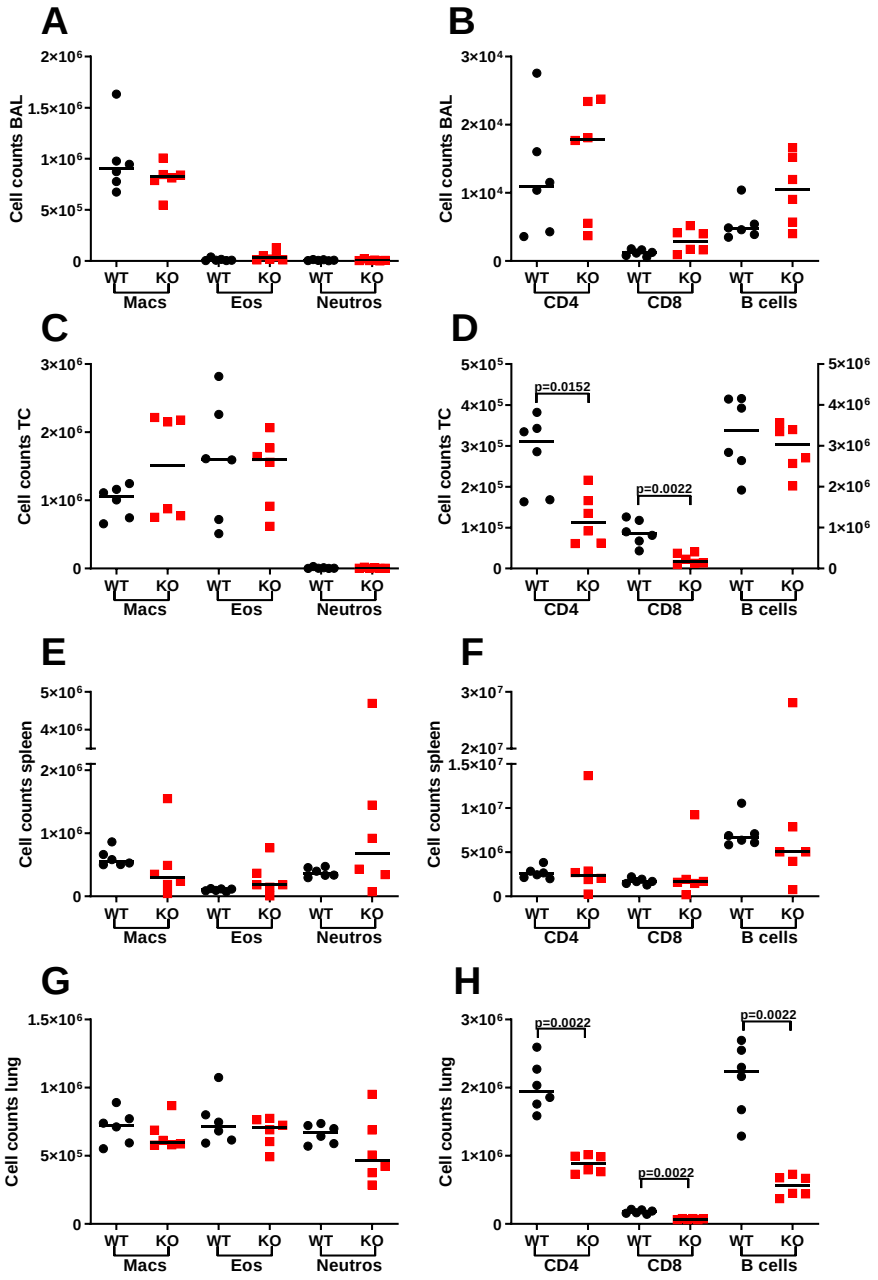

Figure 23: Comparison of cellular composition in different body compartments in BALB/c and M3R$^{-/-}$ mice after 15 dpi. Total cell counts of macrophages (Macs), eosinophils (Eos), and neutrophils (Neutros) (A, C, E, G) as well as CD4^{+} and CD8^{+} T cells and B cells (B, D, F, H) in (A, B) bronchio-alveolar lavage (BAL), (C,D) thoracic cavity lavage (TC), (E, F) spleen and (G, H) lung following *L. sigmodontis* infection at 15 dpi. Statistical significance was analysed by two-tailed non-parametric Mann-Whitney-U-test. Data represented is one experiment with 6 mice per group representative of 2 out of 3 experiments.

The systemic immune response within the spleen did not reveal any significant changes in immune cell infiltration regarding myeloid or lymphoid cell numbers, although B cells were reduced by trend in M3R$^{-/-}$ mice in all performed experiments compared to WT mice (Fig.23E,F).

In addition, the immune cell populations of the lung itself were analysed. Here, macrophages (WT = ~7.10 x 10^5 cells; KO = ~6.53 x 10^5 cells) and eosinophils (WT = ~7.52 x 10^5 cells; KO = ~6.75 x 10^5 cells) were present in equal numbers in WT and M3R$^{-/-}$ mice (Fig.23G). Neutrophil cell numbers were slightly lower in M3R$^{-/-}$ mice compared to WT mice but this difference did not reach statistical significance (WT = ~6.60 x 10^5 cells; KO = ~5.83 x 10^5 cells). However, cell counts of lymphoid cells in the lung tissue at 15 dpi showed significantly lower cell numbers of CD4$^+$ (WT = ~2.02 x 10^6 cells; KO = ~8.81 x 10^5 cells), CD8$^+$ T cells (WT = ~1.78 x 10^5 cells; KO= ~6.95 x 10^4 cells) and B cells in M3R$^{-/-}$ mice (WT = ~2.11 x 10^6 cells; KO = ~5.56x 10^5 cells, Fig.23H).

Additionally, cytokine levels were analysed within the thoracic cavity. The cytokine measurements for IL-5, IFN-γ and TNF were below the detection limit of the ELISA. CXCL-5 and elastase were detectable but did not reveal any differences between WT and M3R$^{-/-}$ mice (Fig.24).

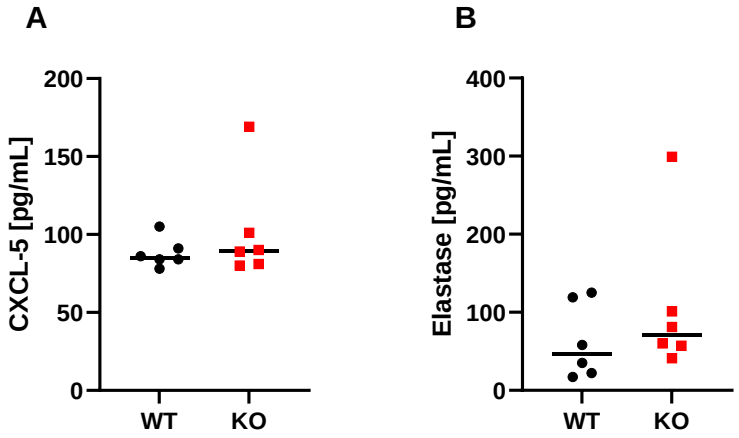

Figure 24: Cytokine release within the thoracic cavity of BALB/c and M3R$^{-/-}$ mice after 15 days of infection. CXCL-5 (A) and elastase (B) concentration in the thoracic cavity after 15 days of natural *L. sigmodontis* infection. Statistical significance was analysed by two-tailed non-parametric Mann-Whitney-U-test. Data represented is one representative experiment out of 2 with 6 mice per group.

3.3.4 Cellular composition in different body compartments at 37 days of natural *L. sigmodontis* infection

To get an overview of the immune responses during the course of infection we next analysed the immune responses at 37 dpi. At this time point worms already developed into adult worms but did not start with the release of MF, yet.

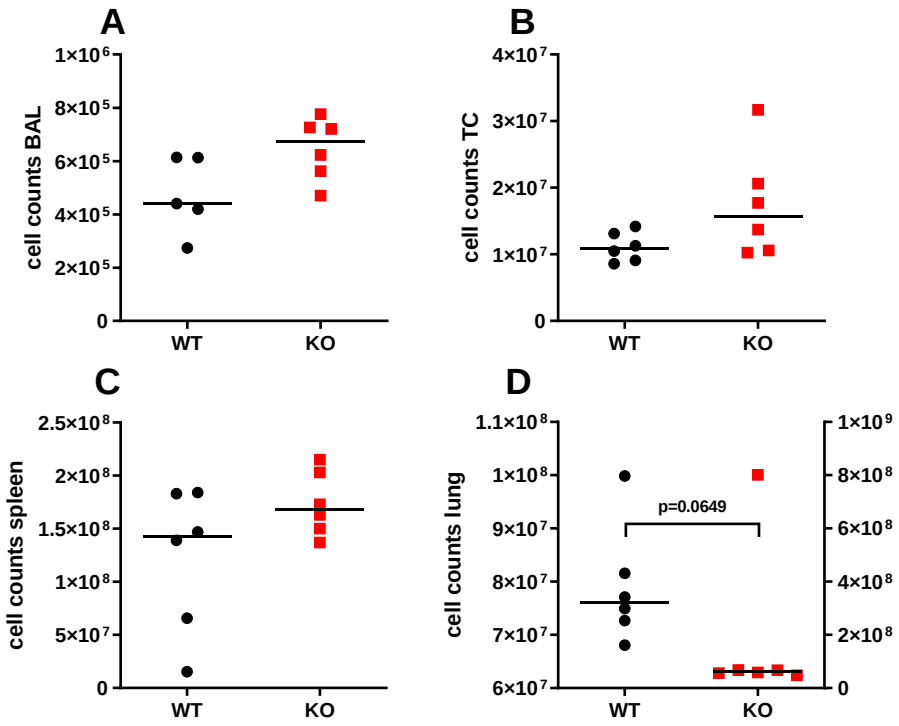

Figure 25: Comparison of total cell counts in different body compartments in BALB/c and M3R$^{-/-}$ mice at 37 dpi. Total cell counts of (A) bronchio-alveolar lavage (BAL), (B) thoracic cavity (TC), (C) spleen and (D) lung at 37 dpi. Statistical significance was analysed by two-tailed non-parametric Mann-Whitney-U-test. *p<0.05, **p<0.01. Data represented is one experiment with 6 mice per group.

The total cell counts of BAL revealed no differences at the two early time points at 9 and 15 dpi but at 37 dpi a slight increase of cell counts in the BAL of infected M3R$^{-/-}$ mice compared to WT mice was observed (WT = ~4,72 x 10^5 cells; KO = ~6,46 x 10^5 cells; Fig.25A). Spleen and thoracic cavity cell numbers were reduced in the M3R$^{-/-}$ mice in the beginning of the infection at 9 dpi. At 15 dpi, the cell numbers were equal between both groups and at 37 dpi there was an increase visible that did not reach statistical significance in the thoracic cavity (WT = ~1.11 x 10^7 cells; KO = ~1.74 x 10^7 cells; Fig.25B) and spleen (WT = ~1.22 x 10^8 cells; KO = ~1.74 x 10^8 cells, Fig.25C). In contrast, lung cell numbers were significantly reduced at the two early infection time points as well as at 37 dpi (WT = ~7.90 x 10^7 cells; KO = ~1.83x 10^8 cells; Fig.25D), although the reduction of lung cells did not reach statistical significance.

The cellular composition of the different body compartments was investigated in more detail by flow cytometry. Eosinophils were slightly increased in all investigated tissues and neutrophils decreased by trend in the thoracic cavity and lung (Fig.26A,C,E, G). Alveolar macrophages were the prominent cell type in BAL fluid and were increased in M3R$^{-/-}$ mice compared to WT mice but this difference did not reach statistical significance, however the

difference was observed in all repeat attempts (WT= ~3.80 x 10^5 cells; KO= ~5.37 x 10^5 cells; Fig.26A). Eosinophil cell numbers were significantly elevated (WT = ~2.40 x 10^3 cells; KO = ~5.94 x 10^3 cells; Fig.26A). Neutrophil numbers were significantly decreased in $M3R^{-/-}$ mice (WT = ~5.47 x 10^3 cells; KO = ~2.32 x 10^3 cells) within the BAL fluid compared to WT controls (Fig.26A), but this reduction of neutrophils was not confirmed in the repeat experiments (data not shown). Lymphoid cell populations like $CD4^+$ and $CD8^+$ T cells as well as B cells did not show any differences in cell numbers between both groups in the BAL fluid (Fig.26B).

Analysis of the thoracic cavity revealed the same trend for myeloid cell numbers in infected mice of both groups like in the BAL fluid. Macrophage (WT = ~1.59 x 10^6 cells; KO = ~3.89 x 10^6 cells; Fig.26C) and eosinophil (WT = ~4.75 x 10^6 cells; KO = ~7.86 x 10^6 cells) cell numbers were higher in $M3R^{-/-}$ mice than in WT mice reaching statistical significance for eosinophil numbers, whereas neutrophil (WT = ~1.65 x 10^6 cells; KO = ~9.8 x 10^5 cells) numbers were significantly lower (Fig.26C). Although the differences of macrophages cell numbers were not significant, the higher numbers in $M3R^{-/-}$ mice were confirmed in the repeat experiments. $CD4^+$ T cell numbers were comparable between both groups (WT = ~2.27 x 10^5 cells; KO = ~3.06 x 10^5 cells), while $CD8^+$ T cell numbers were significantly reduced in the thoracic cavity of $M3R^{-/-}$ compared to WT mice (WT = ~6.17 x 10^4 cells; KO = ~2.76 x 10^4 cells, Fig.26D). B cell numbers of the thoracic cavity of $M3R^{-/-}$ mice showed a huge variance for the individual mice within the group, leading to no statistical significant differences between both groups, but the repeat experiments showed elevated numbers of $CD4^+$ T and B cells (data not shown).

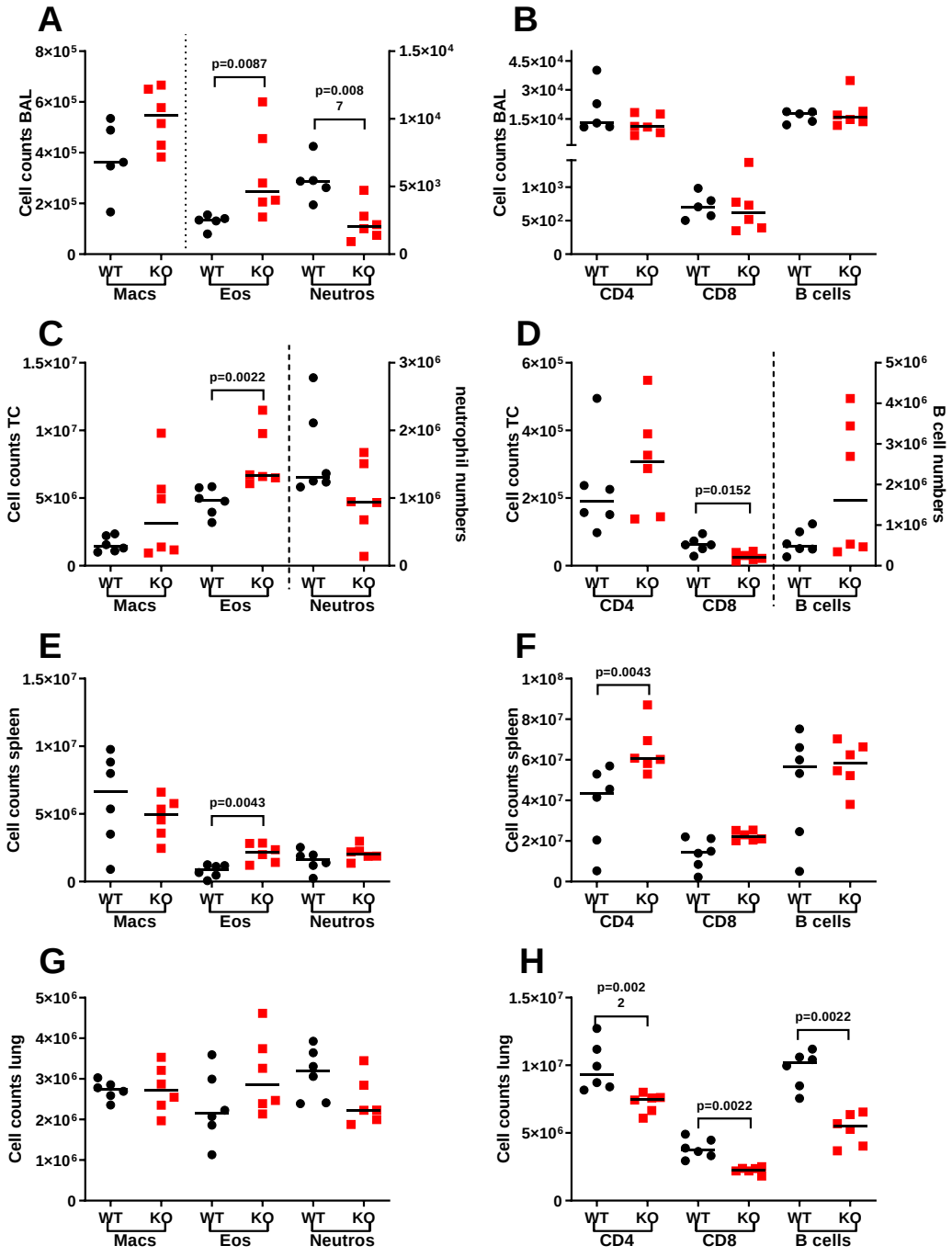

Figure 26: Cellular composition of different body compartments following *L. sigmodontis* infection in M3R$^{-/-}$ mice at 37 dpi. Total cell counts of macrophages (Macs), eosinophils (Eos), and neutrophils (Neutros) (A, C, E, G) as well as CD4^{+} and CD8^{+} T cells and B cells (B, D, F, H) in (A,B) bronchio-alveolar lavage (BAL), (C,D) thoracic cavity lavage (TC), (E, F) spleen and (G, H) lung following *L. sigmodontis* infection at 37 dpi. Statistical significance was analysed by two-tailed non-parametric Mann-Whitney-U-test. *p<0.05, **p<0.01. Data represented is one representative experiment out of 2-3 with 5-6 mice per group.

M3R$^{-/-}$ mice and WT mice demonstrated no differences in numbers of macrophages (WT = ~6.06 x 10^6 cells; KO = ~4.72 x 10^6 cells; Fig.26E) in the spleen, which was consistent with the results of the repeat experiments. Eosinophil cell numbers (WT = ~7.92 x 10^5 cells; KO = ~2.10 x 10^6 cells) were significantly elevated in the spleen and neutrophil numbers

showed no differences between both groups (Fig.26E), similar as in the repeat experiments. $CD4^+$ T cells numbers (WT = ~3.17 x 10^7 cells; KO = ~6.48 x 10^7 cells, Fig.26F) were significantly increased in infected $M3R^{-/-}$ mice compared to controls. Cell numbers of B cells were comparable between WT mice and $M3R^{-/-}$ mice (Fig.26F).

The lung tissue showed no differences in macrophage, eosinophil and neutrophils numbers (Fig.26G). In contrast, lymphoid cell numbers of $CD4^+$ T cells (WT = ~9.86 x 10^6 cells; KO = ~7.23 x 10^6 cells), $CD8^+$ T cells (WT = ~3.86 x 10^6 cells; KO = ~2.24 x 10^6 cells) and B cells (WT = ~9.70 x 10^6 cells; KO = ~5.26 x 10^6 cells) were significantly lower in lungs of infected $M3R^{-/-}$ mice compared to BALB/c mice (Fig.26G, H), but this effect was not confirmed by the repeat experiments (data not shown).

Furthermore, the cytokine levels of BAL fluid and thoracic cavity were investigated using ELISA. No differences in IFN-γ and IL-5 levels were observed in infected BALB/c or $M3R^{-/-}$ mice (Fig.27A, B). However, concentrations of Eotaxin 1 and Eotaxin 2 were increased in the thoracic cavity of infected $M3R^{-/-}$ mice compared to infected WT mice (Fig.27). As Eotaxin is responsible for the recruitment of eosinophils during infection, the higher cytokine levels are in accordance with the higher eosinophil numbers in the thoracic cavity of $M3R^{-/-}$ mice compared to WT mice. In addition, there was a higher release of elastase in the thoracic cavity of $M3R^{-/-}$ mice (Fig.27E), although the numbers of neutrophils were reduced. Cytokine levels of the BAL revealed lower concentrations of IL-5 and MIP-2 (Fig.27F,G) which is in line with the lower neutrophil numbers in the $M3R^{-/-}$ mice compared to WT mice.

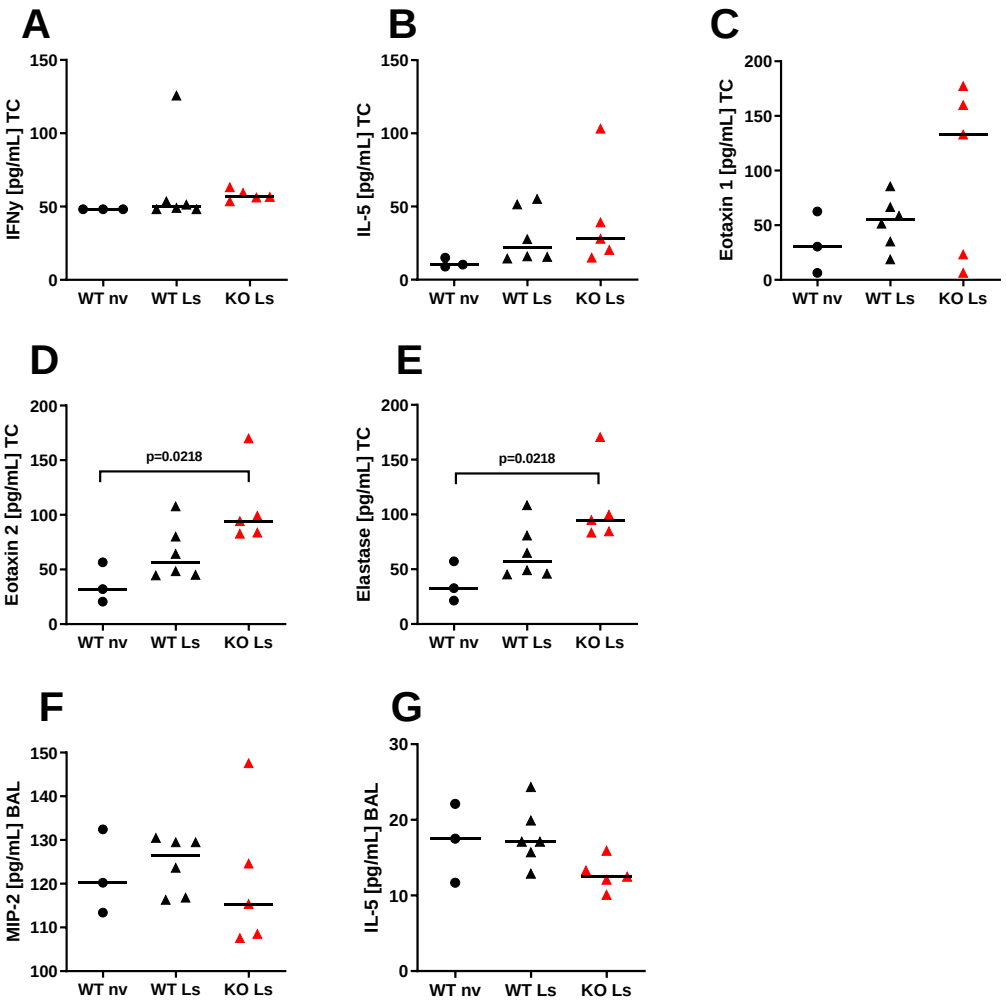

Figure 27: Cytokine milieu within BAL and thoracic cavity at 37 days post natural *L. sigmodontis* infection in M3R$^{-/-}$ mice. Concentrations of IFN-γ (A), IL-5 (B) and Eotaxin 1 and 2 (C, D) as well as elastase (E) in the pleural cavity lavage and concentrations of MIP-2 (F) and IL-5 (G) in bronchio-alveolar lavage at 37 days post *L. sigmodontis* infection in WT and M3R$^{-/-}$ mice. Results are shown as median (A-G). Statistical significance was analysed by two-tailed non-parametric Mann-Whitney-U-test. *p<0.05, **p<0.01. Data represented is one experiment with 5-6 mice per group.

3.3.5 Cellular composition in different body compartments at 70 days of natural *L. sigmodontis* infection

At 70 days post infection the adult worms in the thoracic cavity were patent and released MF into the blood stream. At this time point there were no significant differences in the worm and MF burden of BALB/c and M3R$^{-/-}$ mice (Fig.17A).

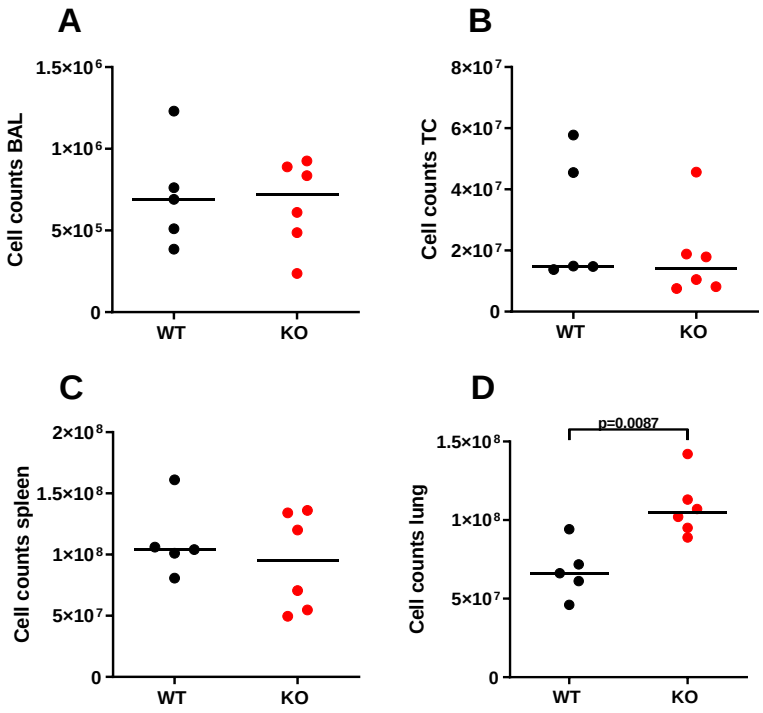

Figure 28: Comparison of total cell counts in different body compartments in BALB/c and M3R$^{-/-}$ mice after 70 dpi. Total cell counts of (A) bronchio-alveolar lavage (BAL), (B) thoracic cavity lavage (TC), (C) spleen and (D) lung at 70 dpi. Statistical significance was analysed by two-tailed non-parametric Mann-Whitney-U-test. *p<0.05, **p<0.01. Data represented is one experiment with 6 mice per group.

The total cell counts of BAL fluid (WT = ~7.61 x 10^5 cells; KO = ~6.64 x 10^5 cells), thoracic cavity (WT = ~2.94 x 10^7 cells; KO = ~1.81 x 10^7 cells) and spleen (WT = ~1.11 x 10^8 cells; KO = ~9.42 x 10^7 cells) showed no differences between both groups (Fig.28A-C) at 70 dpi. Number of lung cells were significantly increased in M3R$^{-/-}$ mice compared to WT mice (WT = ~6.79 x 10^7 cells; KO = ~1.08 x 10^8 cells, Fig.28D). At 70 dpi the composition of the BAL fluid consisted mainly of alveolar macrophages showing no differences in cell numbers between both groups (WT = ~1.50 x 10^5 cells; KO = ~1.46 x 10^5 cells; Fig.29A). Eosinophil (WT = ~6.90 x 10^3 cells; KO = ~9.17 x 10^3 cells) and neutrophil (WT = ~2.64x10^3 cells; KO = ~2.71x10^3 cells) numbers were comparable between WT mice and M3R$^{-/-}$ mice (Fig.19A). Lymphoid cells such as CD4$^+$ T cells (WT = ~6.55 x 10^3 cells; KO = ~2.75 x 10^3 cells; Fig.29B), CD8$^+$ T cells (WT = ~5.75 x 10^3 cells; KO = ~1.89 x 10^3 cells) T and B cells (WT = ~1.08 x 10^3 cells; KO= ~1.16 x 10^3 cells) were also present in comparable numbers within the BAL fluid at 70 dpi (Fig.29B).

Analysis of the thoracic cavity revealed eosinophils as the prominent cell type of myeloid cells but comparable numbers were found in WT mice and M3R$^{-/-}$ mice (WT = ~8.51 x 10^6 cells; KO = ~6.94 x 10^6 cells; Fig.29C). There was also no difference in macrophage

(WT = ~7.96 x 10^5 cells; KO = ~4.36 x 10^5 cells) and neutrophil (WT = ~3.58 x 10^5 cells; KO = ~5.72 x 10^5 cells) numbers between both groups (Fig.29C). The cell population of $CD4^+$and $CD8^+$ T cells, as well as B cells did not show any differences in the thoracic cavity of infected WT and $M3R^{-/-}$ mice (Fig.29D).

Myeloid cell populations in the spleen revealed comparable numbers of macrophages (WT = ~3.55 x 10^6 cells; KO = ~2.68 x 10^6 cells) and eosinophils (WT = ~1.90 x 10^6 cells; KO = ~3.17 x 10^6 cells, Fig.29E). Although neutrophil numbers were increased in $M3R^{-/-}$ mice compared to WT mice in the depicted experiment (WT = ~4.81 x 10^6 cells; KO = ~8.13 x 10^6 cells), the numbers were comparable between both groups in the repeat experiments (data not shown). $CD4^+$ T cell (WT = ~1.31 x 10^7 cells; KO = ~1.72 x 10^7 cells) and $CD8^+$ T cell (WT = ~9.91 x 10^6 cells; KO = ~1.09 x 10^7 cells) and B cell (WT = ~3.14 x 10^7 cells; KO = ~1.95 x 10^7 cells) populations, showed no significant differences in total cell numbers between infected WT and $M3R^{-/-}$ mice (Fig.29F). However, $CD4^+$ and $CD8^+$ T cells were slightly elevated which was confirmed in the repeat experiments (data not shown).

Also the myeloid and lymphoid cell numbers of the lungs of infected animals showed no significant differences between both groups at 70 dpi, and trends seen in Fig.29G, H) were not confirmed in a second experiment.

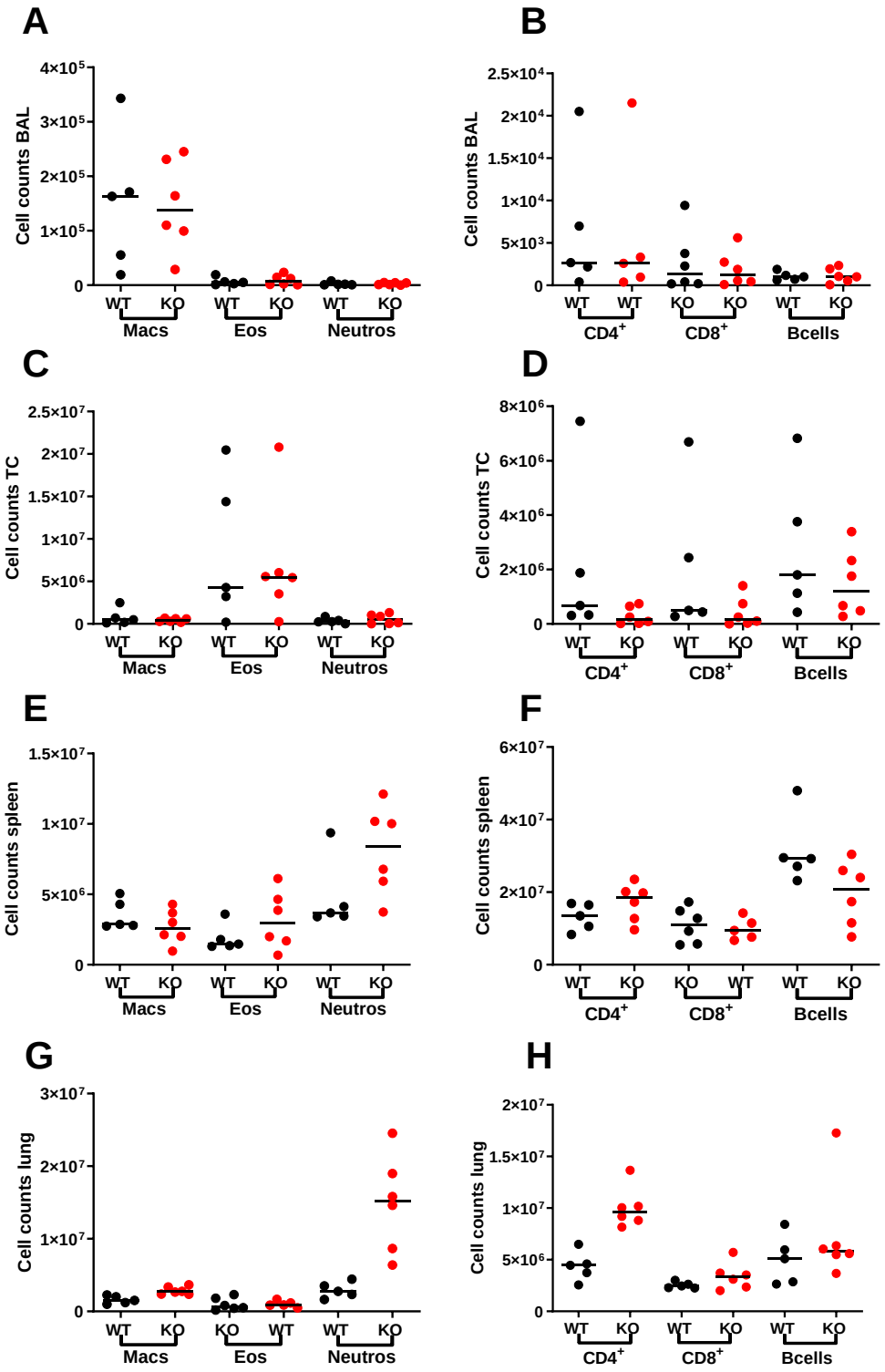

Figure 29: Cellular composition of different body compartments following *L. sigmodontis* infection in M3R$^{-/-}$ mice at 70 dpi. Total cell counts of macrophages (Macs), eosinophils (Eos), and neutrophils (Neutros) (A, C, E, G) as well as CD4$^+$ and CD8$^+$ T cells and B cells (B, D, F, H) in (A,B) bronchio-alveolar lavage (BAL), (C,D) thoracic cavity lavage (TC), (E, F) spleen and (G, H) lung following *L. sigmodontis* infection at 70 dpi. Statistical significance was analysed by two-tailed non-parametric Mann-Whitney-U-test. *p<0.05, **p<0.01. Data represented is one representative out of 2 experiments with 5-6 mice per group.

Cytokine measurements in the thoracic cavity showed increased IFN-γ levels in infected WT mice compared to naïve WT mice and infected M3R$^{-/-}$ mice (WT naïve (nv) = ~3.08 pg/mL; WT *L. sigmodontis* (Ls) = ~300.45 pg/mL; KO Ls = ~64.85 pg/mL; Fig.30A). IL-5 levels were elevated in infected mice, but did not show differences between WT mice and M3R$^{-/-}$ mice (WT nv = ~35.83 pg/mL; WT Ls = ~86.60 pg/mL; KO Ls = ~95.93 pg/mL; Fig.20B). Neutrophil elastase (WT nv = ~38.90 pg/mL; WT Ls = ~110.69 pg/mL; KO Ls = ~186.9 pg/mL) and Eotaxin 1 (WT nv = ~20.86 pg/mL; WT Ls = ~172.02 pg/mL; KO Ls = ~94.56 pg/mL) were increased in infected mice as well, and were comparable between WT and M3R$^{-/-}$ mice (Fig.30C,D). Eotaxin 2 on the other hand was reduced in infected M3R$^{-/-}$ mice compared to infected WT mice (WT nv =~51.38 pg/mL; WT Ls = ~1332.32 pg/mL; KO Ls = ~573.22 pg/mL, Fig.30E). MIP-2 concentrations did not show any differences between naïve or infected WT and M3R$^{-/-}$ mice (Fig.30F).

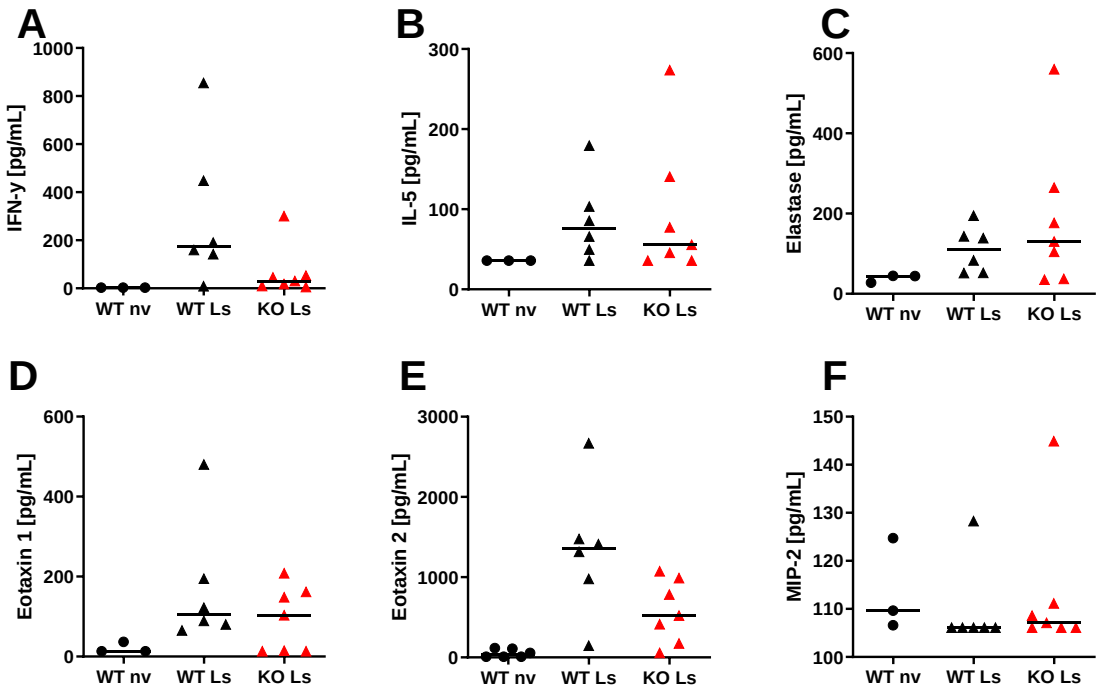

Figure 30: Cytokine milieu within BAL and thoracic cavity at 70 days of natural *L. sigmodontis* infection in M3R$^{-/-}$ mice. Concentrations of IFN-γ (A), IL-5 (B) and Eotaxin 1 and 2 (D, E) in the pleural cavity lavage and concentrations of elastase (C) and MIP-2 (F) at 37 days of *L. sigmodontis* infection in WT and M3R$^{-/-}$ mice. Results are shown as median (A-F). Statistical significance was analysed by Kruskal Wallis and Dun's post hoc test. Data represented is one experiment with 3-6 mice per group.

3.4 Summary of the cellular analysis at the different time points of *L. sigmodontis* infection

In conclusion, it is shown that the number of immune cells such as eosinophils, neutrophils, $CD4^+$ and $CD8^+$ T cells as well as B cells in the thoracic cavity of $M3R^{-/-}$ mice is decreased compared to WT mice shortly after the arrival of the L3 larvae in the thoracic cavity (9 dpi, table 5). This delayed immune response is associated with a delayed migration of L3 larvae into the thoracic cavity in $M3R^{-/-}$ mice. At day 15 of infection, the number of granulocytes in the thoracic cavity of $M3R^{-/-}$ mice increased leading to comparable cell numbers of both infected groups. However, $CD4^+$ and $CD8^+$ T cells were still reduced in the thoracic cavity of $M3R^{-/-}$ animals 15 dpi. In addition, B cells in the spleen and lymphocytes in the lung were reduced in the $M3R^{-/-}$ mice compared to WT mice. By 37 dpi macrophages, eosinophils, $CD4^+$ T and B cells were increased in the thoracic cavity of the $M3R^{-/-}$ animals compared to the WT animals, while neutrophils were reduced (table 5). Similarly, in the spleen the numbers of eosinophils, $CD4^+$ and $CD8^+$ T cells were increased in the $M3R^{-/-}$ mice compared to the WT mice, but B cells remained reduced. With the development of a patent infection (70 dpi), neutrophils increased within the BAL of $M3R^{-/-}$ mice compared to WT mice and immune cell numbers in the thoracic cavity of WT mice and $M3R^{-/-}$ mice were comparable at 70 dpi. However, eosinophils, $CD4^+$ and $CD8^+$ T cells increased in the spleen of $M3R^{-/-}$ mice compared to WT mice. Overall, the obtained data suggest that $M3R^{-/-}$ mice possess a delayed immune response against *L. sigmodontis* compared to WT mice, but this difference in the cellular composition wanes with the development of chronic infection, leading to a comparable worm elimination.

Table 5: Overview of cellular changes at different infection time points of natural *L. sigmodontis* infection. Shown are cellular increases (⇧) and decreases (⇩) in M3R$^{-/-}$ mice compared to WT mice following natural *L. sigmodontis* infection at 9, 15, 37 and 70 dpi that were confirmed in repeat experiments. Comparable cell numbers (⟷) between both infected mouse groups are displayed as well. Oblique arrows indicate repeated differences that did not reach statistical significance, while straight arrows indicate statistical significant differences.

BAL	**9 dpi**	**15 dpi**	**37 dpi**	**70 dpi**
Alv macs	⟷	⟷	⟷	⟷
Eos	⟷	↗	⇧	⟷
Neutros	⟷	⟷	⟷	↗
CD4+	⟷	⟷	⟷	⟷
CD8+	⟷	⟷	⟷	⟷
B cells	↗	⟷	⟷	⟷
TC				
Macs	⟷	⟷	⟷	⟷
Eos	↘	⟷	⇧	⟷
Neutros	↘	⟷	↘	⟷
CD4+	⇩	⇩	↗	⟷
CD8+	⇩	⇩	↗	⟷
B cells	⟷	⟷	⟷	⟷
Spleen				
Macs	⟷	⟷	⟷	⟷
Eos	⟷	⟷	⇧	↗
Neutros	⟷	⟷	↘	⟷
CD4+	⟷	⟷	⇧	↗
CD8+	⟷	⟷	↗	↗
B cells	↘	↘	⟷	⟷
Lung				
Alv macs	⟷	⟷	⟷	⟷
Eos	⟷	⟷	⟷	⟷
Neutros	⟷	⟷	⟷	⟷
CD4+	⟷	⇩	⟷	⟷
CD8+	⟷	⇩	⟷	⟷
B cells	⟷	⇩	⟷	⟷

3.5 Intravenous *L. sigmodontis* infection abolishes the higher worm recovery in M3R$^{-/-}$ mice

Mice lacking the type 3 muscarinic receptor showed a delayed but higher worm recovery during the course of a natural infection with *L. sigmodontis*. Although, there was a reduction

of $CD4^+$ and $CD8^+$ T cells within the thoracic cavity and lung accompanied by a delayed neutrophil infiltration into the thoracic cavity, this does probably not account for the higher susceptibility of $M3R^{-/-}$ mice to *L. sigmodontis* infection immediately after L3 larvae reached the thoracic cavity. Therefore, an intravenous (iv) infection was performed with a defined number of 40 L3 larvae to circumvent the skin barrier and migration route via the lymphatics. Importantly, following iv infection, the migration of L3 to the thoracic cavity is faster and analysis were performed at 9 dpi (43). Interestingly, the difference in worm recovery observed during natural infection was abolished 9 dpi after iv infection (Fig.31A). Total cell numbers within BAL, thoracic cavity, spleen und lung did not show any significant differences between WT mice and $M3R^{-/-}$ mice (Fig.31B-E).

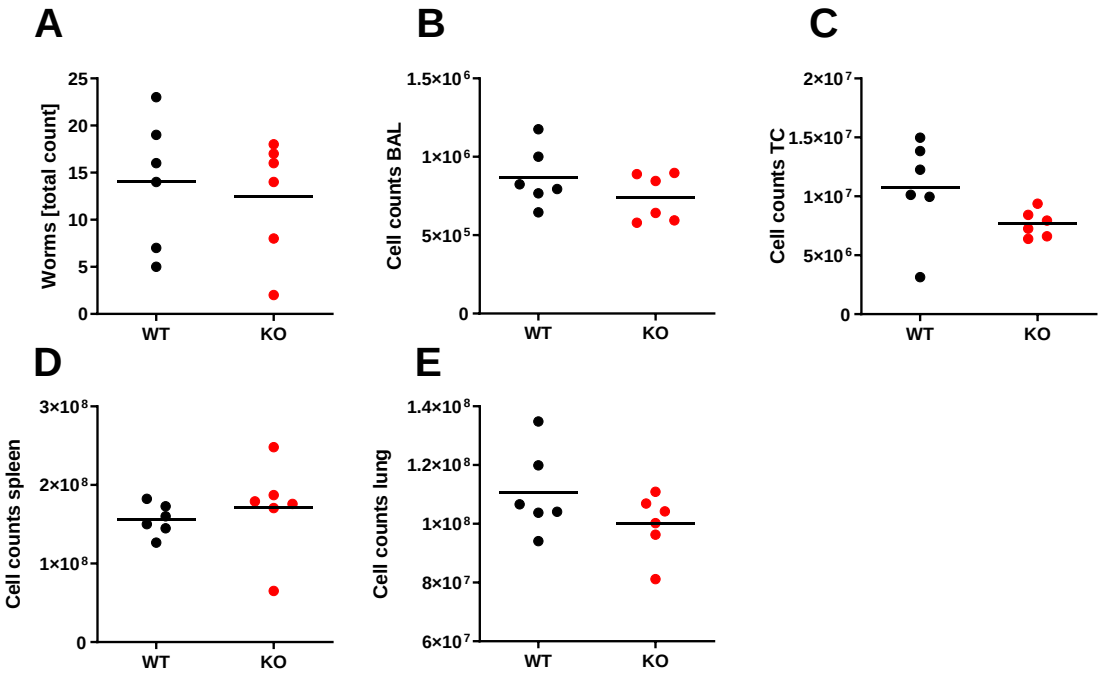

Figure 31: Comparison of worm burden and total cell counts in different body compartments in BALB/c and $M3R^{-/-}$ mice after iv infection. Worm burden at 9 days of intravenous infection with 40 L3 larvae (A). Total cell counts of bronchio-alveolar lavage (BAL) (B), thoracic cavity lavage (TC) (C), spleen (D) and lung cells (E) at 9 days post iv infection. Statistical significance was analysed by two-tailed non-parametric Mann-Whitney-U-test. *p<0.05, **p<0.01. Data represented is one experiment with 6 mice per group.

3.4.1 Cellular recruitment to different body compartments at 9 days post intravenous *L. sigmodontis* infection

Intravenous infection abolished the higher worm recovery in $M3R^{-/-}$ mice compared to WT mice. The cellular analysis of the BAL fluid showed no differences of the analysed myeloid and lymphoid cell populations between WT and $M3R^{-/-}$ mice (Fig.32A,B). The cellular composition in the thoracic cavity at 9 days post iv infection showed no differences in

macrophage and neutrophil numbers (Fig.32C). However, eosinophil numbers were slightly reduced (WT = ~2.13 x 10^6 cells; KO = ~1.78 x 10^6 cells), but this did not reach statistical significance in infected M3R$^{-/-}$ mice compared to WT mice (Fig.32C). Additionally, CD4$^+$ T cells (WT = ~5.58 x 10^5 cells; KO = ~2.74 x 10^5 cells) and CD8$^+$ T cell numbers (WT = ~4.03 x 10^5 cells; KO = ~1.19 x 10^5 cells; Fig.32D) in the thoracic cavity were significantly reduced in M3R$^{-/-}$ mice compared to controls. B cell numbers were reduced as well but this did not reach statistical significance (WT = ~4.40 x 10^6 cells; KO = ~2.26 x 10^6cells, Fig.32D).

The cellular composition of the spleen revealed no differences in macrophage (WT = ~7.54 x 10^5 cells; KO = ~5.77 x 10^5 cells) or eosinophil numbers (WT = ~1.26 x 10^6 cells; KO = ~1.76 x 10^6 cells; Fig.32E), but showed slightly increased neutrophil numbers that did not reach statistical significance (WT = ~1.94 x 10^6 cells; KO = ~4.9 x 10^6 cells). While CD4$^+$ T cells and CD8$^+$ T cell numbers in the spleen were lower in M3R$^{-/-}$ mice compared to WT mice following natural infection, intravenous infection led to an increase of those, although it did not reach statistical significance (CD4$^+$ T cells: WT = ~2.37 x 10^7 cells; KO = ~3.46 x 10^7 cells; CD8$^+$ T cells: WT = ~1.19 x 10^7 cells; KO = ~1.85 x 10^7 cells; respectively, Fig.32F). B cell numbers in the spleen were equal between both infected groups (WT = ~5.22 x 10^7 cells; KO = ~4.83 x 10^7 cells; Fig.32F).

Furthermore, the lung tissue was investigated and the cellular composition showed comparable numbers of macrophages (WT = ~2.24 x 10^6 cells; KO = ~2.34 x 10^6 cells; Fig22G) and eosinophils (WT = ~1.59 x 10^6 cells; KO = ~1.44 x 10^6 cells) at 9 days post iv infection. In contrast, neutrophil numbers were significantly increased in the lung of M3R$^{-/-}$ mice ($p = 0.0173$; WT = ~1.73 x 10^6 cells; KO = ~2.67 x 10^6 cells, Fig.32G). Lymphoid cells within the lung were all reduced, however only CD8$^+$ T cells were significantly lower in M3R$^{-/-}$ mice compared to WT mice ($p = 0.0087$; WT = ~3.55 x 10^6 cells; KO = ~2.24 x 10^6 cells; Fig.32H).

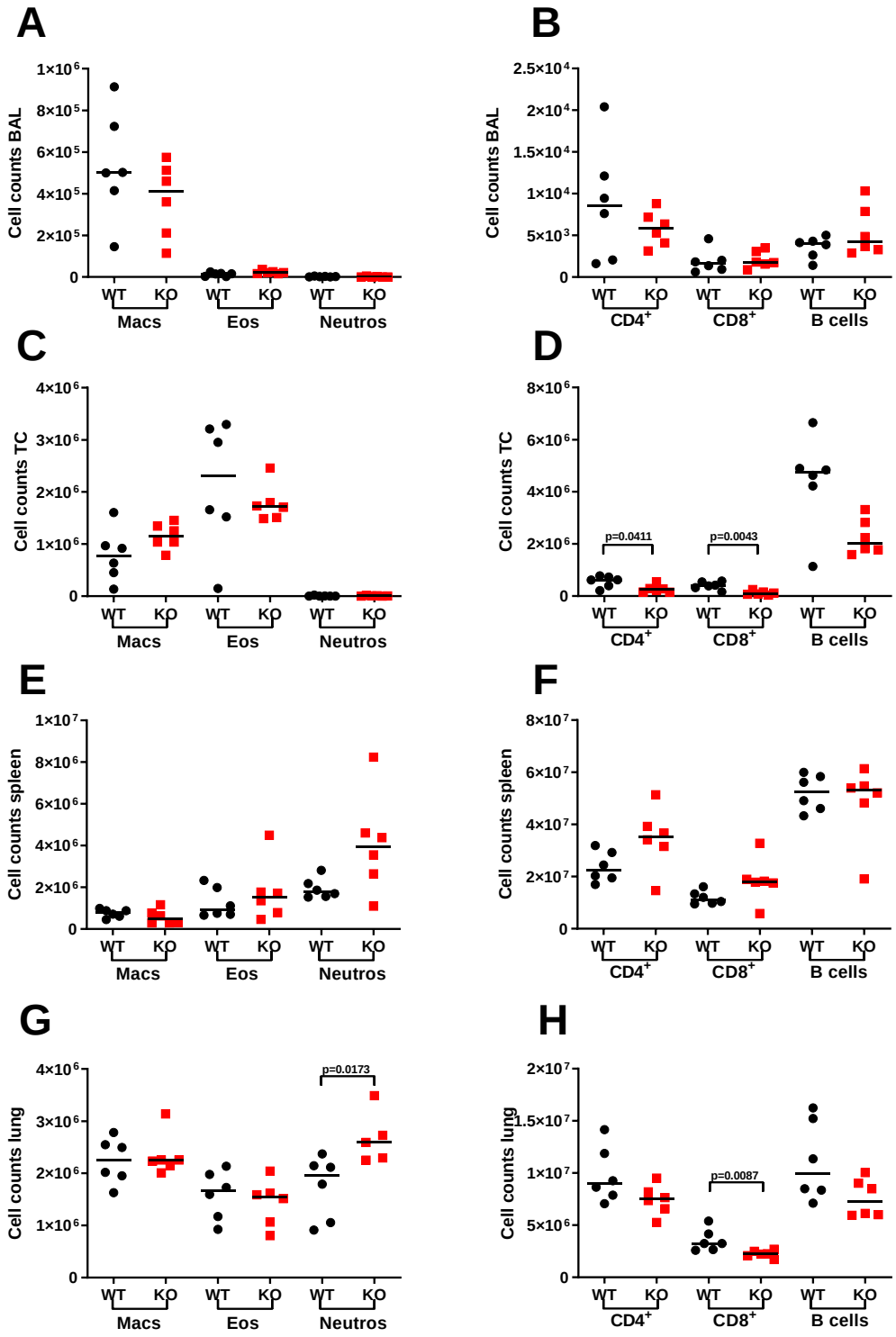

Figure 32: Cellular composition of different body compartments following intravenous L3 injection in M3R$^{-/-}$ mice at 9 dpi. Total cell counts of macrophages (Macs), eosinophils (Eos), and neutrophils (Neutros) (A, C, E, G) as well as CD4$^+$ and CD8$^+$ T cells and B cells (B, D, F, H) in (A, B) bronchio-alveolar lavage (BAL), (C, D) thoracic cavity lavage (TC), (E, F) spleen and (G, H) lung following intravenous L3 injection at 9 dpi. Statistical significance was analysed by two-tailed non-parametric Mann-Whitney-U-test. Data represented is one representative experiment out of two with 6 mice per group.

In summary, intravenous infection led to higher CD4$^+$ T cell and CD8$^+$ T cell numbers in the spleen accompanied by higher neutrophil numbers in M3R$^{-/-}$ mice compared to WT mice. In

general, comparable trends were observed as at 9 days after natural infection with *L. sigmodontis*.

Table 6: Comparison of immune cells in the different body compartments following natural and iv infection of M3R$^{-/-}$ and WT mice with *L. sigmodontis* at 9 dpi. Shown are cellular increases (⇧) and decreases (⇩) in M3R$^{-/-}$ mice compared to WT mice following natural and intravenous infection with *L. sigmodontis* infection at 9 dpi that were confirmed in repeat experiments. Comparable cell numbers (⟷) between both infected mouse groups are displayed as well. Oblique arrows indicate repeated differences that did not reach statistical significance, while straight arrows indicate statistical significant differences.

BAL	Iv infection 9 dpi	Natural infection 9 dpi
Alv macs	⟷	⟷
Eos	⟷	⟷
Neutros	⟷	⟷
CD4+	⟷	⟷
CD8+	⟷	⟷
B cells	⟷	↗
TC		
Macs	⟷	⟷
Eos	↘	↘
Neutros	⟷	↘
CD4+	⇩	⇩
CD8+	⇩	⇩
B cells	↘	⟷
Spleen		
Macs	⟷	⟷
Eos	↗	⟷
Neutros	↗	⟷
CD4+	↗	⟷
CD8+	↗	⟷
B cells	⟷	↘
Lung		
Alv macs	⟷	⟷
Eos	⟷	⟷
Neutros	⇧	⟷
CD4+	⟷	⟷
CD8+	⇧	⟷
B cells	⟷	⟷

Interestingly, there are small differences in the immune cell distribution between WT and M3R$^{-/-}$ mice following iv or natural infection. In the thoracic cavity, no differences in the cell number of macrophages between WT and M3R$^{-/-}$ mice following natural infection were detected (table 6). However, macrophages were elevated upon iv infection. Eosinophils, CD4^{+} and CD8^{+} T cells as well as B cells were reduced in the thoracic cavity of M3R$^{-/-}$ mice following natural and iv infection. However, WT mice and M3R$^{-/-}$ mice both had comparable numbers of neutrophils after iv infection, whereas these were reduced in M3R$^{-/-}$ mice following natural infection compared to WT mice. In the spleen, eosinophils and neutrophils were equally elevated in the M3R$^{-/-}$ animals regardless of the route of infection. Observed differences in immune cell numbers support the assumption of a delayed immune response during natural infection due to a delayed arrival of the L3 larvae in the thoracic cavity of M3R$^{-/-}$ mice compared to WT mice.

3.5 Innate lymphoid cells during natural and intravenous *L. sigmodontis* infection

Innate lymphoid cells are tissue resident cells that are involved in immune responses by releasing signalling molecules in response to tissue damage. Innate lymphoid type 1 cells (ILC1) are predominantly triggered by intracellular microorganisms like viruses, bacteria or protozoan parasites and induce a type 1 immune response. ILC2 cells are responsible for type 2 immunity and can be induced by extracellular molecules like allergens and helminths. ILC3 are responsible for tissue repair and phagocytosis as well as a source for the cytokines IL-22 and IL-17 (165). Innate lymphoid cells were investigated during the course of infection within the thoracic cavity. While ILC3 showed no consisting differences for each infection time point (data not shown), ILC2 illustrated consistent differences in the independent experiments. Natural infection with *L. sigmodontis* showed by trend lower numbers of ILC2 in M3R$^{-/-}$ mice compared to WT mice at 9 dpi (WT = ~3.93 x 10^4 cells; KO = ~1.90 x 10^4 cells; Fig.33A). At 15 dpi both infected groups possessed equal numbers of ILC 2 (WT = ~2.84 x 10^3 cells; KO = ~3.33 x 10^3 cells). Interestingly, at 37 dpi ILC2 increased in both infected groups but M3R$^{-/-}$ mice possessed significantly increased numbers of ILC2 in the thoracic cavity compared to infected WT mice ($p = 0.0087$; WT = ~3.83 x 10^5 cells, KO = ~9.12 x 10^5 cells, Fig.33A). At 70 dpi ILC2 decreased in both infected groups to equal numbers (WT = ~2.01 x 10^4 cells; KO = ~2.79 x 10^4 cells). After intravenous infection, ILC2 numbers were quite low at 9 dpi and by trend lower in M3R$^{-/-}$ mice than in WT mice (WT = ~713 cells; KO = ~271 cells; Fig.33B) similar to the 9 dpi time point after natural infection. This trend was confirmed in the repeat experiment.

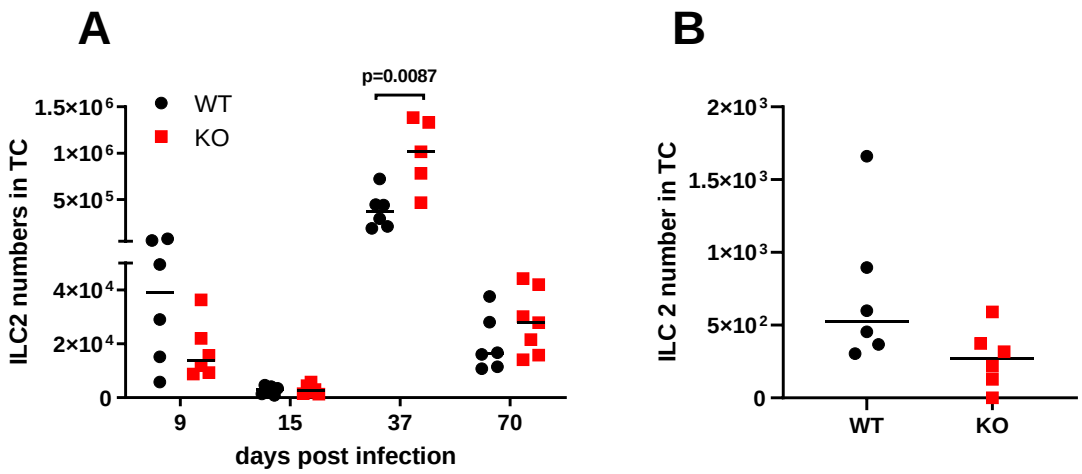

Figure 33: Innate lymphoid type 2 cells during *L. sigmodontis* infection. ILC 2 were measured in the thoracic cavity after natural infection (A) at 9, 15, 37 and 70 dpi and after intravenous infection at 9 dpi (B). (A) Represents 2 out of 3 independent experiments for each infection time point. (B) Data represented is one out of 2 experiments. Statistical significance was analysed by two-tailed non-parametric Mann-Whitney-U-test.

Furthermore, ILC1 subsets within the lung revealed significantly lower numbers of Lin^- mNK cells at 9 dpi in $M3R^{-/-}$ mice compared to WT mice ($p = 0.0043$; WT = ~2.14 x 10^6 cells; KO = ~7.09 x 10^5 cells; Fig.34A). Cell numbers of Lin^- mNK cells decreased at 15 dpi in both WT and $M3R^{-/-}$ mice showing no difference any more between both groups (WT = ~2.32 x 10^5 cells; KO = ~1.52 x 10^5 cells). At 37 dpi there was a comparable gain of Lin^- mNK cells in both infected groups. However, at 70 dpi cell numbers of Lin^- mNK cells increased further than at 37 dpi, resulting in significantly higher numbers in $M3R^{-/-}$ mice compared to WT mice ($p = 0.0260$; WT = ~1.27 x 10^6 cells; KO = ~1.84 x 10^6 cells, Fig.34A). Interestingly, after intravenous infection Lin^- mNK cells were present in equal numbers in WT and $M3R^{-/-}$ mice (WT = ~2.49 x 10^6 cells; KO = ~2.43 x 10^6 cells; Fig.34D), while after natural infection $M3R^{-/-}$ mice possessed reduced numbers compared to WT mice. In addition, Lin^+ mNK cell numbers increased during natural infection with a peak at 70 dpi (Fig.34B), while $M3R^{-/-}$ mice possessed reduced numbers of Lin^+ mNK cells at each time point. At 9 dpi the numbers were slightly reduced (WT = ~1.51 x 10^5 cells; KO = ~3.10 x 10^3 cells) and did not reach statistical significance. However, starting at 15 dpi cell numbers increased ($p = 0.0095$; WT = ~5.92 x 10^5 cells; KO = ~7.26 x 10^4 cells, Fig.34B) and were significantly higher in the lungs of WT mice compared to $M3R^{-/-}$ mice.

Lin^+ mNK numbers increased further at 37 dpi ($p = 0.0043$; WT = ~2.82 x 10^6 cells; KO = ~4.19 x 10^5 cells) and peaked at 70 dpi ($p = 0.0012$; WT = ~6.54 x 10^6 cells; KO = ~2.31 x 10^6 cells), but at both time points numbers were significantly reduced in $M3R^{-/-}$

mice compared to WT mice (Fig.34B). Cell numbers of Lin^+ mNK cells were also reduced at 9 days after intravenous infection (WT = ~4.45 x 10^6 cells; KO = ~1.80 x 10^6 cells; Fig.34D) where the worm recovery was similar in both groups. Besides, ILC1 cell numbers were comparable at each time point between both groups following natural infection (Fig.34C), as well as intravenous infection (Fig.34D).

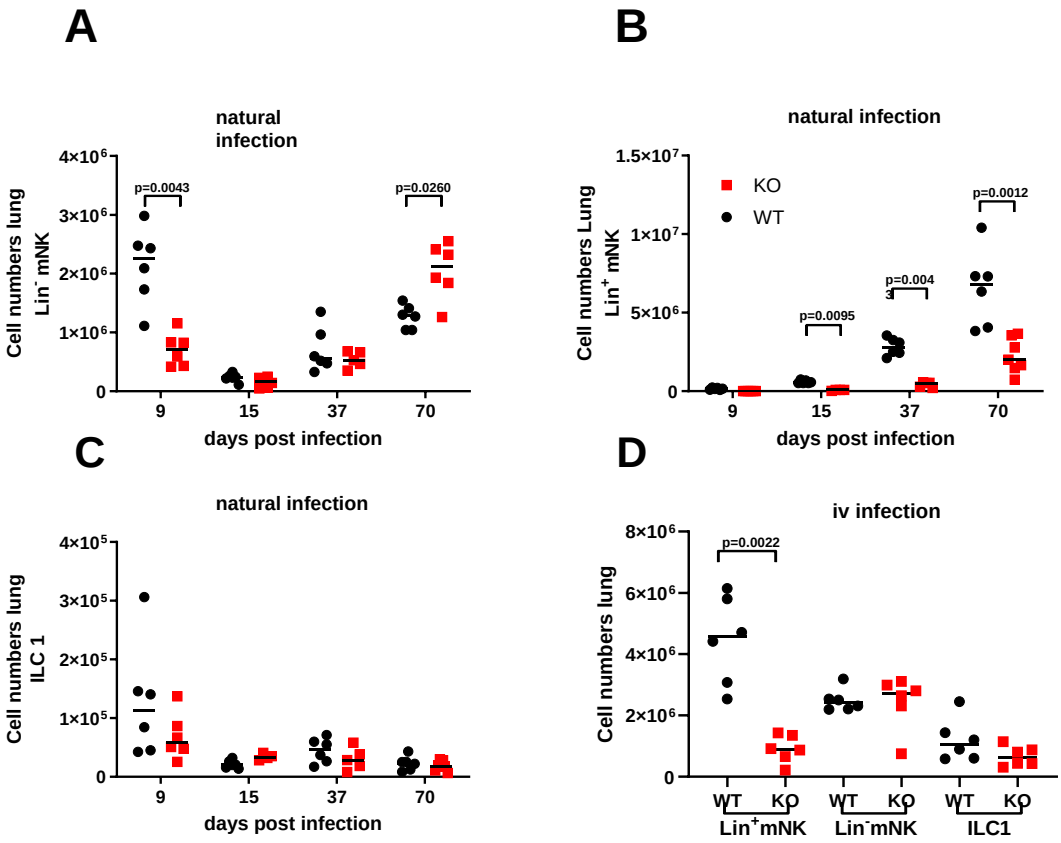

Figure 34: Innate lymphoid type 1 cells during *L. sigmodontis* infection. ILC subsets were measured in the lung after natural infection at 9, 15, 37 and 70 dpi showing Lin^-mNK cells (A), Lin^+mNK cells (B) and ILC1 (C). ILC populations after intravenous infection (D) were measured in the lung at 9 dpi. (A) Data represented is 2 out of 3 independent experiments for each infection time point. (B) Data represents 1 out of 2 experiments. Statistical significance was analysed by two-tailed non-parametric Mann-Whitney-U-test.

In summary, ILC2s were present in the thoracic cavity shortly after the L3 reached the thoracic cavity (9 dpi) but to a lesser extent in $M3R^{-/-}$ mice than in WT mice. However, the tide turned at day 37 post-infection, where $M3R^{-/-}$ mice showed significantly increased numbers of ILC2s compared to WT animals. In addition, there was an increase in Lin^+ mNK cells during the course of infection in WT and $M3R^{-/-}$ animals, but $M3R^{-/-}$ mice possessed lower numbers at each time point.

3.6 Intradermal infection with *L. sigmodontis* leads to reduced granulocyte activation in M3R$^{-/-}$ mice

As the reduced worm burden after natural infection was circumvented by an intravenous infection and the cellular analysis of the different body compartments did not reveal differences on the cellular level that might be responsible for the increased worm burden in M3R$^{-/-}$ mice, either L3 migration through the skin or lymphatics might be affected. Therefore, an intradermal injection with 10 infective L3 larvae was performed to analyse the local immune response by flow cytometry within the skin after 3 hours of infection. The same mice were infected intradermally with L3 larvae in the upper hind leg region on the right side and 10 µL PBS were injected on the left side as control. Eosinophil frequencies were by trend lower in M3R$^{-/-}$ mice compared to WT mice, but the variance among the individual mice was high and L3 injection did not increase the eosinophil frequencies at that time point (Fig.35A). However, L3 injection increased MHCII (PBS: WT = ~3904 MFI; KO = ~4350 MFI; WT L3 = ~7396 MFI; KO L3 = ~2472 MFI; Fig.35B) and CD86 expression (PBS: WT = ~1165 MFI; KO = ~1262 MFI; WT L3 = ~2384 MFI; KO L3 = ~780 MFI; Fig.35C) on eosinophils of WT mice, while the expression of both markers was unchanged in M3R$^{-/-}$ mice. Thus, eosinophil activation after 3 hours of intradermal L3 injection was significantly reduced in M3R$^{-/-}$ mice compared to WT mice. With regard to neutrophils, their frequencies were comparable between both control groups (Fig.35D). L3 injection slightly increased the neutrophil frequency in both M3R$^{-/-}$ and WT mice, confirming previous studies with regards to WT animals (58, 59). Upon L3 exposure, neutrophil frequencies were by trend higher in M3R$^{-/-}$ mice compared to WT mice, but this did not reach statistical significance (PBS: WT = ~0.53 %; KO = ~0.68 %; WT L3 = ~1.7 %; KO L3 = ~3.08 %; Fig.35C). Neutrophil activation was slightly increased after L3 injection in WT mice in terms of CD86 (WT = ~15785 MFI; KO = ~10944 MFI; WT L3 = ~18208 MFI; KO L3 = ~10392 MFI) and CD54 expression (WT = ~47057 MFI; KO = ~30383 MFI; WT L3 = ~55477 MFI; KO L3 = ~26982 MFI; Fig.35.E,F). Importantly, the activation status of neutrophils in the skin of M3R$^{-/-}$ mice remained unchanged after L3 injection, leading to a lower neutrophil activation compared to WT mice after L3 injection.

In conclusion, L3 injection into the skin led to an increase of neutrophil frequencies in WT mice and M3R$^{-/-}$ mice. Although, the infiltration of neutrophils was slightly higher in M3R$^{-/-}$ mice compared to WT mice, CD86 and CD54 expression was unchanged in M3R$^{-/-}$ mice upon L3 injection, while WT mice possessed a higher expression of both activation markers

following L3 injection. Furthermore, activation of eosinophils was lower in the M3R$^{-/-}$ mice than in WT mice. In summary, M3R$^{-/-}$ mice showed a reduced granulocyte activation compared to WT mice after intradermal L3 injection, which may impair their protective response against the invading L3 larvae.

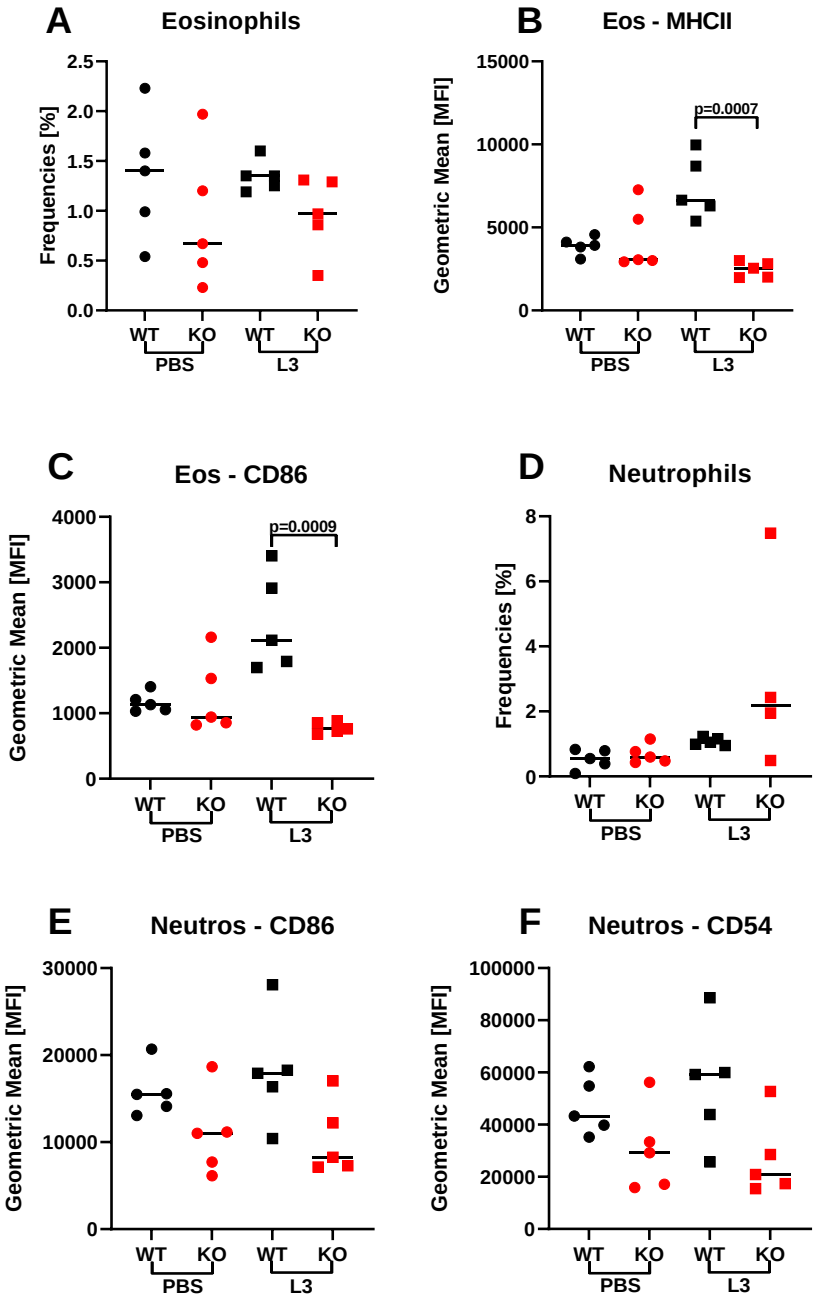

Figure 35: Increased neutrophil infiltration but reduced neutrophil and eosinophil activation following intradermal L3 injection in M3R$^{-/-}$ mice. Proportions of eosinophils (A) and neutrophils (D) 3 hours after intradermal L3 or PBS injection in WT and M3R$^{-/-}$ mice. The activation of eosinophils concerning MHCII (B) and CD86 (C) expression and neutrophil activation concerning CD86 (E) and CD54 (F) is displayed. Statistical significance was analysed by two-tailed non-parametric Mann-Whitney-U-test. *p<0.05, **p<0.01. Data represented is one experiment with 6 mice per group.

3.7 *In vitro* stimulation of bone marrow-derived neutrophils

Previous experiments revealed a reduced neutrophil and eosinophil activation after intradermal L3 injection. Therefore, bmd neutrophils were isolated from both WT and $M3R^{-/-}$ mice and stimulated *in vitro* with PMA and Zymosan as positive control or left untreated as control. Additional conditions included L3 larvae and the stimulation with LsAg. Isolated neutrophils already possessed a high baseline expression of MHCII in the untreated condition after 6 hours of culture (WT= ~23038 MFI; KO= ~18483 MFI; Fig.36A) with no difference in both groups. Stimulation with PMA up-regulated MHCII expression in both neutrophils derived from WT and $M3R^{-/-}$ mice showing no differences between both groups. Stimulation with L3 larvae and LsAg did not increase MHCII expression and resulted in no differences in the mean fluorescence intensity between neutrophils derived from WT or $M3R^{-/-}$ mice.

In contrast, CD54 expression on bmd neutrophils was up-regulated upon LPS (WT = ~9014 MFI; KO = ~4477 MFI; Fig.36B) and Zymosan (WT = ~10763 MFI; KO = ~6014 MFI) stimulation with a higher expression in neutrophils from WT mice than $M3R^{-/-}$ mice. Stimulation with L3 larvae did not change the expression of CD54 in both groups (WT = ~3066 MFI; KO = ~3645 MFI), whereas LsAg stimulation slightly increased expression of CD54 on neutrophils from $M3R^{-/-}$ mice (WT = ~3351 MFI; KO = ~5513 MFI; Fig.36B), but this did not reach statistical significance.

Given the lack of activation following LsAg and L3 stimulation, it was subsequently investigated if the cells were still viable after 6 hours of stimulation. Stimulation with PMA and Zymosan led to a strong activation and cell death after 6 hours with up to 60 % and 80% dead cells (Fig.36C) in both groups, respectively. However, in all other conditions >80 % of the neutrophils remained viable after 6 hours of stimulation (Fig.36C).

In addition, bmd neutrophils were co-cultured with isolated L3 larvae to investigate the motility of the larvae for 48 hours as it is known that neutrophils can inhibit L3 larval motility by NETosis (59). As control L3 larvae were cultured in medium alone. Bmd neutrophils of WT and $M3R^{-/-}$ mice were co-cultured with L3 larvae with and without DNase to degrade released DNA nets. Larval motility was measured using a motility score from 0 meaning no movement to 4, which indicated rapid and continuous movement. In the beginning, all L3 larvae were rapidly moving with a score of 4 in all conditions (Fig.36D). After 24 hours, L3 larvae co-cultured with neutrophils from $M3R^{-/-}$ mice were already affected in their movement compared to neutrophils from WT mice (WT = score 4; KO = score 3.5). While larvae cultured with WT neutrophils still moved very quickly around themselves and in all directions

performing the filarial dance (score 4), this movement was already restricted and slowed down in the co-culture with M3R$^{-/-}$ neutrophils (score 3). One day later, the motility of L3 larvae co-cultured with neutrophils from WT mice started to decrease as well, but the motility inhibition remained stronger with neutrophils derived from M3R$^{-/-}$ mice (WT = score 3.2; KO = score 2.8). Addition of DNase had only a marginal impact on larval motility compared to the corresponding group without DNase (Fig.36D), indicating that DNA nets are not essentially involved in impairing the motility. L3 larvae cultured in the absence of neutrophils remained rapidly moving until the end of the experiment at 48 hours.

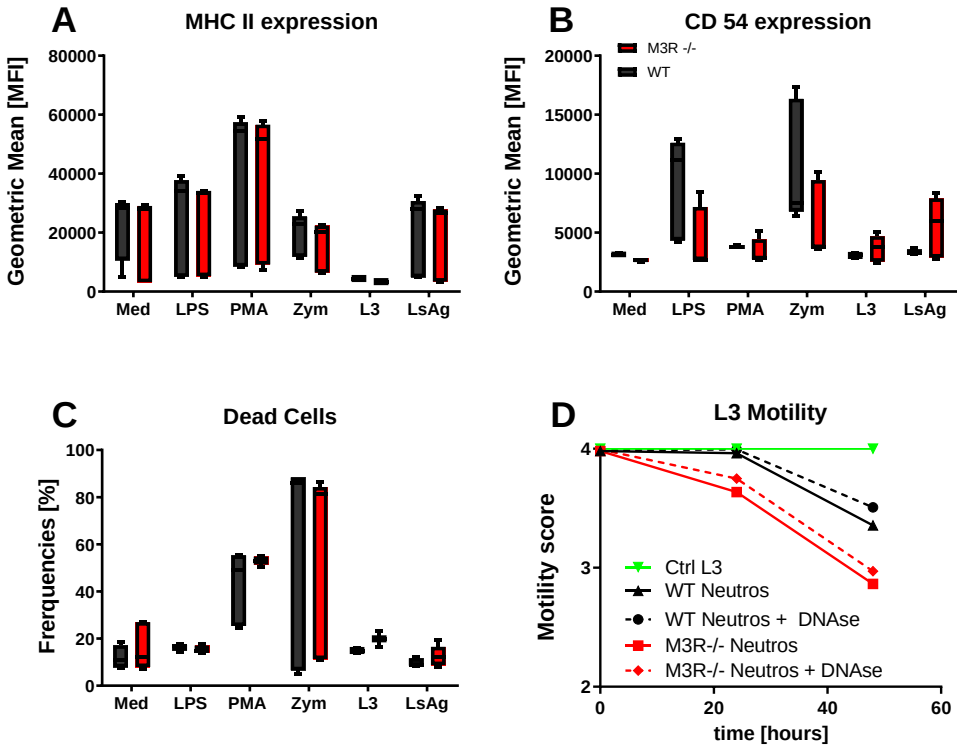

Figure 36: *In vitro* larval motility is impaired by co-cultured neutrophils generated from M3R$^{-/-}$ mice. Neutrophils were isolated from bone marrow of WT and M3R$^{-/-}$ mice and stimulated with LPS, LsAg, PMA and Zymosan or left untreated. After 6 hours the activation status of stimulated neutrophils was measured by flow cytometry, showing MCHII expression (A), CD54 expression (B) and frequencies of dead neutrophils (C). Neutrophils from WT and M3R$^{-/-}$ were co-cultured *in vitro* with isolated L3 larvae and motility was determined for 2 days (D) by using a motility score from 0 meaning no movement to 4, rapid and continuous movement. Statistical significance was analysed by two-tailed non-parametric Mann-Whitney-U-test. *p<0.05, **p<0.01. Data represented are two experiments pooled with cells from 5 mice per group are shown.

Based on those results, bmd neutrophils from M3R$^{-/-}$ mice inhibited larval motility more effectively *in vitro* than bmd neutrophils from WT mice. Given that neutrophils infiltrated the site of infection within the skin of M3R$^{-/-}$ mice successfully and are able to inhibit L3 motility *in vitro*, these data indicate that differences in neutrophil recruitment and function are probably not the cause for the observed differences in the worm burden of M3R$^{-/-}$ mice.

3.8 Vascular permeability and whole blood *in vitro* assay

M3R$^{-/-}$ mice showed a reduced neutrophil and eosinophil activation after intradermal L3 injection compared to WT mice. However, bmd neutrophils from M3R$^{-/-}$ mice induced a stronger inhibition of L3 motility *in vitro* compared to neutrophils from WT mice, which does not explain the higher worm recovery in M3R$^{-/-}$ animals. Therefore, it was suggested that vascular permeability might be affected in M3R$^{-/-}$ mice, which would facilitate larval migration (62). A whole blood assay was performed to investigate basophil activation, as basophiles are the main cell type in the peripheral blood releasing histamine, which could increase vascular permeability. Basophil activation was determined by measuring expression of CD200R after stimulation with different concentrations of anti-FcεR and LsAg (166). Ionomycin was used as a positive control. WT and M3R$^{-/-}$ mice possessed similar frequencies of CD200R positive basophils when left unstimulated (WT = ~12.2 %; KO = 11.35 %; Fig.37A). Stimulation with concentrations ranging from 0.4 to 6.25 µg/mL of anti-FcεR induced higher frequencies of CD200R positive, activated basophils in WT mice compared to M3R$^{-/-}$ mice (1.6 µg/mL: WT = ~38 %; KO = ~12 %). Similarly, LsAg concentrations of 0.2 and 2 µg/mL induced CD200R expressing basophils (0.2 µg/mL: WT = ~24 %; KO = ~17.45 %; 2 µg/mL: WT = ~30 %; KO = ~17.4 %, respectively), showing higher frequencies in WT mice compared to M3R$^{-/-}$ mice. Ionomycin was used as a positive control and induced about 41 % CD200R expressing basophils in WT mice compared to 18 % in M3R$^{-/-}$ mice (Fig.37B). Furthermore, histamine release was measured via ELISA after 30 minutes after iv injection of L3 in WT and M3R$^{-/-}$ mice (Fig.37C). In accordance, with the lower activation of basophils after *in vitro* stimulation, the histamine release after iv infection was significantly lower in M3R$^{-/-}$ mice compared to WT mice (WT= 1.565 ng/mL; KO= 1.553 ng/mL).

Although, the lower basophil activation and histamine release contradict the theory of a higher vascular permeability, a vascular permeability assay was performed to generate direct proof. Therefore, PBS and LsAg were injected into the left and right ear of a mouse, respectively. After 3 minutes, Evans blue was injected iv and 10 minutes later the ears were cut to investigate leakage of Evans blue in the tissue. LsAg injection led to a higher leakage of Evans blue in the WT and M3R$^{-/-}$ mice (Fig.37D). Interestingly, M3R$^{-/-}$ mice showed a significantly higher vascular permeability after LsAg injection compared to PBS control ($p = 0.0025$; KO PBS = ~0.012 OD; KO LsAg = ~0.036 OD). Importantly, the optical density after LsAg injection was significantly higher in M3R$^{-/-}$ mice compared to WT mice

(p = 0.0404; WT LsAg= ~0.019 OD; KO LsAg = ~0.026 OD), indicating a higher vascular permeability in M3R$^{-/-}$ mice.

In summary, M3R$^{-/-}$ mice showed a reduced *in vivo* basophil activation accompanied by a lower histamine release compared to WT mice, but possessed a significantly higher vascular permeability that might facilitate L3 larval migration to the thoracic cavity that may lead to the observed increased worm burden in the M3R$^{-/-}$ mice.

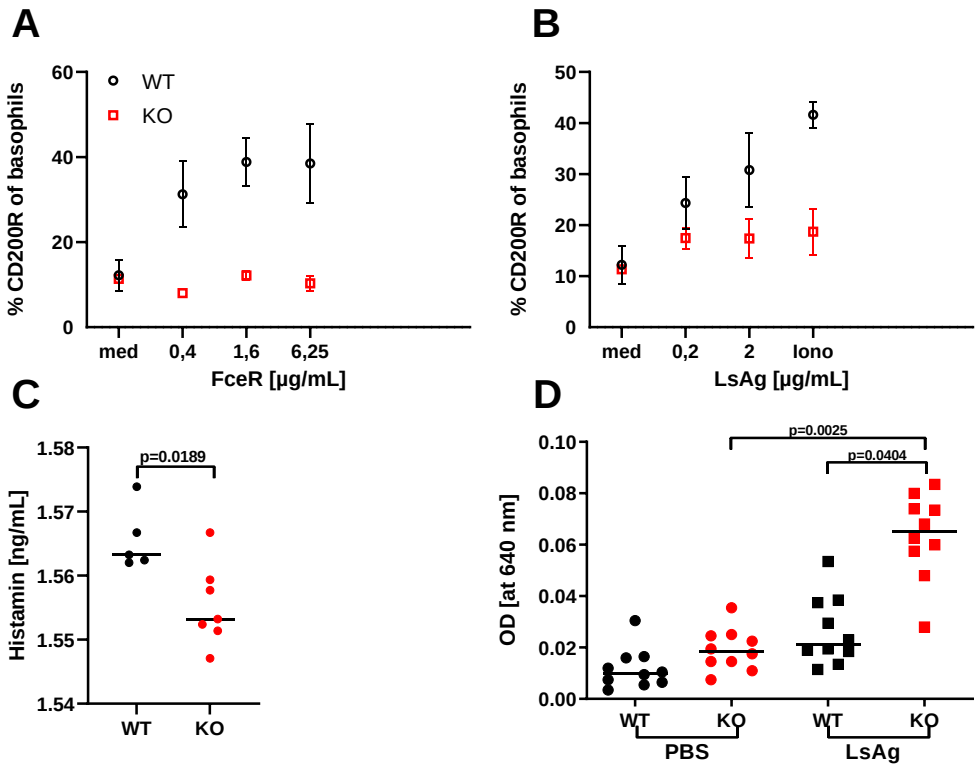

Figure 37. M3R$^{-/-}$ mice possess higher vascular permeability despite lower basophil activation. Basophil activation is displayed by CD200R expression after whole blood stimulation with different concentrations of FcεR (A) and LsAg (B). Histamine release (C) in the blood of infected animals 30 minutes after iv infection with 40 L3 Larvae. Vascular permeability (D) was determined by injecting 10 µg LsAg oder PBS intradermally in the ear, after 3 minutes Evans blue was injected intravenously. After 10 minutes ears were added into formamide for 48 hours at 56°C and leakage of evens blue was determined by measuring OD at 620nm. Data represented is pooled from two independent experiments with n=5 mice per group. Statistical significance was analysed by Kruskal-Wallis followed by Dunn's post hoc test: p<0.05, **p<0.01.

3.9 Migration kinetics during natural *L. sigmodontis* infection

As the previous experiments using natural infection were not infected with the same batch of mites due to limitations of the M3R$^{-/-}$ mouse numbers, a natural infection kinetic was performed. Here, all mice were naturally infected using the same batch of mites. The worm burden and cellular composition of the thoracic cavity was analysed at 7, 9, 12 and 15 dpi. At 7 dpi WT and M3R$^{-/-}$ mice possessed equal numbers of worms in the thoracic cavity (WT = ~21 worms; KO = ~22 worms; Fig.38A). Worm recovery at 9 dpi resulted by trend in

lower numbers in the M3R$^{-/-}$ mice compared to WT mice (WT = ~70 worms; KO = ~57 worms), confirming our previous results. At 12 dpi worm recovery was still by trend lower in M3R$^{-/-}$ mice compared to WT mice (WT = ~25 worms; KO = ~12 worms). At 15 dpi, worm recovery increased in the M3R$^{-/-}$ mice and was significantly higher compared to WT mice (p = 0.0079; WT = ~33 worms; KO = ~97 worms). While the high worm burden in WT mice and M3R$^{-/-}$ mice at 9 dpi seems to be an outlier, the overall worm recovery data from this experiment indicates that in M3R$^{-/-}$ mice there is a delayed migration of L3 leading to an increased worm burden by 15 dpi, whereas in WT animals the majority of L3 larvae reached the thoracic cavity by 7 dpi, which is in line with the literature (42, 43). The cell numbers of the thoracic cavity increased with infection time and M3R$^{-/-}$ mice had lower numbers at 9 (WT = ~1.98x10^7 cells; KO = ~1.00x10^7 cells) and 12 dpi (WT = ~1.48x10^7 cells; KO= ~4.05x10^6 cells) compared to WT mice but comparable numbers at 15 dpi (WT = ~1.51x10^7 cells; KO = ~1.72x10^7 cells, Fig.38B).

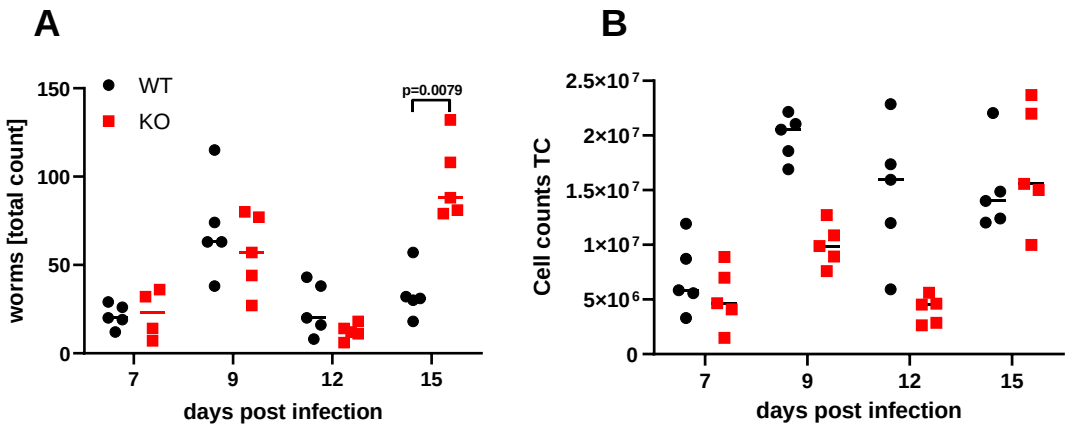

Figure 38. Migration kinetic during natural *L. sigmodontis* infection. Worm burden (A) and total cell numbers (B) were determined within the thoracic cavity at 7, 9, 12 and 15 dpi. Data represented is one experiment with 5 mice per group. Statistical significance was analysed by two-tailed Mann-Whitney t-test: p<0.05, **p<0.01.

The cellular composition of the thoracic cavity revealed lower numbers of myeloid and lymphoid cells at 7, 9 and 12 dpi in infected M3R$^{-/-}$ mice compared to WT mice (Fig.39A-C), which is in line with the in general lower numbers of thoracic cavity cells. Eosinophils (9 dpi: WT = 8.29 x 10^6 cells, KO = 2.69 x 10^6 cells; 12 dpi: WT = 3.80 x 10^6 cells, KO = 4.52 x 10^5 cells) and B cells (9 dpi: WT = 6.13 x 10^6 cells, KO = 3.35 x 10^6 cells; 12 dpi: WT = 5.60 x 10^6 cells, KO = 2.24 x 10^6 cells) were significantly reduced at 9 and 12 dpi in M3R$^{-/-}$ mice compared to WT mice (Fig.39C-F). In addition, neutrophils were reduced by trend at 9 dpi (WT = 9.71 x 10^4 cells, KO = 6.00 x 10^4 cells, Fig.39C) and 12 dpi (WT = 2.27 x 10^4 cells, KO = 4.04 x 10^3 cells, Fig.39E), while CD4$^+$ T cells

(WT = 5.98 x 10^5 cells, KO = 5.18 x 10^5 cells) and $CD8^+$ T cells (WT = 3.52 x 10^5 cells, KO = 2.20 x 10^5 cells, Fig.39D) were comparable at 9 dpi but significantly lower at 12 dpi ($CD4^+$: WT = 7.69 x 10^5 cells, KO = 1.62 x 10^5 cells; $CD8^+$: WT = 2.87 x 10^5 cells, KO = 3.61 x 10^4 cells, Fig.39F). Although, T cell numbers were not consistent with the previous experiments, the kinetic experiment confirmed the reduction of eosinophils, neutrophils and B cells at 9 dpi.

At 15 dpi, cell numbers increased in the $M3R^{-/-}$ mice, so that WT and $M3R^{-/-}$ mice possessed equal numbers of macrophages (WT = ~2.09 x 10^6 cells; KO = ~2.21 x 10^6 cells) and eosinophils (WT = ~5.2 x 10^6 cells; KO = ~7.45 x 10^6 cells), but by trend higher numbers of neutrophils (WT = ~9.71 x 10^3 cells; KO = ~1.42 x 10^4 cells, Fig.39G). However, $CD4^+$ T cell (WT = ~1.40 x 10^6 cells; KO = ~5.80 x 10^5 cells) and $CD8^+$ T cell numbers (WT = 3.93 x 10^5 cells; KO = ~9.32 x 10^4 cells) were significantly reduced in $M3R^{-/-}$ mice compared to WT mice (Fig.39H), which confirms our previous data. B cell numbers were comparable (WT = ~4.48 x 10^6 cells; KO = ~4.78 x 10^6 cells, Fig.39H) between both groups at 15 dpi. Overall, the migration kinetics experiment confirmed that at the onset of infection, migration of L3 larvae is delayed in $M3R^{-/-}$ mice compared to WT mice. This is accompanied by a reduced number of eosinophils, neutrophils, $CD4^+$ T cells and $CD8^+$ T cells as well as B cells in the thoracic cavity of $M3R^{-/-}$ mice. Thus, the reduction of $CD4^+$ T cells and $CD8^+$ T cells in the thoracic cavity of infected $M3R^{-/-}$ mice compared to WT mice at 15 dpi was confirmed as shown in table 5.

Therefore, we conclude that there is a delayed migration of L3 Larvae in the thoracic cavity accompanied by a delayed infiltration of immune cells to the site of infection in $M3R^{-/-}$ mice. Especially, numbers of $CD4^+$ and $CD8^+$ T cells as well as eosinophils and neutrophils were reduced in the thoracic cavity of $M3R^{-/-}$ mice compared to WT mice during early infection. We further observed that L3 larvae reached the thoracic cavity at around 15 dpi and $M3R^{-/-}$ mice possessed a higher worm recovery than WT mice, which might be due to a higher vascular permeability and a minor granulocyte activation in the skin.

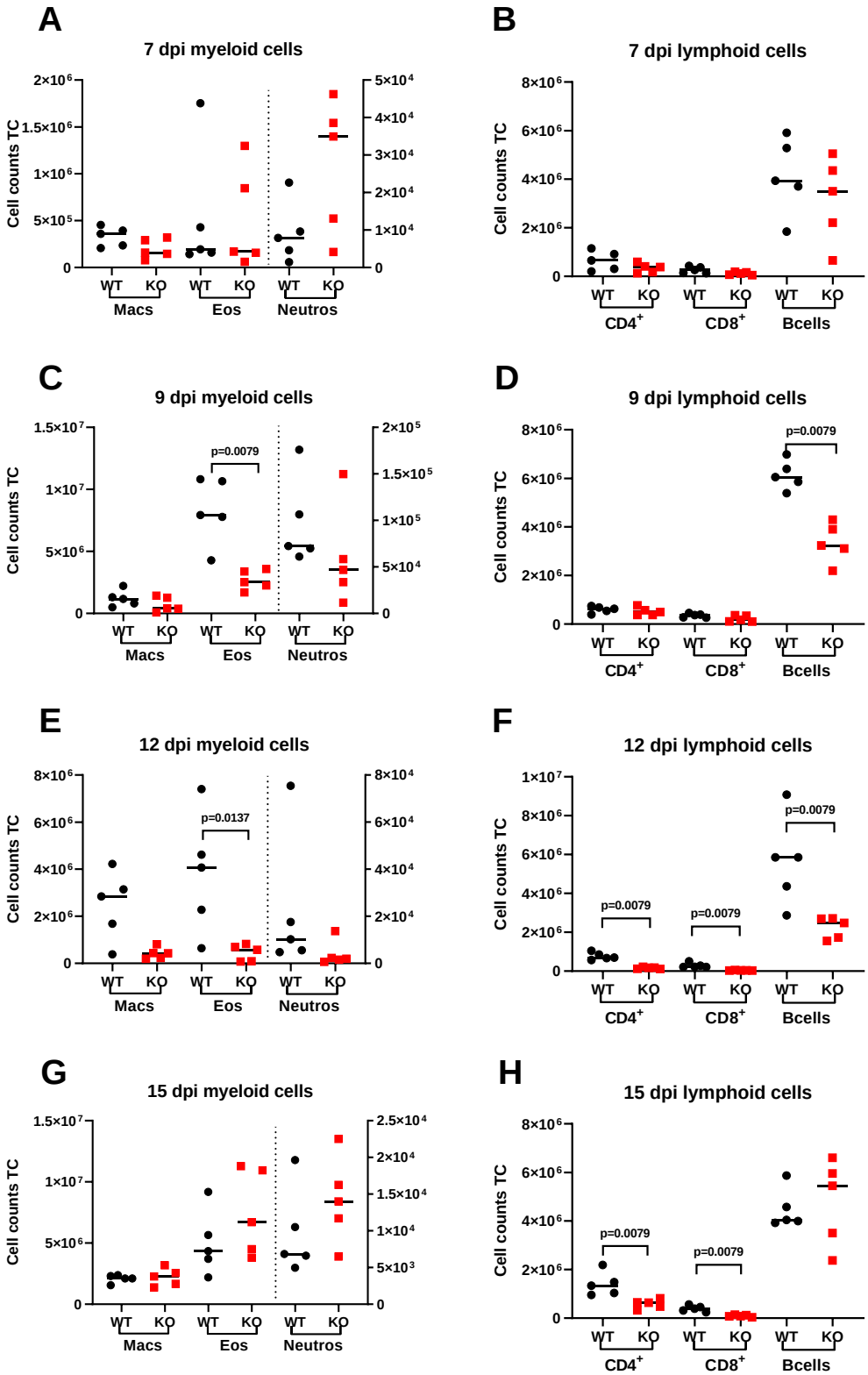

Figure 39. Cellular composition of the thoracic cavity during different time points of natural *L. sigmodontis* infection. Total cell counts of macrophages (Macs), eosinophils (Eos), and neutrophils (Neutros) (A, C, E, G) as well as $CD4^+$ and $CD8^+$ T cells and B cells (B, D, F, H) in the thoracic cavity lavage (TC) at 7 (A,B), 9 (C,D), 12 (E,F) and 15 (G, H) days of natural *L. sigmodontis* infection. Data represented is one experiment with 5 mice per group. Statistical significance was analysed using two-tailed Mann-Whitney t-test: $p<0.05$, $^{**}p<0.01$.

4. Discussion

Helminth infections are widespread in tropical and subtropical areas of the world. Due to the debilitating symptoms, infected persons are socially stigmatised and sometimes no longer physically able to pursue their profession. On the other hand, helminths modulate the immune response of the host to survive and these modulations have also positive attributes for example, they can protect against allergies (49, 167) and autoimmune diseases such as diabetes mellitus (98, 105, 168) and rheumatoid arthritis (104). The protective effect of helminth modulation is particularly characterised by the induced type 2 immune response (48, 49, 169, 170), as well as the regulatory, anti-inflammatory T cell response and TGF-ß or IL-10 release (67, 105, 171). Recently, there is an increased interest to investigate the cooperation between the nervous system and the immune system (111, 118) as it has already been shown that the nervous system and the immune system work together. This immune-nervous co-ordination is achieved by the release of different neurological peptides in the periphery such as substance P, CGRP (116) and the neurotransmitter ACh (142, 172, 173), cytokines and hormones (norepinephrine and epinephrine) as well as direct influence by the vagal nerve (111, 117). Additionally, it was already shown that immune cells themselves like T cells and B cells as well as NK cells and macrophages can produce and react to ACh via nAChRs or mAChRs (149, 173, 174). Further, it was shown that ACh signalling through the m3AChR is necessary for proper clearance of bacteria and intestinal helminth infection with *N. brasiliensis* (156). Therefore, the aim of this thesis was to investigate the influence of ACh signalling during a helminth infection with *L. sigmodontis* in order to better understand the immune response and possibly discover targets for treatment.

4.1 ChAt expression during natural *L. sigmodontis* infection

Firstly, ChAt reporter mice were infected with *L. sigmodontis* to analyse if immune cells produce ACh during infection. In naïve mice there was a small portion of immune cells present in the fluid of the thoracic cavity, which mainly comprise macrophages, T and B cells, NK cells and few dendritic cells (46). Natural infection with *L. sigmodontis* of ChAt reporter mice revealed a cellular increase of immune cells within the thoracic cavity of infected animals at 35 dpi. Especially, myeloid and lymphoid cells as macrophages, eosinophils, neutrophils, $CD4^+$ and $CD8^+$ T as well as B cells were increased at 35 dpi, which is in line with previous reports (46, 70). It has already been described that neutrophils are the first line of defence against helminths infection within the skin where they attack L3 larvae (59, 61). Furthermore, they are important for granuloma formation and necessary for adult worm

elimination within the thoracic cavity (76, 175). Similarly, eosinophils start infiltrating the thoracic cavity around 9 dpi and are able to target MF, L3 and adult worms (176) by releasing toxic proteins like MBP, MPO (74) or by extracellular trap formation (75). Accordingly, mice lacking IL-4R/IL-5 have an impaired maturation of eosinophils and mice lacking eosinophils (dblGATA), possess a higher worm burden and MF load than the susceptible BALB/c mice (163, 177).

All myeloid cells (macrophages, eosinophils and neutrophils) analysed in the thoracic cavity showed a baseline expression of ChAt in naïve mice (see 3.1 table 1). At 35 dpi, neutrophils showed an increased ChAt expression while eosinophilic ChAt expression was rather reduced. Although, the expression of ChAt by neutrophils is not published yet, the ability of neutrophils to respond to ACh via m3AChR has been described (178).

ACh signalling through m3AChR is important to induce neutrophil extracellular trap formation in levamisole-induced autoimmunity (178). Since neutrophils are largely responsible for the elimination of L3 larvae in the skin, which is also partly caused by NETosis, this might also be induced by ACh signalling (178, 179). Furthermore, ChAt expression of macrophages was observed in infected and non-infected animals at comparable levels, and confirmed by PCR (see 3.1, figure 3). The ability of macrophages to produce ACh has already been published (174).

Additionally, T cells are important during helminth infection as they are primed to differentiate into Th2 cells and are essential for worm clearance (46, 89, 180). Therefore, an increase of these cell types during infection with *L. sigmodontis* in the thoracic cavity was expected. Interestingly, increased ACh production by $CD4^+$ T cells and $CD8^+$ T cells in the thoracic cavity started already at 5 dpi, immediately after the L3 larvae reached the thoracic cavity (see 3.1, Fig.1). ACh production of $CD8^+$ T cells and B cells peaked at 35 dpi, the time when elimination of young adult worms starts in C57BL/6 mice (44, 180), while $CD4^+$ T cells stopped ACh production at that time point. It is already known that T cells and B cells are in general able to produce ACh, e.g. during bacterial infections (118) and infection with the intestinal helminth *N. brasiliensis* (156). Thus, these results confirm the ability of $CD4^+$ T cells and $CD8^+$ T cells (121) and B cells (142, 181) to produce ACh (174) and suggest that ACh signalling might be required to control infection with *L. sigmodontis* as ACh is increasingly produced during a time point when worm clearance starts.

Looking at the systemic immune response in the spleen, we observed an increase in macrophage numbers, especially on day 35 of the infection. In contrast, neutrophils were reduced and eosinophil frequencies showed no difference (see 3.1). However, these myeloid cells in the spleen showed a comparable ChAt expression compared to non-infected animals. In contrast, $CD8^+$ T cells and B cells increased significantly at 35 dpi while $CD4^+$ T cell frequencies rather declined. However, ChAt expression of $CD8^+$ T cells and B cells was comparable to uninfected animals in the spleen, whereas ChAt expression of $CD4^+$ T cells increased in the spleen at 35 dpi indicating a local impact of ACh signalling in the thoracic cavity for myeloid cell populations, but a systemic influence for $CD4^+$ T cells. The vagal nerve triggers ACh production by T cells via epinephrine release within the spleen after recognition of inflammatory processes to dampen pro-inflammatory responses by macrophages (111). Macrophages play an important role during helminth infection as AAMΦ impede $CD4^+$ T cell proliferation in murine filarial infections, although no direct impact on worm killing was observed (78, 182, 183). AAMΦ are also crucial for maintaining Th2 dominated anti-inflammatory responses and are dependent on IL-10 during schistosomiasis (79). The induction of AAMΦ during *L. sigmodontis* infection is dependent on $CD4^+$ T cells and TGF-β (182). Furthermore, ACh signalling through α7-nAChR leads to a reduction of pro-inflammatory cytokines (TNF, IL-6) and antigen-specific antibody release (174). Therefore, ACh released by T cells in the spleen and thoracic cavity might modulate the pro-inflammatory cytokine release by macrophages and affect other immune cells as well during infection with *L. sigmodontis*, thus inducing Th2- dominated immune response.

4.2 Influences of cholinergic signalling during *L. sigmodontis* infection in BALB/c mice

Since we observed that macrophages, $CD4^+$ and $CD8^+$ T cells as well as B cells release ACh during *L. sigmodontis* infection at the site of infection and in the spleen at crucial infection time points, we proceeded to investigate the immune response to infection while blocking ACh signalling. To investigate if ACh signalling affects the immune response to *L. sigmodontis*, BALB/c mice were infected naturally and treated either with AB or vehicle as control prior to infection and the four following days to block mAChRs. AB binds to mAChRs, but it has a higher affinity to the m3AChR, as the binding here lasts longer than to the other mAChRs (184). This effect was desired because m3AChR is expressed in lung tissue and on immune cells, both of which play an important role during *L. sigmodontis* infection (185). Interestingly, we observed a higher worm recovery in mice where cholinergic

signalling was inhibited (see 3.2.1). The higher worm recovery was accompanied by a trend to an increased infiltration of immune cells in the thoracic cavity, especially higher numbers of neutrophils and eosinophils at 9 dpi compared to untreated control mice. This increased number of immune cells might be due to the higher worm burden. Accordingly, it was shown that $RAG^{-/-}$ mice, which lack T cells and B cells, possess a higher worm burden that is accompanied by slightly increased numbers of immune cells, especially neutrophils compared to C57BL/6 control mice (186).

As ACh signalling was inhibited for the duration of L3 migration (up to 5dpi) to the thoracic cavity (43, 59) and there were no significant differences found in individual cell populations in the thoracic cavity when ACh signalling was blocked that may explain the differences in worm burden, we next infected animals intravenously to bypass the skin barrier and migration through the lymphatic system. After bypassing the skin and lymphatic system by iv infection with a defined number of L3 larvae, there was no increase in worm recovery (Fig.5). Furthermore, the immune cell populations in the thoracic cavity did not show significant differences. Thus, either the immune response in the skin or the migration through the vascular vessels was influenced by the inhibition of the cholinergic signalling. Several studies have already shown, that immune responses in the skin play an important role in the initial elimination of L3 larvae (58, 60) and vascular permeability facilitates L3 larval migration (62). Therefore, we first investigated the effect of AB treatment on the vascular permeability. Animals were treated with AB or vehicle, subsequently intradermally injected with LsAg and PBS into the left and right ear, respectively. After intravenous application of Evans Blue, vascular permeability could be visualized (187). Although, LsAg treatment resulted in an increased vasodilation, there was no difference in AB-treated and untreated animals. Thus, the blocking of ACh signalling by AB did not affect vascular permeability.

Next, to assess the impact of ACh signalling inhibition on skin immune responses, animals were treated with AB or vehicle and then infected intradermally with 10 L3 larvae. After 3 hours, the infected skin areal was removed, the immune cells were extracted and examined by flow cytometry (58). We observed that L3 injection led to an increased infiltration of neutrophils to the skin in both AB-treated and vehicle control mice. Neutrophil infiltration to the site of L3 injection was in line with the results from previous studies (46, 59). Interestingly, AB-treated mice showed a reduced neutrophil activation (MHCII, CD86, CD54) within the skin compared to untreated mice indicating that an impaired ACh signalling might impair neutrophil activation within the skin of infected animals. However, it must be

noted that neutrophil activation was generally lower in infected animals than in naïve animals. This was unexpected, as neutrophils were previously reported to be recruited and activated in the skin after L3 injection (58, 59). This discrepancy is likely due to differences in the timing between injection and removal of the treated skin, which was 3 hours in this study. According to the literature, ACh stimulation through mAChRs induces the release of chemotactic substances, which leads to the recruitment of neutrophils (158, 160, 188). Therefore, it would have been expected that a reduced recruitment of neutrophils occurs after inhibition of ACh signalling, but in the experiments presented in this thesis, the frequencies of neutrophils were comparable in AB-treated and untreated animals. This might be again explained by the experimental design and the chosen 3h time point after infection. Alternatively, the intranasal application of the inhibitor may predominantly act in the lung tissue and the systemic effect to the infected skin areal, which was at the upper hind leg regions, might be less prominent.

In summary, we observed that inhibition of cholinergic signalling leads to a higher susceptibility to *L. sigmodontis*, which was accompanied by increased immune cell infiltration to the site of infection. However, the improved survival of L3 larvae was not associated with an altered vascular permeability but rather with a reduced neutrophil activity (MHCII, CD54, CD86) in the skin after intradermal infection. Thus, bypassing the skin barrier by intravenous infection with L3 larvae reversed the increased worm recovery of AB-treated mice compared to untreated mice.

4.3 Lack of muscarinic type 3 receptor signalling during natural *L. sigmodontis* infection

The mAChR inhibitor AB blocks the m3AChR but also binds briefly to all other mAChRs (162). To confirm the data obtained with the AB inhibitor, additional experiments in M3R-deficient mice during natural *L. sigmodontis* infection were performed. First, the worm burden in WT and $M3R^{-/-}$ mice at different infection time points was examined, when the larvae/worms undergo important developmental stages. At 9 dpi, when all L3 larvae should have reached the thoracic cavity (43), the $M3R^{-/-}$ mice displayed a reduced worm burden compared to WT mice. This was surprising as we initially observed a higher worm recovery in mice treated with AB. This discrepancy may be due to the fact that AB does not exclusively bind to m3AChR, although the binding of AB to m3AChR lasts the longest compared to the other mAChRs (162). In addition, AB has an elimination half-life of 2 to 3 hours and is rapidly transformed into ineffective metabolites in human plasma, but its local effect should last 24 hours (162, 189). This has the advantage that severe systemic side effects

are reduced as the systemic bioavailability is less than 5 % (162). Therefore, it might be that AB acts locally in the lung and has only a short systemic effect, whereas M3R$^{-/-}$ mice show a consistently systemic blockade of M3R signalling that might explain the different outcomes at 9 dpi. However, M3R$^{-/-}$ mice showed an increased worm recovery after 15 and 37 dpi compared to WT mice (Fig.7); which is in agreement with the results from the experiments with AB-treated animals. Furthermore, it is in line with the results obtained for the intestinal nematode *N. brasiliensis*, which was expelled to a lesser degree in M3R$^{-/-}$ mice (156). Accordingly, it appears that ACh signalling via the m3AChR has an impact on both intestinal and tissue dwelling helminth and both have a similar larval migration process.

In addition, the length of the female adult worms was shorter at 37 dpi in the M3R$^{-/-}$ mice compared to the WT mice while male worms showed no differences in length between both groups. On the one hand, this could be associated with a lack of space due to the increased number of worms in the thoracic cavity of M3R$^{-/-}$ mice, or the development of worms could be impaired. In addition, there were more female worms than male worms in both infected mouse groups, representing sexual dimorphism. It was already shown that female worms represent the dominant sex during *L. sigmodontis* infection (~70%) (34, 190). On day 70, when the adult worms already started to produce MFs, there was no difference in worm load or development of MF^{+} and MF^{-} individuals between both groups. In addition, the length of the female adult worms of the M3R$^{-/-}$ mice has also adapted and no longer showed any significant difference to the female adult worms of the WT mice. However, the number of MFs in the blood increased from 58 dpi to 70 dpi and was elevated by trend in the M3R$^{-/-}$ mice compared to WT mice (Fig.17). Given that the M3R$^{-/-}$ mice had an increased number of adult worms, the slightly higher numbers of MFs in the blood might be due to an increased number of female worms in the M3R$^{-/-}$ mice. Embryogenesis in the individual experiments at this point showed exactly the opposing trends in WT and M3R$^{-/-}$ animals as far as embryonic development is concerned and therefore cannot influence the MF release. However, the spleen is essential for the elimination of MF (82) and showed increased numbers of eosinophils, CD4^{+} and CD8^{+} T cells at 37 and 70 dpi in M3R$^{-/-}$ mice (table 6).

Next, we examined the immune cell populations during the different infection time points in different tissues like BAL, thoracic cavity, spleen and lung. At 9 dpi M3R$^{-/-}$ mice revealed reduced numbers of eosinophils, neutrophils, CD4^{+} T cells and CD8^{+} T cells within the thoracic cavity compared to WT mice, which was in line with the lower worm burden at that time point. In contrast, increased levels of CXCL-5 and IL-5 were measured in the thoracic

cavity of infected M3R$^{-/-}$ mice compared to WT mice at 9 dpi (Fig.21). The increased secretion of CXCL-5 and IL-5 may be due to the later arrival of L3 larvae in the thoracic cavity of M3R$^{-/-}$ mice and subsequently lead to a delayed recruitment of eosinophils and neutrophils (191-193). In contrast, MPO was reduced in the thoracic cavity of infected M3R$^{-/-}$ mice compared to WT mice at 9 dpi. MPO is mainly released by neutrophils (194) and induces reactive oxygen species for pathogen elimination (195) and is additionally involved in neutrophil extracellular trap formation (196). Thus, its reduction might be associated with the lower neutrophil numbers in M3R$^{-/-}$ mice.

In the further course of infection, no differences in neutrophil and eosinophil numbers in the thoracic cavity were detected on day 15. At this time, the levels of secreted CXCL-5 and elastase were comparable in WT and M3R$^{-/-}$ mice (Fig.14), while IL-5 levels were below the detection limit of the ELISA. However, the cell numbers of CD4^{+} T cells and CD8^{+} T cells in the thoracic cavity were still lower in the M3R$^{-/-}$ mice compared to WT mice. By 37 dpi macrophage, eosinophil and CD4^{+} T cell numbers increased in M3R$^{-/-}$ mice compared to WT mice, while neutrophils were reduced in the thoracic cavity (Fig.17). This might indicate that the immune response is delayed in M3R$^{-/-}$ mice and just now starts to target the worms, as cell populations that are needed for proper worm clearance increase (44, 48, 163, 177). Additionally, this may explain why there was no difference in the adult worm burden at the late time point (70 dpi). The measured cytokine levels in the thoracic cavity of IL-5 and IFN-γ, as indicators of type 2 and type 1 immune responses, respectively, were comparable between WT and M3R$^{-/-}$ mice (Fig.28). Besides, it was shown that IL-5 is essential for proper worm elimination in mice and a lack of IL-5 leads to reduced recruitment of neutrophils and eosinophils (163, 197, 198). However, MIP-2 and IL-5 levels in the BAL were by trend lower in M3R$^{-/-}$ mice than in WT mice, which might be related to the lower neutrophil numbers in those animals as MIP-2 is released by neutrophils at the site of infection and can recruit them (199). Previous studies already showed a relation of increased MIP-2 levels and higher neutrophil accumulation during *L. sigmodontis* infection in S100A8/S100A9-deficient mice (59). In contrast, Eotaxin 1 and 2 as well as elastase levels were increased in the thoracic cavity of M3R$^{-/-}$ mice compared to WT mice. Although neutrophil numbers were reduced, the elastase levels were increased in the M3R$^{-/-}$ mice, which is surprising as elastase is released by neutrophils and can drive extracellular trap formation against invading pathogens (59, 200). One explanation might be that neutrophils are reduced in the M3R$^{-/-}$ mice but are more activated than in the WT mice, although we did not measure activation parameters here and activation of neutrophils in the skin after intradermal infection was reduced. The increased

Eotaxin levels in the thoracic cavity of M3R$^{-/-}$ are consistent with the increased eosinophil counts and it was already shown that Eotoxin is crucial for parasite clearance (193, 201).

Regarding the patent infection at 70 dpi eosinophils, CD4^{+} T cell and CD8^{+} T cell numbers were slightly increased within the thoracic cavity of M3R$^{-/-}$ mice compared to WT mice (table 6). The cytokine levels in the thoracic cavity of IL-5, Eotaxin 1 and MIP-2 were comparable in both mouse strains at day 70. Thus, the immune response in the M3R$^{-/-}$ mice seems to have caught up and is at a similar level as in the WT mice.

These data indicate a delayed immune response within the thoracic cavity, the site of infection, in the M3R$^{-/-}$ mice that initially leads to a higher worm recovery at early time points but in the end to a similar clearance of the adult worms at 70 dpi.

4.4 Different infection routs of *L. sigmodontis* in M3R$^{-/-}$ mice

Even though we observed a delayed immune response indicated by a reduction of neutrophils, CD4^{+} T cells and CD8^{+} T cells in the thoracic cavity and spleen during natural infection in M3R$^{-/-}$ mice, this does not explain the higher susceptibility of M3R$^{-/-}$ mice persuasively. Therefore, the animals were infected intravenously with a defined number of L3 larvae to bypass the skin barrier and the lymphatic system, two body compartments that play an important role in the immune response against infiltrating L3 larvae (59, 62, 68). We investigated the worm recovery at 9 dpi, because it was previously shown that after 8 days following intravenous infection all larvae reached the thoracic cavity (43). Interestingly, iv infection abolished the reduced worm recovery in M3R$^{-/-}$ mice compared to WT mice (Fig.21). In addition, the cell numbers within BAL, thoracic cavity, spleen and lung were comparable between both groups. Similarly to the natural infection with *L. sigmodontis*, M3R$^{-/-}$ mice possessed lower numbers of eosinophils, CD4^{+} and CD8^{+} T cells as well as B cells (table 7). In contrast, macrophages were slightly elevated in frequencies in the thoracic cavity after iv infection in M3R$^{-/-}$ mice while the numbers were comparable between both groups during natural infection. In addition, neutrophil numbers were comparable as well after iv infection, whereas they were reduced in M3R$^{-/-}$ mice after natural infection. Furthermore, CD4^{+} and CD8^{+} T cells in the spleen were increased in M3R$^{-/-}$ compared to WT mice after iv infection while they were lower during natural infection. These changes in cell numbers between natural and iv infection further highlight a delayed immune response in the M3R$^{-/-}$ mice during natural infection that is associated with the delayed arrival of the L3 larvae in the thoracic cavity, but does not explain the higher worm recovery following natural infection.

Furthermore, ILC2s were reduced in the lung of M3R$^{-/-}$ mice compared to WT mice at 9 days post natural infection, but the same trend was observed after iv infection (Fig.23). ILC2s are induced by alarmins (damage-associated molecular patterns; DAMP) that might be triggered by tissue damage caused by migrating L3 larvae. Thus, increased ILC2s numbers can be found at several barrier organs during helminth infection and are crucial for maintenance of the Th2 dominated immune response (64, 108, 202). In addition, ILC2s produce ACh in response to helminth infection and stimulation of these cells increased type 2 cytokine release (140, 141). Interestingly, ILC2s increased during the course of infection showing an association with the higher numbers in M3R$^{-/-}$ mice than in WT mice at 37 dpi, but this still does not explain the delayed arrival of the larvae.

ILC1s and Lin^{+} mNK cells were reduced at 9 dpi in the lung of infected M3R$^{-/-}$ mice compared to WT mice independent of the infection route. Additionally, Lin^{+} mNK cells were reduced in the M3R$^{-/-}$ mice at each infection time point following natural infection compared to WT mice. Interestingly, Lin^{-} mNK cells were reduced in the M3R$^{-/-}$ mice following natural infection but comparable after intravenous infection at 9 dpi. NK cells do not only contribute to control *L. sigmodontis* infection (86), but are also producers of ACh, which can modulate infiltrating macrophages (203). Interestingly, M3R$^{-/-}$ and WT mice possessed comparable numbers of Lin^{-} mNK cells following iv infection but macrophage numbers in the thoracic cavity were increased in M3R$^{-/-}$ compared to WT mice, which was not seen after a natural infection. Although we did see minor changes on the cellular level between WT and M3R$^{-/-}$ mice following iv infection this does not explain the delayed but increased larval entry to the thoracic cavity in the M3R$^{-/-}$ mice following natural infection.

Subsequently, the cellular immune response in the skin was investigated, as the majority of the infiltrating L3 larvae are already eliminated during natural infection (68, 204). As expected, the L3 injection led to a recruitment of neutrophils (58-60) in both mouse types compared to the PBS control. The increase in neutrophil frequency was slightly more pronounced in the M3R$^{-/-}$ mice. Importantly, the activation state of neutrophils, as assessed by the expression of CD54 and CD86 on the neutrophils, was elevated upon L3 injection in the WT mice, but did not increase in the M3R$^{-/-}$ mice (Fig.25). The same was observed for eosinophil activation markers (MHCII, CD86) showing a significantly lower activation in the M3R$^{-/-}$ mice compared to WT mice. As both granulocytes are important for L3 clearance (52, 75, 205) the reduced activation of both cell types may impair the protective response against invading L3 larvae in the skin.

In order to investigate this further, the activity of neutrophils co-cultured with L3 larvae *in vitro* was analysed (Fig.26). Although, stimulation with LPS and Zymosan revealed a slightly lower expression of CD54 in neutrophils derived from $M3R^{-/-}$ mice, stimulation with LsAg and L3 larvae led to comparable CD54 expression in neutrophils from $M3R^{-/-}$ and WT mice. Interestingly, bmd neutrophils from $M3R^{-/-}$ mice showed a stronger inhibitory effect on larval motility than bmd neutrophils from WT mice. Furthermore, the minor differences on larval motility impairment when DNase was added might indicate that not DNA traps but granular proteins are sufficient for the inhibition of larval motility. Thus, neutrophils from $M3R^{-/-}$ mice seem to be less activated than neutrophils from WT mice but they do show an improved inhibition of L3 motility in the *in vitro* assays performed here. In addition, there were more neutophils recruited to the skin of $M3R^{-/-}$ following intradermal L3 injection than in WT mice, thus the L3 larvae are more likely to be held back so that less reach the thoracic cavity at 9 dpi. However, neutrophils were less activated and the relation changes afterwards as activated neutrophils die within 24 hours (206). Given that, the results from the *in vitro* L3 experiments did not explain the increased worm burden in the $M3R^{-/-}$ mice compared to WT mice, it was next suggested that the migration of the larvae through the lymphatics may be affected by an increased vascular permeability. To further investigate the aspects of vascular permeability, basophil activity was investigated, as they are the dominant producers of histamine in the peripheral blood and histamine induces vasodilation (62). The activation of basophils was determined by CD200R expression after stimulation with anti-FcεR and LsAg (166). In contrast to the expectations, both LsAg and anti-FcεR stimulation of blood cells from WT mice increased the frequencies of $CD200R^{+}$ basophils *in vitro* compared to $M3R^{-/-}$ mice (Fig.27) and histamine levels in the blood of infected WT mice was higher compared to $M3R^{-/-}$ mice. Despite the reduced histamine levels in the blood of $M3R^{-/-}$ mice and minor basophil activation compared to WT mice, the $M3R^{-/-}$ possessed an increased vascular permeability after LsAg injection compared to WT mice, which might facilitate larval migration. Given the drastically increased vascular permeability in $M3R^{-/-}$ mice, it was speculated if the increased vascular permeability might cause the L3 larvae to stray along its path to the thoracic cavity, thereby increasing the migration time. Therefore, migration kinetic experiments were performed and analysed at four different time points following natural infection to check when all L3 larvae have arrived in the thoracic cavity. The L3 larvae were counted at 7, 9, 12 and 15 dpi. Here we observed that the higher worm recovery in $M3R^{-/-}$ was detected earliest at 15 dpi. Based on these results, L3 migration was facilitated by a higher

vascular permeability in the $M3R^{-/-}$ mice, although the larval arrival in the thoracic cavity was delayed.

In summary, the results of this thesis demonstrate that ACh signalling via m3AChR is necessary for a proper control of filarial infection with *L. sigmodontis*. Lack of ACh signalling leads to a reduced granulocyte activation that may impair the local clearance of L3 in the skin. Increased vascular permeability in $M3R^{-/-}$ mice allows more L3 larvae to reach the thoracic cavity, although the migration is delayed. This delayed larval migration leads to a delayed immune response at the site of infection, which is compensated over time and leads to a comparable worm elimination at the late time points.

Complimentary projects

Complimentary project - 1 - Absence of the Aryl hydrocarbon receptor impairs protective immune responses and enhances vascular permeability during *Litomosoides sigmodontis* infection

Stefan J. Frohberger, **Anna-Lena Neumann,** Fabian Gondorf, Wiebke Stamminger, Jayagopi Surendar, Alexandra Ehrens, Achim Hoerauf, Irmgard Förster, Marc P. Hübner

Manuscript under preparation.

The aryl hydrocarbon receptor (AhR) is a transcription factor that belongs to the pattern recognition receptors (PRR) and in particular senses environmental changes. It is widely distributed in the immune system and secondary lymphatic organs. It is also found in immune cells and tissues that serve as a barrier to invading pathogens such as lung, intestine and skin tissue (207, 208). It has already been shown that within barrier organs innate lymphocytes play an important role in the initial immune response regulated by the AhR. AhR-deficient mice showed increased susceptibility to infection with bacteria such as *Listeria monocytogenes* and improved survival of pathogens (209-211). Since the skin is an important barrier organ during filarial infection and most L3 larvae are already killed there, the impact of AhR during the immune response against *L. sigmodontis* was investigated. The lack of AhR resulted in an increased worm burden at early infection time points (5 and 14 dpi) compared to WT controls, that was associated with and impaired immune response. The higher worm recovery was accompanied by decreased proportions of $CD4^{+}$ T cells, eosinophils, neutrophils and mast cells. In addition, the analysis of immune cells within the

skin after intradermal infection of filarial crude extract revealed lower frequencies of macrophages, monocytes, neutrophils and eosinophils as wells as reduced expression of activation markers (CD86 on macrophages, CD69 on neutrophils). These results indicate that AhR plays a pivotal role during the immune response against *L. sigmodontis*. In addition, AhR-deficient mice possessed an increased vascular permeability that was associated with higher histamine release and reduced CCL17 levels. Accordingly, when the natural infection route was bypassed by infecting the animals intravenously, WT and $AhR^{-/-}$ mice show no difference in worm burden anymore, indicating that differences in the vascular permeability may account for the higher worm burden in $AhR^{-/-}$ mice. In summary, AhR is important for early immune response against invading *L. sigmodontis* L3 larvae within the skin as its deficiency leads to an impaired immune response and enhances histamine release, which facilitates larval migration by increasing vascular permeability.

Complimentary project - 2 - ILC2s control microfilaremia during *Litomosoides sigmodontis* infection.

Julia J. Reichwald, **Anna-Lena Neumann**, Frederic Risch, Stefan J. Frohberger, Johanna F. Scheunemann, Alexandra Ehrens, Wiebke Strutz, Achim Hoerauf, Beatrix Schumak, Marc P. Hübner. Manuscript under preparation.

Innate lymphoid cells are a recently discovered cell population that play an important role in innate immune defence. Initial studies showed that ILCs are involved in the immune response to various different infectious diseases (212, 213). However, little is known about their role during filarial infections (214). To investigate the role of ILCs during filariasis, susceptible BALB/c WT mice and semi-susceptible C57BL/6 WT mice were infected naturally with *Litomosoides sigmodontis* and investigated at different infection time points. In contrast to BALB/c WT mice, C57BL/6 mice had significantly increased numbers of ILC2s in the thoracic cavity. In addition, elevated IL-5 levels were found that could be assigned to ILC2s, thus they exhibited a higher secretion of IL-5 than $CD4^{+}$ T cells. Furthermore, ILC2s and eosinophils were still the main sources of IL-5 in the absence of T cells, as seen in case of $Rag2^{-/-}$ C57BL/6 mice, which lack T and B lymphocytes and show an increased worm recovery compared to isotype controls. Importantly, depletion of ILC2s using an anti-CD90.2 antibody in these animals did not lead to a further increase in adult worm burden, but enhanced the MF load in the blood. In general, it was observed that ILC2s are not essential

for the immune response during the moulting of L4 to adult worms but control the MF load in absences of T and B cells in Rag2$^{-/-}$ C57BL/6 mice.

Complimentary project - 3 - S100A8/S100A9 deficiency increases neutrophil activation and protective immune responses against invading infective L3 larvae of the filarial nematode *Litomosoides sigmodontis*

Stefan J Frohberger, Frederic Fercoq, **Anna-Lena Neumann**, Jayagopi Surendar, Wiebke Stamminger, Alexandra Ehrens , Indulekha Karunakaran , Estelle Remion , Thomas Vogl, Achim Hoerauf , Coralie Martin, Marc P Hübner ; **PloS Neglected Tropical Diseases. 2020 Feburary 27;14(2):e0008119.**

As mentioned earlier, human pathogenic filariae are responsible for several devastating diseases such as LF and tissue filariasis. Using the rodent filariae *L. sigmodontis,* some important immunoregulatory processes during filarial infection have already been uncovered. Among others, it was shown that neutrophilic granulocytes have an important function in the protective immune response against migrating larvae of filariae. Therefore, we investigated the function of the heterodimer calprotectin (S100A8/S100A9) during infection with *L. sigmodontis*. Calprotectin is found in both monocytes and neutrophils and can exacerbate or reduce tissue damage depending on the environment. S100A8/A9-deficient mice were naturally infected with *L. sigmodontis* and showed a significantly lower worm burden than control animals after 12 dpi. Even bypassing the skin barrier by subcutaneous infection with a defined number of L3 larvae still resulted in a reduced worm burden in the S100A8/A9$^{-/-}$ mice compared to controls. Interestingly, intradermal injection of L3 larvae led to an increased recruitment of neutrophils, eosinophils and macrophages to the site of infection (skin) in S100A8/A9-deficient mice compared to controls. In addition, the lower worm burden in S100A8/A9$^{-/-}$ mice was accompanied by elevated levels of elastase, CXCL-1, CXCL-2 and CXCL-5. Furthermore, *in vitro* co-culture experiments of neutrophils and L3 larvae revealed higher activation of neutrophils from S100A8/A9$^{-/-}$ mice compared to neutrophils from WT animals. Also, motility of the L3 was more effectively impaired when co-cultured with neutrophils from S100A8/A9$^{-/-}$ mice. In further experiments, we showed that the protective effect by neutrophils in S100A8/A9$^{-/-}$ mice was attenuated when the neutrophils were depleted before infection and during the first 5 days after infection, indicated by an increased worm burden. However, we also observed that bypassing the skin and lymphatic system through

intravenous administration of the L3 larvae completely reversed the phenotype. Thus, there was a higher worm burden than in the WT mice. In conclusion, the experiments revealed that calprotectin increases neutrophil recruitment and activation and inhibits larval motility.

Complimentary project - 4 - Microfilariae Trigger Eosinophil Extracellular DNA Traps in a Dectin-1-Dependent Manner

Alexandra Ehrens , Benjamin Lenz , **Anna-Lena Neumann** , Samuela Giarrizzo , Julia Jennifer Reichwald , Stefan Julian Frohberger , Wiebke Stamminger , Benedikt Christian Buerfent , Frédéric Fercoq, Coralie Martin , Daniel Kulke , Achim Hoerauf , Marc Peter Hübner ; **Cell Reports. 2021 Janurary 12;34(2):108621**

Eosinophils present only a small percentage of the cells in our blood in healthy people (<5%). However, they are particularly elevated in the immune response to allergies and parasitic helminth diseases. They are effector cells recruited by Th2 immune activation (215). It was already shown by *in vitro* cultures that they have the capability to eliminate helminth larvae of *Schistosoma mansoni* (216) and *Trichinella sprialis* (217). In addition, it has already been shown that *L. sigmodontis* infection in mice lacking eosinophils leads to a significantly increased burden of MF and adult worms as well as prolonged survival of these (163). However, the exact function of how eosinophils attack helminths is not yet well understood. Therefore, in this study we performed in vitro co-cultures of MF and L3 larvae of *L. sigmodontis* with eosinophils to investigate this further. We showed that the motility of MF is inhibited in direct contact with eosinophils. This occurs through extracellular DNA traps (EETosis) formed by eosinophils. Further, in vivo injection of MF triggered eosinophil-dependent DNA release and MF covered with DNA traps were more rapidly removed from the peripheral blood. To investigate the mechanism of EETosis, different C-type lectin receptors were blocked in co-cultures of MF and eosinophils. It was found that dectin-1 is the receptor necessary to induce EETosis. In addition, it was shown that the released DNA is mostly mitochondrial DNA. Moreover, the DNA-dependent inhibition of MF motility is a conserved mechanism, as EETosis was induced in eosinophils from human and mice after contact with MF from *L. sigmodontis* as well as the heartworm *Dirofilaria immitis*.

Complimentary project - 5 - IL-6 is required for protective immune responses against early filarial infection

Muhsin Muhsin, Jesuthas Ajendra , Katrin Gentil , Afiat Berbudi, **Anna-Lena Neumann** , Lil Klaas , Kim E Schmidt , Achim Hoerauf , Marc P Hübner; **International Journal for Parasitology. 2018 October;48(12):925-935.**

The pro-inflammatory cytokine IL-6 plays an important role during the innate immune response and is also a mediator between innate and adaptive immune response as it can act on leucocytes like granulocytes, lymphocytes, monocytes and dendritic cells. IL-6-deficient mice showed an increased worm burden after infection with *L. sigmodontis*. Since the worm burden was already increased at early infection time points, the immune response during migration from the skin to the thoracic cavity seemed to be affected. Therefore, vascular permeability was investigated, as it can facilitate larval migration when enhanced. However, inhibition of histamine release, which increases vascular permeability, had no impact on vascular permeability and worm recovery in $IL6^{-/-}$ mice and corresponding controls. In contrast, blocking the degranulation of mast cells in $IL6^{-/-}$ mice resulted in a reduced worm burden. This suggests that mediators released by mast cells improve larval migration at least partially. In addition, it was shown that subcutaneous administration of L3 larvae abolished the higher worm recovery in $IL\text{-}6^{-/-}$ mice, indicating the importance of IL-6 during early immune response within the skin. Therefore, local immune response within the skin were investigated after intradermal L3 or filarial crude extract inoculation. Mice lacking IL-6 showed an impaired recruitment of neutrophils and macrophages to the skin. Thus, IL-6 is required for optimal early immune response within the skin to impair migration of L3 larvae

Complimentary project - 6 - Filarial extract of *Litomosoides sigmodontis* induces a type 2 immune response and attenuates plaque development in hyperlipidemic ApoE-knockout mice

Constanze Kuehn, Miyuki Tauchi, Roman Furtmair, Katharina Urschel, Dorette Raaz-Schrauder, **Anna-Lena Neumann**, Stefan J Frohberger, Achim Hoerauf, Susanne Regus, Werner Lang, Tolga Atilla Sagban, Florian Matthias Stumpfe, Stephan Achenbach, Marc P Hübner , Barbara Dietel ; **The FASEB Journal. 2019 May;33(5):6497-6513**.

Hyperlipidemic ApoE-knockout mice ($ApoE^{-/-}$) are particularly suitable for the study of atherosclerosis due to a reduced ability to remove lipoprotein, resulting in an accumulation of

cholesterol ester-containing particles in the blood. The increased accumulation of cholesterol in the blood can lead to the formation of atherosclerotic plaques. Therefore, these mice show a particularly generalized pro-inflammatory phenotype. In contrast, helminths induce a Th2 immune response that tends to protect the host from pro-inflammatory diseases. Therefore, the effect of a shift to Th2 immunomodulation by administration of *L. sigmodontis* crude extract on atherosclerosis in $ApoE^{-/-}$ mice was investigated. In general, we observed that intraperitoneal administration of 50 µg crude extract induced a Th2 immune response as it increased frequencies of eosinophil and AAMΦ. In addition, the influence of LsAg application on the development of arteriosclerosis was investigated. For this purpose, $ApoE^{-/-}$ mice were given a high-fat diet for a period of 12 weeks and were treated with 50 µg LsAg weekly at the beginning of the diet. In addition, the therapeutic use of LsAg was also investigated. For this purpose, mice were studied that were fed a high-fat diet for 12 weeks, after which the same animals were fed a normal diet for 12 weeks and received weekly LsAg injections. A significant reduction in plaque size was observed in both models, preventive and therapeutic LsAg treatment. When LsAg was used as a therapeutic agent, a regression of plaque size and macrophage density in the aortic root was observed. In addition, Th1-specific gene expression and intraplaque inflammation were reduced. Further, *in vitro* assays have shown that LsAg affects endothelial signalling pathways. Here, the inhibition of JNK1/2 appears to be involved in the suppression of monocyte cell adhesion under proatherogenic shear stress. The switch to an enhanced Th2 immune response by LsAg exhibited an antiatherogenic effect due to the reduced plaque size and its reduction in the advanced arteriosclerosis experiment. Thus, inhibition of the Th1 immune response appears to mediate the protective role.

Complimentary project - 7 - Comparative study on serum-induced arthritis in the temporomandibular and limb joint of mice

Sema Safi, David Frommholz, Susanne Reimann, Werner Götz, Christoph Bourauel, **Anna-Lena Neumann**, Achim Hoerauf, Harald Ilges, Ali-Farid Safi, Andreas Jäger, Marc P Hübner, Lina Gölz; International Journal of rheumatic Diseases. 2019 April;22(4):636-645.

Rheumatoid arthritis is an autoimmune disease that causes severe inflammatory reactions within the joints. These inflammatory episodes can lead to great pain and physical impairment of the patient. It affects approximately 1.0% of adults in industrialised countries (5-50

cases/100,000 annually) (218). As the disease progresses, systemic inflammatory reactions can also occur, which can lead to concomitant cardiovascular disease. Using the K/BxN serum transfer model, rheumatoid arthritis can be induced in WT animals. The knee joints of the animals swell up already after 8 days and the mobility is limited. In this study, the K/BxN model was used to investigate the pathological mechanisms of rheumatoid arthritis in the temporomandibular joint (219, 220). The study revealed a significant paw swelling in affected animals compared to healthy control animals and before arthritis induction. In addition, the locomotor activity of the sick animals was reduced. The joints of the diseased animals also showed clear signs of inflammation, which were confirmed by histological and immunohistochemical methods. Interestingly, no inflammation or swelling was detected in the temporomandibular joint. Thus, the temporomandibular joint seems to be less susceptible to a rheumatoid inflammatory reactions than the joints of the extremities.

Complimentary project - 8 - Adiponectin Limits IFN-γ and IL-17 Producing CD4 T Cells in Obesity by Restraining Cell Intrinsic Glycolysis

Jayagopi Surendar, Stefan J Frohberger, Indulekha Karunakaran, Vanessa Schmitt, Wiebke Stamminger , **Anna-Lena Neumann**, Christoph Wilhelm, Achim Hoerauf , Marc P Hübner ; **Frontiers in Immunology. 2019 October 29;10:2555.**

The incidence of obesity is steadily increasing and has already caused 3.4 million deaths in 2010. Moreover, people often suffer from overweight, which leads to physical and social limitations (221). Therefore, it is of great interest not only to reduce or prevent the emergence but also to better understand the immune response during obesity. To study the immune response during obesity, C57BL/6 mice were set on a high fat diet (HFD) and compared to mice fed a normal diet. HFD shifted the immune response of affected animals to a pro-inflammatory milieu. The adipose tissue of HFD mice showed increased proportions of $CD4^+$ and $CD8^+$ T cells, as well as T cells that were IFN-γ and IL-17 positive. As depletion of antigen-presenting cells like macrophages and B cells did not lead to a reduction in $CD4^+$ inflammation during early HFD, we investigated the influence of the hormone adiponectin, which contributes to tissue insulin sensitivity. *In vitro* studies showed that adiponectin dampens $CD4^+$ IFN-γ and IL-17 positive T cells, which reduced priming of Th1 and Th17 cells in HFD mice. When HFD mice were treated with the crude extract of *L. sigmodontis* it led to an increased release of adiponectin as well as reduced Th1 and Th17 cell proportions.

In addition, the frequency of Th1 and Th17 cells was also reduced *in vitro* after T cell stimulation with adipocyte-conditioned media from LsAg-treated animals. Importantly, when an adiponectin neutralising antibody was added to the medium, the effect disappeared. This suggests that the positive effect of helminth infection and treatment with their products on glucose tolerance and obesity in mice may be due to the regulatory function of adiponectin on $CD4^+$ T cells.

5. References

1. Windsor, D. A. 1998. Controversies in parasitology, Most of the species on Earth are parasites. *International journal for parasitology* 28: 1939-1941.
2. Lucius RL-F, B. 1997. *Parasitologie. Grundlagen für Biologen, Mediziner und Veterinärmediziner*. Spektrum, Heidelberg.
3. Bruschi, F. 2014. *Helminth Infections and their Impact on Global Public Health* Springer, Vienna.
4. Taylor, M. J., A. Hoerauf, and M. Bockarie. 2010. Lymphatic filariasis and onchocerciasis. *Lancet (London, England)* 376: 1175-1185.
5. Savioli, L., D. Engels, D. Daumerie, J. Jannin, J. Alvar, K. Asiedu, M. Gastellu-Etchegorry, P. Simarro, and S. P. Mariotti. 2006. Response from Savioli and colleagues from the Department of Neglected Tropical Diseases, World Health Organization. *PLoS medicine* 3: e283.
6. 2021. About Parasites. Centers for disease control and prevention.
7. Collaborators, G. D. a. I. I. a. P. 2018. Global, regional, and national incidence, prevalence, and years lived with disability for 354 diseases and injuries for 195 countries and territories, 1990–2017: a systematic analysis for the Global Burden of Disease Study 2017. *The Lancet* 392.
8. Abiose, A. 1998. Onchocercal eye disease and the impact of Mectizan treatment. *Annals of tropical medicine and parasitology* 92 Suppl 1: S11-22.
9. Katawa, G., L. E. Layland, A. Y. Debrah, C. von Horn, L. Batsa, A. Kwarteng, S. Arriens, W. T. D, S. Specht, A. Hoerauf, and T. Adjobimey. 2015. Hyperreactive onchocerciasis is characterized by a combination of Th17-Th2 immune responses and reduced regulatory T cells. *PLoS neglected tropical diseases* 9: e3414.
10. Allen, J. E., O. Adjei, O. Bain, A. Hoerauf, W. H. Hoffmann, B. L. Makepeace, H. Schulz-Key, V. N. Tanya, A. J. Trees, S. Wanji, and D. W. Taylor. 2008. Of mice, cattle, and humans: the immunology and treatment of river blindness. *PLoS neglected tropical diseases* 2: e217.
11. Abraham, D., R. Lucius, and A. J. Trees. 2002. Immunity to Onchocerca spp. in animal hosts. *Trends in parasitology* 18: 164-171.
12. Nutman, T. B. 1998. Filariasis, Lymphatic. In *Encyclopedia of Immunology (Second Edition)*. P. J. Delves, ed. Elsevier, Oxford. 913-915.
13. King, C. L., J. Suamani, N. Sanuku, Y. C. Cheng, S. Satofan, B. Mancuso, C. W. Goss, L. J. Robinson, P. M. Siba, G. J. Weil, and J. W. Kazura. 2018. A Trial of a Triple-Drug Treatment for Lymphatic Filariasis. *The New England journal of medicine* 379: 1801-1810.
14. Weil, G. J., J. Bogus, M. Christian, C. Dubray, Y. Djuardi, P. U. Fischer, C. W. Goss, M. Hardy, P. Jambulingam, C. L. King, V. S. Kuttiat, K. Krishnamoorthy, M. Laman, J. F. Lemoine, K. K. O'Brian, L. J. Robinson, J. Samuela, K. B. Schechtman, A. Sircar, A. Srividya, A. C. Steer, T. Supali, and S. Subramanian. 2019. The safety of double- and triple-drug community mass drug administration for lymphatic filariasis: A multicenter, open-label, cluster-randomized study. *PLoS medicine* 16: e1002839.
15. Al-Kubati, A. S., A. R. Al-Samie, S. Al-Kubati, and R. M. R. Ramzy. 2020. The story of Lymphatic Filariasis elimination as a public health problem from Yemen. *Acta Tropica* 212: 105676.

16. Vercruysse, J., B. Levecke, and R. Prichard. 2012. Human soil-transmitted helminths: implications of mass drug administration. *Current opinion in infectious diseases* 25: 703-708.
17. Hoerauf, A., K. Pfarr, S. Mand, A. Y. Debrah, and S. Specht. 2011. Filariasis in Africa--treatment challenges and prospects. *Clin Microbiol Infect* 17: 977-985.
18. Hoerauf, A. 2008. Filariasis: new drugs and new opportunities for lymphatic filariasis and onchocerciasis. *Current opinion in infectious diseases* 21: 673-681.
19. Martin, R. J., A. P. Robertson, and S. Choudhary. 2021. Ivermectin: An Anthelmintic, an Insecticide, and Much More. *Trends in parasitology* 37: 48-64.
20. Verma, S., S. S. Kashyap, A. P. Robertson, and R. J. Martin. 2020. Diethylcarbamazine activates TRP channels including TRP-2 in filaria, Brugia malayi. *Communications biology* 3: 398.
21. Walker, M., S. D. S. Pion, H. Fang, J. Gardon, J. Kamgno, M. G. Basáñez, and M. Boussinesq. 2017. Macrofilaricidal Efficacy of Repeated Doses of Ivermectin for the Treatment of River Blindness. *Clinical infectious diseases : an official publication of the Infectious Diseases Society of America* 65: 2026-2034.
22. Bandi, C., A. J. Trees, and N. W. Brattig. 2001. Wolbachia in filarial nematodes: evolutionary aspects and implications for the pathogenesis and treatment of filarial diseases. *Veterinary parasitology* 98: 215-238.
23. McLaren, D. J., M. J. Worms, B. R. Laurence, and M. G. Simpson. 1975. Micro-organisms in filarial larvae (Nematoda). *Transactions of the Royal Society of Tropical Medicine and Hygiene* 69: 509-514.
24. Kozek, W. J., and H. F. Marroquin. 1977. Intracytoplasmic bacteria in Onchocerca volvulus. *The American journal of tropical medicine and hygiene* 26: 663-678.
25. Taylor, M. J., H. F. Cross, L. Ford, W. H. Makunde, G. B. Prasad, and K. Bilo. 2001. Wolbachia bacteria in filarial immunity and disease. *Parasite immunology* 23: 401-409.
26. Hoerauf, A., S. Mand, O. Adjei, B. Fleischer, and D. W. Büttner. 2001. Depletion of wolbachia endobacteria in Onchocerca volvulus by doxycycline and microfilaridermia after ivermectin treatment. *Lancet (London, England)* 357: 1415-1416.
27. Kramer, L., S. Crosara, G. Gnudi, M. Genchi, C. Mangia, A. Viglietti, and C. Quintavalla. 2018. Wolbachia, doxycycline and macrocyclic lactones: New prospects in the treatment of canine heartworm disease. *Veterinary parasitology* 254: 95-97.
28. Hoerauf, A., S. Mand, L. Volkmann, M. Büttner, Y. Marfo-Debrekyei, M. Taylor, O. Adjei, and D. W. Büttner. 2003. Doxycycline in the treatment of human onchocerciasis: Kinetics of Wolbachia endobacteria reduction and of inhibition of embryogenesis in female Onchocerca worms. *Microbes and infection* 5: 261-273.
29. Tamarozzi, F., A. Halliday, K. Gentil, A. Hoerauf, E. Pearlman, and M. J. Taylor. 2011. Onchocerciasis: the role of Wolbachia bacterial endosymbionts in parasite biology, disease pathogenesis, and treatment. *Clinical microbiology reviews* 24: 459-468.
30. Bockarie, M. J., and R. M. Deb. 2010. Elimination of lymphatic filariasis: do we have the drugs to complete the job? *Current opinion in infectious diseases* 23: 617-620.
31. Wormser, G. P., R. P. Wormser, F. Strle, R. Myers, and B. A. Cunha. 2019. How safe is doxycycline for young children or for pregnant or breastfeeding women? *Diagnostic microbiology and infectious disease* 93: 238-242.
32. Rajan, T. V., F. K. Nelson, E. Cupp, L. D. Schultz, and D. L. Greiner. 1992. Survival of Onchocerca volvulus in nodules implanted in immunodeficient rodents. *The Journal of parasitology* 78: 160-163.
33. Maréchal, P., L. Le Goff, G. Petit, M. Diagne, D. W. Taylor, and O. Bain. 1996. The fate of the filaria Litomosoides sigmodontis in susceptible and naturally resistant mice. *Parasite (Paris, France)* 3: 25-31.
34. Petit, G., M. Diagne, P. Marechal, D. Owen, D. Taylor, and O. Bain. 1992. Maturation of the filaria Litomosoides sigmodontis in BALB/c mice; comparative susceptibility of nine other inbred strains. *Ann Parasitol Hum Comp* 67: 144-150.
35. Morris, C. P., H. Evans, S. E. Larsen, and E. Mitre. 2013. A comprehensive, model-based review of vaccine and repeat infection trials for filariasis. *Clinical microbiology reviews* 26: 381-421.

36. Hoffmann, W., G. Petit, H. Schulz-Key, D. Taylor, O. Bain, and L. Le Goff. 2000. Litomosoides sigmodontis in mice: reappraisal of an old model for filarial research. *Parasitology today (Personal ed.)* 16: 387-389.
37. Risch, F., M. Ritter, A. Hoerauf, and M. P. Hübner. 2021. Human filariasis-contributions of the Litomosoides sigmodontis and Acanthocheilonema viteae animal model. *Parasitology research*.
38. Babayan, S., M. N. Ungeheuer, C. Martin, T. Attout, E. Belnoue, G. Snounou, L. Rénia, M. Korenaga, and O. Bain. 2003. Resistance and susceptibility to filarial infection with Litomosoides sigmodontis are associated with early differences in parasite development and in localized immune reactions. *Infection and immunity* 71: 6820-6829.
39. Bosshardt, S. C., J. W. McCall, S. U. Coleman, K. L. Jones, T. A. Petit, and T. R. Klei. 1993. Prophylactic activity of tetracycline against Brugia pahangi infection in jirds (Meriones unguiculatus). *The Journal of parasitology* 79: 775-777.
40. Hoerauf, A., K. Nissen-Pähle, C. Schmetz, K. Henkle-Dührsen, M. L. Blaxter, D. W. Büttner, M. Y. Gallin, K. M. Al-Qaoud, R. Lucius, and B. Fleischer. 1999. Tetracycline therapy targets intracellular bacteria in the filarial nematode Litomosoides sigmodontis and results in filarial infertility. *The Journal of clinical investigation* 103: 11-18.
41. Hoerauf, A., L. Volkmann, C. Hamelmann, O. Adjei, I. B. Autenrieth, B. Fleischer, and D. W. Büttner. 2000. Endosymbiotic bacteria in worms as targets for a novel chemotherapy in filariasis. *The Lancet* 355: 1242-1243.
42. Hubner, M. P., M. N. Torrero, J. W. McCall, and E. Mitre. 2009. Litomosoides sigmodontis: a simple method to infect mice with L3 larvae obtained from the pleural space of recently infected jirds (Meriones unguiculatus). *Experimental parasitology* 123: 95-98.
43. Karadjian, G., F. Fercoq, N. Pionnier, N. Vallarino-Lhermitte, E. Lefoulon, A. Nieguitsila, S. Specht, L. M. Carlin, and C. Martin. 2017. Migratory phase of Litomosoides sigmodontis filarial infective larvae is associated with pathology and transient increase of S100A9 expressing neutrophils in the lung. *PLoS neglected tropical diseases* 11: e0005596.
44. Layland, L. E., J. Ajendra, M. Ritter, A. Wiszniewsky, A. Hoerauf, and M. P. Hubner. 2015. Development of patent Litomosoides sigmodontis infections in semi-susceptible C57BL/6 mice in the absence of adaptive immune responses. *Parasites & vectors* 8: 396.
45. Medzhitov, R., and C. A. Janeway, Jr. 1997. Innate immunity: impact on the adaptive immune response. *Current opinion in immunology* 9: 4-9.
46. Finlay, C. M., and J. E. Allen. 2020. The immune response of inbred laboratory mice to Litomosoides sigmodontis: A route to discovery in myeloid cell biology. *Parasite immunology* 42: e12708.
47. Maizels, R. M., A. Balic, N. Gomez-Escobar, M. Nair, M. D. Taylor, and J. E. Allen. 2004. Helminth parasites--masters of regulation. *Immunol Rev* 201: 89-116.
48. Allen, J. E., and T. E. Sutherland. 2014. Host protective roles of type 2 immunity: parasite killing and tissue repair, flip sides of the same coin. *Seminars in immunology* 26: 329-340.
49. Henry, E. K., J. M. Inclan-Rico, and M. C. Siracusa. 2017. Type 2 cytokine responses: regulating immunity to helminth parasites and allergic inflammation. *Curr Pharmacol Rep* 3: 346-359.
50. Gazzinelli-Guimaraes, P. H., and T. B. Nutman. 2018. Helminth parasites and immune regulation. *F1000Research* 7.
51. Allen, J. E., and R. M. Maizels. 1996. Immunology of human helminth infection. *International archives of allergy and immunology* 109: 3-10.
52. Abraham, D., O. Leon, S. Schnyder-Candrian, C. C. Wang, A. M. Galioto, L. A. Kerepesi, J. J. Lee, and S. Lustigman. 2004. Immunoglobulin E and eosinophil-dependent protective immunity to larval Onchocerca volvulus in mice immunized with irradiated larvae. *Infection and immunity* 72: 810-817.
53. Pearlman, E. 1997. Immunopathology of onchocerciasis: a role for eosinophils in onchocercal dermatitis and keratitis. *Chemical immunology* 66: 26-40.
54. Hall, L. R., J. T. Kaifi, E. Diaconu, and E. Pearlman. 2000. CD4(+) depletion selectively inhibits eosinophil recruitment to the cornea and abrogates Onchocerca volvulus keratitis (River blindness). *Infection and immunity* 68: 5459-5461.

55. Knab, J., K. Darge, and D. W. Büttner. 1997. Immunohistological studies on macrophages in lymph nodes of onchocerciasis patients after treatment with ivermectin. *Tropical medicine & international health : TM & IH* 2: 1156-1169.
56. Boyd, A., J. M. Ribeiro, and T. B. Nutman. 2014. Human CD117 (cKit)+ innate lymphoid cells have a discrete transcriptional profile at homeostasis and are expanded during filarial infection. *PloS one* 9: e108649.
57. O'Regan, N. L., S. Steinfelder, G. Venugopal, G. B. Rao, R. Lucius, A. Srikantam, and S. Hartmann. 2014. Brugia malayi microfilariae induce a regulatory monocyte/macrophage phenotype that suppresses innate and adaptive immune responses. *PLoS neglected tropical diseases* 8: e3206-e3206.
58. Ajendra, J., S. Specht, S. Ziewer, A. Schiefer, K. Pfarr, M. Parčina, T. A. Kufer, A. Hoerauf, and M. P. Hübner. 2016. NOD2 dependent neutrophil recruitment is required for early protective immune responses against infectious Litomosoides sigmodontis L3 larvae. *Scientific reports* 6: 39648.
59. Frohberger, S. J., F. Fercoq, A. L. Neumann, J. Surendar, W. Stamminger, A. Ehrens, I. Karunakaran, E. Remion, T. Vogl, A. Hoerauf, C. Martin, and M. P. Hübner. 2020. S100A8/S100A9 deficiency increases neutrophil activation and protective immune responses against invading infective L3 larvae of the filarial nematode Litomosoides sigmodontis. *PLoS neglected tropical diseases* 14: e0008119.
60. Pionnier, N., E. Brotin, G. Karadjian, P. Hemon, F. Gaudin-Nome, N. Vallarino-Lhermitte, A. Nieguitsila, F. Fercoq, M. L. Aknin, V. Marin-Esteban, S. Chollet-Martin, G. Schlecht-Louf, F. Bachelerie, and C. Martin. 2016. Neutropenic Mice Provide Insight into the Role of Skin-Infiltrating Neutrophils in the Host Protective Immunity against Filarial Infective Larvae. *PLoS Negl Trop Dis* 10: e0004605.
61. Porthouse, K. H., S. R. Chirgwin, S. U. Coleman, H. W. Taylor, and T. R. Klei. 2006. Inflammatory responses to migrating Brugia pahangi third-stage larvae. *Infection and immunity* 74: 2366-2372.
62. Specht, S., J. K. Frank, J. Alferink, B. Dubben, L. E. Layland, G. Denece, O. Bain, I. Forster, C. J. Kirschning, C. Martin, and A. Hoerauf. 2011. CCL17 Controls Mast Cells for the Defense against Filarial Larval Entry. *J Immunol* 186: 4845-4852.
63. Allen, J. E., and T. E. Sutherland. 2014. Host protective roles of type 2 immunity: parasite killing and tissue repair, flip sides of the same coin. *Seminars in immunology* 26: 329-340.
64. Boyd, A., K. Killoran, E. Mitre, and T. B. Nutman. 2015. Pleural cavity type 2 innate lymphoid cells precede Th2 expansion in murine Litomosoides sigmodontis infection. *Experimental parasitology* 159: 118-126.
65. Herbert, D. B. R., B. Douglas, and K. Zullo. 2019. Group 2 Innate Lymphoid Cells (ILC2): Type 2 Immunity and Helminth Immunity. *International journal of molecular sciences* 20: 2276.
66. Babu, S., and T. B. Nutman. 2014. Immunology of lymphatic filariasis. *Parasite immunology* 36: 338-346.
67. Specht, S., L. Volkmann, T. Wynn, and A. Hoerauf. 2004. Interleukin-10 (IL-10) counterregulates IL-4-dependent effector mechanisms in Murine Filariasis. *Infection and immunity* 72: 6287-6293.
68. Porthouse, K. H., S. R. Chirgwin, S. U. Coleman, H. W. Taylor, and T. R. Klei. 2006. Inflammatory responses to migrating Brugia pahangi third-stage larvae. *Infection and immunity* 74: 2366-2372.
69. Weatherhead, J. E., P. Gazzinelli-Guimaraes, J. M. Knight, R. Fujiwara, P. J. Hotez, M. E. Bottazzi, and D. B. Corry. 2020. Host Immunity and Inflammation to Pulmonary Helminth Infections. *Front Immunol* 11: 594520-594520.
70. Maizels, R. M., and H. J. McSorley. 2016. Regulation of the host immune system by helminth parasites. *The Journal of allergy and clinical immunology* 138: 666-675.
71. Allen, J. E., and R. M. Maizels. 2011. Diversity and dialogue in immunity to helminths. *Nature reviews. Immunology* 11: 375-388.

72. Gentil, K., A. Hoerauf, and E. Pearlman. 2012. Differential induction of Th2- and Th1-associated responses by filarial antigens and endosymbiotic Wolbachia in a murine model of river blindness. *European journal of microbiology & immunology* 2: 134-139.
73. Torrero, M. N., M. P. Hübner, D. Larson, H. Karasuyama, and E. Mitre. 2010. Basophils amplify type 2 immune responses, but do not serve a protective role, during chronic infection of mice with the filarial nematode Litomosoides sigmodontis. *Journal of immunology (Baltimore, Md. : 1950)* 185: 7426-7434.
74. Specht, S., M. Saeftel, M. Arndt, E. Endl, B. Dubben, N. A. Lee, J. J. Lee, and A. Hoerauf. 2006. Lack of eosinophil peroxidase or major basic protein impairs defense against murine filarial infection. *Infection and immunity* 74: 5236-5243.
75. Ehrens, A., B. Lenz, A. L. Neumann, S. Giarrizzo, J. J. Reichwald, S. J. Frohberger, W. Stamminger, B. C. Buerfent, F. Fercoq, C. Martin, D. Kulke, A. Hoerauf, and M. P. Hübner. 2021. Microfilariae Trigger Eosinophil Extracellular DNA Traps in a Dectin-1-Dependent Manner. *Cell reports* 34: 108621.
76. Al-Qaoud, K. M., E. Pearlman, T. Hartung, J. Klukowski, B. Fleischer, and A. Hoerauf. 2000. A new mechanism for IL-5-dependent helminth control: neutrophil accumulation and neutrophil-mediated worm encapsulation in murine filariasis are abolished in the absence of IL-5. *International immunology* 12: 899-908.
77. Chen, F., W. Wu, A. Millman, J. F. Craft, E. Chen, N. Patel, J. L. Boucher, J. F. Urban, Jr., C. C. Kim, and W. C. Gause. 2014. Neutrophils prime a long-lived effector macrophage phenotype that mediates accelerated helminth expulsion. *Nature immunology* 15: 938-946.
78. Kreider, T., R. M. Anthony, J. F. Urban, Jr., and W. C. Gause. 2007. Alternatively activated macrophages in helminth infections. *Current opinion in immunology* 19: 448-453.
79. Herbert, D. R., C. Hölscher, M. Mohrs, B. Arendse, A. Schwegmann, M. Radwanska, M. Leeto, R. Kirsch, P. Hall, H. Mossmann, B. Claussen, I. Förster, and F. Brombacher. 2004. Alternative macrophage activation is essential for survival during schistosomiasis and downmodulates T helper 1 responses and immunopathology. *Immunity* 20: 623-635.
80. Van Dyken, S. J., and R. M. Locksley. 2013. Interleukin-4- and interleukin-13-mediated alternatively activated macrophages: roles in homeostasis and disease. *Annual review of immunology* 31: 317-343.
81. Saeftel, M., L. Volkmann, S. Korten, N. Brattig, K. Al-Qaoud, B. Fleischer, and A. Hoerauf. 2001. Lack of interferon-gamma confers impaired neutrophil granulocyte function and imparts prolonged survival of adult filarial worms in murine filariasis. *Microbes Infect* 3: 203-213.
82. Ajendra, J., S. Specht, A. L. Neumann, F. Gondorf, D. Schmidt, K. Gentil, W. H. Hoffmann, M. J. Taylor, A. Hoerauf, and M. P. Hubner. 2014. ST2 deficiency does not impair type 2 immune responses during chronic filarial infection but leads to an increased microfilaremia due to an impaired splenic microfilarial clearance. *PloS one* 9: e93072.
83. Maizels, R. M., E. J. Pearce, D. Artis, M. Yazdanbakhsh, and T. A. Wynn. 2009. Regulation of pathogenesis and immunity in helminth infections. *The Journal of experimental medicine* 206: 2059-2066.
84. Hoerauf, A., J. Satoguina, M. Saeftel, and S. Specht. 2005. Immunomodulation by filarial nematodes. *Parasite immunology* 27: 417-429.
85. Al-Qaoud, K. M., A. Taubert, H. Zahner, B. Fleischer, and A. Hoerauf. 1997. Infection of BALB/c mice with the filarial nematode Litomosoides sigmodontis: role of CD4+ T cells in controlling larval development. *Infection and immunity* 65: 2457-2461.
86. Korten, S., L. Volkmann, M. Saeftel, K. Fischer, M. Taniguchi, B. Fleischer, and A. Hoerauf. 2002. Expansion of NK cells with reduction of their inhibitory Ly-49A, Ly-49C, and Ly-49G2 receptor-expressing subsets in a murine helminth infection: contribution to parasite control. *Journal of immunology (Baltimore, Md. : 1950)* 168: 5199-5206.
87. Murphy K, T. P., Walport M. 2008. *Janeways´s Immunology*.
88. Satoguina, J. S., T. Adjobimey, K. Arndts, J. Hoch, J. Oldenburg, L. E. Layland, and A. Hoerauf. 2008. Tr1 and naturally occurring regulatory T cells induce IgG4 in B cells through GITR/GITR-L interaction, IL-10 and TGF-beta. *European journal of immunology* 38: 3101-3113.

89. White, M. P. J., C. M. McManus, and R. M. Maizels. 2020. Regulatory T-cells in helminth infection: induction, function and therapeutic potential. *Immunology* 160: 248-260.
90. Babu, S., S. Q. Bhat, N. Pavan Kumar, A. B. Lipira, S. Kumar, C. Karthik, V. Kumaraswami, and T. B. Nutman. 2009. Filarial lymphedema is characterized by antigen-specific Th1 and th17 proinflammatory responses and a lack of regulatory T cells. *PLoS neglected tropical diseases* 3: e420.
91. Smith, K. A., K. J. Filbey, L. A. Reynolds, J. P. Hewitson, Y. Harcus, L. Boon, T. Sparwasser, G. Hämmerling, and R. M. Maizels. 2016. Low-level regulatory T-cell activity is essential for functional type-2 effector immunity to expel gastrointestinal helminths. *Mucosal immunology* 9: 428-443.
92. Specht, S., M. D. Taylor, M. A. Hoeve, J. E. Allen, R. Lang, and A. Hoerauf. 2012. Over expression of IL-10 by macrophages overcomes resistance to murine filariasis. *Experimental parasitology* 132: 90-96.
93. Lightowlers, M. W., and M. D. Rickard. 1988. Excretory-secretory products of helminth parasites: effects on host immune responses. *Parasitology* 96 Suppl: S123-166.
94. Harnett, M. M., A. J. Melendez, and W. Harnett. 2010. The therapeutic potential of the filarial nematode-derived immunodulator, ES-62 in inflammatory disease. *Clinical and experimental immunology* 159: 256-267.
95. Pineda, M. A., F. Lumb, M. M. Harnett, and W. Harnett. 2014. ES-62, a therapeutic anti-inflammatory agent evolved by the filarial nematode Acanthocheilonema viteae. *Molecular and biochemical parasitology* 194: 1-8.
96. Harnett, W., I. B. McInnes, and M. M. Harnett. 2004. ES-62, a filarial nematode-derived immunomodulator with anti-inflammatory potential. *Immunology letters* 94: 27-33.
97. Berbudi, A., J. Surendar, J. Ajendra, F. Gondorf, D. Schmidt, A. L. Neumann, A. P. Wardani, L. E. Layland, L. S. Hoffmann, A. Pfeifer, A. Hoerauf, and M. P. Hübner. 2016. Filarial Infection or Antigen Administration Improves Glucose Tolerance in Diet-Induced Obese Mice. *Journal of innate immunity* 8: 601-616.
98. Hübner, M. P., J. T. Stocker, and E. Mitre. 2009. Inhibition of type 1 diabetes in filaria-infected non-obese diabetic mice is associated with a T helper type 2 shift and induction of FoxP3+ regulatory T cells. *Immunology* 127: 512-522.
99. Gondorf, F., A. Berbudi, B. C. Buerfent, J. Ajendra, D. Bloemker, S. Specht, D. Schmidt, A. L. Neumann, L. E. Layland, A. Hoerauf, and M. P. Hübner. 2015. Chronic filarial infection provides protection against bacterial sepsis by functionally reprogramming macrophages. *PLoS pathogens* 11: e1004616.
100. Huang, X., L. R. Zeng, F. S. Chen, J. P. Zhu, and M. H. Zhu. 2018. Trichuris suis ova therapy in inflammatory bowel disease: A meta-analysis. *Medicine* 97: e12087.
101. Garg, S. K., A. M. Croft, and P. Bager. 2014. Helminth therapy (worms) for induction of remission in inflammatory bowel disease. *The Cochrane database of systematic reviews*: Cd009400.
102. Wang, M., L. Wu, R. Weng, W. Zheng, Z. Wu, and Z. Lv. 2017. Therapeutic potential of helminths in autoimmune diseases: helminth-derived immune-regulators and immune balance. *Parasitology research* 116: 2065-2074.
103. Smallwood, T. B., P. R. Giacomin, A. Loukas, J. P. Mulvenna, R. J. Clark, and J. J. Miles. 2017. Helminth Immunomodulation in Autoimmune Disease. *Front Immunol* 8: 453.
104. Rodgers, D. T., M. A. Pineda, M. A. McGrath, L. Al-Riyami, W. Harnett, and M. M. Harnett. 2014. Protection against collagen-induced arthritis in mice afforded by the parasitic worm product, ES-62, is associated with restoration of the levels of interleukin-10-producing B cells and reduced plasma cell infiltration of the joints. *Immunology* 141: 457-466.
105. Hübner, M. P., Y. Shi, M. N. Torrero, E. Mueller, D. Larson, K. Soloviova, F. Gondorf, A. Hoerauf, K. E. Killoran, J. T. Stocker, S. J. Davies, K. V. Tarbell, and E. Mitre. 2012. Helminth protection against autoimmune diabetes in nonobese diabetic mice is independent of a type 2 immune shift and requires TGF-β. *Journal of immunology (Baltimore, Md. : 1950)* 188: 559-568.
106. Zaccone, P., and A. Cooke. 2013. Helminth mediated modulation of Type 1 diabetes (T1D). *International journal for parasitology* 43: 311-318.

107. Berbudi, A., J. Ajendra, A. P. Wardani, A. Hoerauf, and M. P. Hübner. 2016. Parasitic helminths and their beneficial impact on type 1 and type 2 diabetes. *Diabetes/metabolism research and reviews* 32: 238-250.
108. Licona-Limón, P., L. K. Kim, N. W. Palm, and R. A. Flavell. 2013. TH2, allergy and group 2 innate lymphoid cells. *Nature Immunology* 14: 536-542.
109. Chico, M. E., M. G. Vaca, A. Rodriguez, and P. J. Cooper. 2019. Soil-transmitted helminth parasites and allergy: Observations from Ecuador. *Parasite immunology* 41: e12590.
110. Maizels, R. M. 2020. Regulation of immunity and allergy by helminth parasites. *Allergy* 75: 524-534.
111. Tracey, K. J. 2002. The inflammatory reflex. *Nature* 420: 853-859.
112. Dantzer, R. 2018. Neuroimmune Interactions: From the Brain to the Immune System and Vice Versa. *Physiological reviews* 98: 477-504.
113. Webster, J. I., L. Tonelli, and E. M. Sternberg. 2002. Neuroendocrine regulation of immunity. *Annual review of immunology* 20: 125-163.
114. Sternberg, E. M. 2006. Neural regulation of innate immunity: a coordinated nonspecific host response to pathogens. *Nature reviews. Immunology* 6: 318-328.
115. Agelaki, S., C. Tsatsanis, A. Gravanis, and A. N. Margioris. 2002. Corticotropin-releasing hormone augments proinflammatory cytokine production from macrophages in vitro and in lipopolysaccharide-induced endotoxin shock in mice. *Infection and immunity* 70: 6068-6074.
116. Cuesta, M. C., L. Quintero, H. Pons, and H. Suarez-Roca. 2002. Substance P and calcitonin gene-related peptide increase IL-1 beta, IL-6 and TNF alpha secretion from human peripheral blood mononuclear cells. *Neurochemistry international* 40: 301-306.
117. Borovikova, L. V., S. Ivanova, M. Zhang, H. Yang, G. I. Botchkina, L. R. Watkins, H. Wang, N. Abumrad, J. W. Eaton, and K. J. Tracey. 2000. Vagus nerve stimulation attenuates the systemic inflammatory response to endotoxin. *Nature* 405: 458-462.
118. Tracey, K. J., C. J. Czura, and S. Ivanova. 2001. Mind over immunity. *FASEB journal : official publication of the Federation of American Societies for Experimental Biology* 15: 1575-1576.
119. Goehler, L. E., R. P. Gaykema, M. K. Hansen, K. Anderson, S. F. Maier, and L. R. Watkins. 2000. Vagal immune-to-brain communication: a visceral chemosensory pathway. *Autonomic neuroscience : basic & clinical* 85: 49-59.
120. Goehler, L. E., R. P. Gaykema, K. T. Nguyen, J. E. Lee, F. J. Tilders, S. F. Maier, and L. R. Watkins. 1999. Interleukin-1beta in immune cells of the abdominal vagus nerve: a link between the immune and nervous systems? *The Journal of neuroscience : the official journal of the Society for Neuroscience* 19: 2799-2806.
121. Rosas-Ballina, M., P. S. Olofsson, M. Ochani, S. I. Valdés-Ferrer, Y. A. Levine, C. Reardon, M. W. Tusche, V. A. Pavlov, U. Andersson, S. Chavan, T. W. Mak, and K. J. Tracey. 2011. Acetylcholine-synthesizing T cells relay neural signals in a vagus nerve circuit. *Science (New York, N.Y.)* 334: 98-101.
122. Renate Huch, K. D. J. 2007. *Mensch Körper Krankheiten*. Klaus D. Jürgens, München.
123. Picciotto, M. R., M. J. Higley, and Y. S. Mineur. 2012. Acetylcholine as a neuromodulator: cholinergic signaling shapes nervous system function and behavior. *Neuron* 76: 116-129.
124. Wess, J. 2003. Novel insights into muscarinic acetylcholine receptor function using gene targeting technology. *Trends in pharmacological sciences* 24: 414-420.
125. Picciotto, M. R., B. J. Caldarone, S. L. King, and V. Zachariou. 2000. Nicotinic receptors in the brain. Links between molecular biology and behavior. *Neuropsychopharmacology : official publication of the American College of Neuropsychopharmacology* 22: 451-465.
126. Douglas, C. L., H. A. Baghdoyan, and R. Lydic. 2002. Postsynaptic muscarinic M1 receptors activate prefrontal cortical EEG of C57BL/6J mouse. *Journal of neurophysiology* 88: 3003-3009.
127. Raiteri, M., R. Leardi, and M. Marchi. 1984. Heterogeneity of presynaptic muscarinic receptors regulating neurotransmitter release in the rat brain. *The Journal of pharmacology and experimental therapeutics* 228: 209-214.
128. Zhang, W., M. Yamada, J. Gomeza, A. S. Basile, and J. Wess. 2002. Multiple muscarinic acetylcholine receptor subtypes modulate striatal dopamine release, as studied with M1-M5

muscarinic receptor knock-out mice. *The Journal of neuroscience : the official journal of the Society for Neuroscience* 22: 6347-6352.
129. Tuchek, S., V. Dolezhal, and I. Richny. 1984. [Regulation of acetylcholine synthesis in presynaptic endings of cholinergic neurons of the central nervous system]. *Neirofiziologiia = Neurophysiology* 16: 603-611.
130. Wang, H., Y. Lu, and Z. Wang. 2007. Function of cardiac M3 receptors. *Autonomic & autacoid pharmacology* 27: 1-11.
131. Wess, J. 2004. Muscarinic acetylcholine receptor knockout mice: novel phenotypes and clinical implications. *Annual review of pharmacology and toxicology* 44: 423-450.
132. McGehee, D. S., M. J. Heath, S. Gelber, P. Devay, and L. W. Role. 1995. Nicotine enhancement of fast excitatory synaptic transmission in CNS by presynaptic receptors. *Science (New York, N.Y.)* 269: 1692-1696.
133. Wonnacott, S. 1997. Presynaptic nicotinic ACh receptors. *Trends in neurosciences* 20: 92-98.
134. Bucher, D., and J. M. Goaillard. 2011. Beyond faithful conduction: short-term dynamics, neuromodulation, and long-term regulation of spike propagation in the axon. *Progress in neurobiology* 94: 307-346.
135. Ge, S., and J. A. Dani. 2005. Nicotinic acetylcholine receptors at glutamate synapses facilitate long-term depression or potentiation. *The Journal of neuroscience : the official journal of the Society for Neuroscience* 25: 6084-6091.
136. Ji, D., R. Lape, and J. A. Dani. 2001. Timing and location of nicotinic activity enhances or depresses hippocampal synaptic plasticity. *Neuron* 31: 131-141.
137. Shen, J.-x., and J. L. Yakel. 2009. Nicotinic acetylcholine receptor-mediated calcium signaling in the nervous system. *Acta Pharmacol Sin* 30: 673-680.
138. Strom, T. B., A. Deisseroth, J. Morganroth, C. B. Carpenter, and J. P. Merrill. 1972. Alteration of the cytotoxic action of sensitized lymphocytes by cholinergic agents and activators of adenylate cyclase. *Proceedings of the National Academy of Sciences of the United States of America* 69: 2995-2999.
139. Cox, M. A., G. S. Duncan, G. H. Y. Lin, B. E. Steinberg, L. X. Yu, D. Brenner, L. N. Buckler, A. J. Elia, A. C. Wakeham, B. Nieman, C. Dominguez-Brauer, A. R. Elford, K. T. Gill, S. P. Kubli, J. Haight, T. Berger, P. S. Ohashi, K. J. Tracey, P. S. Olofsson, and T. W. Mak. 2019. Choline acetyltransferase-expressing T cells are required to control chronic viral infection. *Science (New York, N.Y.)* 363: 639-644.
140. Roberts, L. B., C. Schnoeller, R. Berkachy, M. Darby, J. Pillaye, M. J. Oudhoff, N. Parmar, C. Mackowiak, D. Sedda, V. Quesniaux, B. Ryffel, R. Vaux, K. Gounaris, S. Berrard, D. R. Withers, W. G. C. Horsnell, and M. E. Selkirk. 2021. Acetylcholine production by group 2 innate lymphoid cells promotes mucosal immunity to helminths. *Science immunology* 6.
141. Chu, C., C. N. Parkhurst, W. Zhang, L. Zhou, H. Yano, M. Arifuzzaman, and D. Artis. 2021. The ChAT-acetylcholine pathway promotes group 2 innate lymphoid cell responses and anti-helminth immunity. *Science immunology* 6.
142. Reardon, C., G. S. Duncan, A. Brustle, D. Brenner, M. W. Tusche, P. S. Olofsson, M. Rosas-Ballina, K. J. Tracey, and T. W. Mak. 2013. Lymphocyte-derived ACh regulates local innate but not adaptive immunity. *Proceedings of the National Academy of Sciences of the United States of America* 110: 1410-1415.
143. You, H., C. Liu, X. Du, S. Nawaratna, V. Rivera, M. Harvie, M. Jones, and D. P. McManus. 2018. Suppression of Schistosoma japonicum Acetylcholinesterase Affects Parasite Growth and Development. *International journal of molecular sciences* 19.
144. You, H., C. Liu, X. Du, and D. P. McManus. 2017. Acetylcholinesterase and Nicotinic Acetylcholine Receptors in Schistosomes and Other Parasitic Helminths. *Molecules (Basel, Switzerland)* 22: 1550.
145. Robertson, A. P., and R. J. Martin. 2007. Ion-channels on parasite muscle: pharmacology and physiology. *Invertebrate neuroscience : IN* 7: 209-217.
146. Kaminsky, R., N. Gauvry, S. Schorderet Weber, T. Skripsky, J. Bouvier, A. Wenger, F. Schroeder, Y. Desaules, R. Hotz, T. Goebel, B. C. Hosking, F. Pautrat, S. Wieland-Berghausen, and P. Ducray. 2008. Identification of the amino-acetonitrile derivative

monepantel (AAD 1566) as a new anthelmintic drug development candidate. *Parasitology research* 103: 931-939.
147. Crabtree, J. E., and R. A. Wilson. 1980. Schistosoma mansoni: a scanning electron microscope study of the developing schistosomulum. *Parasitology* 81: 553-564.
148. de Lange, A., U. F. Prodjinotho, H. Tomes, J. Hagen, B. A. Jacobs, K. Smith, W. Horsnell, C. Sikasunge, D. Hockman, M. E. Selkirk, C. Prazeres da Costa, and J. V. Raimondo. 2020. Taenia larvae possess distinct acetylcholinesterase profiles with implications for host cholinergic signalling. *PLoS neglected tropical diseases* 14: e0008966.
149. Baez-Pagan, C. A., M. Delgado-Velez, and J. A. Lasalde-Dominicci. 2015. Activation of the Macrophage alpha7 Nicotinic Acetylcholine Receptor and Control of Inflammation. *Journal of neuroimmune pharmacology : the official journal of the Society on NeuroImmune Pharmacology* 10: 468-476.
150. McLean, L. P., A. Smith, L. Cheung, R. Sun, V. Grinchuk, T. Vanuytsel, N. Desai, J. F. Urban, Jr., A. Zhao, J. P. Raufman, and T. Shea-Donohue. 2015. Type 3 Muscarinic Receptors Contribute to Clearance of Citrobacter rodentium. *Inflammatory bowel diseases* 21: 1860-1871.
151. Kistemaker, L. E., I. S. Bos, M. N. Hylkema, M. C. Nawijn, P. S. Hiemstra, J. Wess, H. Meurs, H. A. Kerstjens, and R. Gosens. 2013. Muscarinic receptor subtype-specific effects on cigarette smoke-induced inflammation in mice. *The European respiratory journal* 42: 1677-1688.
152. Kistemaker, L. E., R. P. van Os, A. Dethmers-Ausema, I. S. Bos, M. N. Hylkema, M. van den Berge, P. S. Hiemstra, J. Wess, H. Meurs, H. A. Kerstjens, and R. Gosens. 2015. Muscarinic M3 receptors on structural cells regulate cigarette smoke-induced neutrophilic airway inflammation in mice. *American journal of physiology. Lung cellular and molecular physiology* 308: L96-103.
153. Abe, S., H. Tsuboi, H. Kudo, H. Asashima, Y. Ono, F. Honda, H. Takahashi, M. Yagishita, S. Hagiwara, Y. Kondo, I. Matsumoto, and T. Sumida. 2020. M3 muscarinic acetylcholine receptor-reactive Th17 cells in primary Sjögren's syndrome. *JCI insight* 5.
154. Felton, J., S. Hu, and J. P. Raufman. 2018. Targeting M3 Muscarinic Receptors for Colon Cancer Therapy. *Current molecular pharmacology* 11: 184-190.
155. Ali, O., M. Tolaymat, S. Hu, G. Xie, and J. P. Raufman. 2021. Overcoming Obstacles to Targeting Muscarinic Receptor Signaling in Colorectal Cancer. *International journal of molecular sciences* 22.
156. Darby, M., C. Schnoeller, A. Vira, F. J. Culley, S. Bobat, E. Logan, F. Kirstein, J. Wess, A. F. Cunningham, F. Brombacher, M. E. Selkirk, and W. G. Horsnell. 2015. The M3 muscarinic receptor is required for optimal adaptive immunity to helminth and bacterial infection. *PLoS pathogens* 11: e1004636.
157. McLean, L. P., A. Smith, L. Cheung, J. F. Urban, Jr., R. Sun, V. Grinchuk, N. Desai, A. Zhao, J. P. Raufman, and T. Shea-Donohue. 2016. Type 3 muscarinic receptors contribute to intestinal mucosal homeostasis and clearance of Nippostrongylus brasiliensis through induction of TH2 cytokines. *American journal of physiology. Gastrointestinal and liver physiology* 311: G130-141.
158. Bühling, F., N. Lieder, U. C. Kühlmann, N. Waldburg, and T. Welte. 2007. Tiotropium suppresses acetylcholine-induced release of chemotactic mediators in vitro. *Respiratory medicine* 101: 2386-2394.
159. Anzueto, A., and M. Miravitlles. 2020. Tiotropium in chronic obstructive pulmonary disease - a review of clinical development. *Respiratory research* 21: 199.
160. Vacca, G., W. J. Randerath, and A. Gillissen. 2011. Inhibition of granulocyte migration by tiotropium bromide. *Respiratory research* 12: 24.
161. Malerba, M., A. Radaeli, G. Santini, J. Morjaria, N. Mores, C. Mondino, G. Macis, and P. Montuschi. 2018. The discovery and development of aclidinium bromide for the treatment of chronic obstructive pulmonary disease. *Expert opinion on drug discovery* 13: 563-577.
162. Gavaldà, A., M. Miralpeix, I. Ramos, R. Otal, C. Carreño, M. Viñals, T. Doménech, C. Carcasona, B. Reyes, D. Vilella, J. Gras, J. Cortijo, E. Morcillo, J. Llenas, H. Ryder, and J. Beleta. 2009. Characterization of Aclidinium Bromide, a Novel Inhaled Muscarinic

Antagonist, with Long Duration of Action and a Favorable Pharmacological Profile. *Journal of Pharmacology and Experimental Therapeutics* 331: 740-751.
163. Frohberger, S. J., J. Ajendra, J. Surendar, W. Stamminger, A. Ehrens, B. C. Buerfent, K. Gentil, A. Hoerauf, and M. P. Hübner. 2019. Susceptibility to L. sigmodontis infection is highest in animals lacking IL-4R/IL-5 compared to single knockouts of IL-4R, IL-5 or eosinophils. *Parasites & vectors* 12: 248.
164. Hubner, M. P., D. Larson, M. N. Torrero, E. Mueller, Y. Shi, K. E. Killoran, and E. Mitre. 2011. Anti-FcepsilonR1 antibody injections activate basophils and mast cells and delay Type 1 diabetes onset in NOD mice. *Clinical immunology (Orlando, Fla.)* 141: 205-217.
165. Montaldo, E., K. Juelke, and C. Romagnani. 2015. Group 3 innate lymphoid cells (ILC3s): Origin, differentiation, and plasticity in humans and mice. *European journal of immunology* 45: 2171-2182.
166. Torrero, M. N., D. Larson, M. P. Hübner, and E. Mitre. 2009. CD200R surface expression as a marker of murine basophil activation. *Clinical and experimental allergy : journal of the British Society for Allergy and Clinical Immunology* 39: 361-369.
167. Daniłowicz-Luebert, E., S. Steinfelder, A. A. Kühl, G. Drozdenko, R. Lucius, M. Worm, E. Hamelmann, and S. Hartmann. 2013. A nematode immunomodulator suppresses grass pollen-specific allergic responses by controlling excessive Th2 inflammation. *International journal for parasitology* 43: 201-210.
168. Zaccone, P., and S. W. Hall. 2012. Helminth infection and type 1 diabetes. *The review of diabetic studies : RDS* 9: 272-286.
169. King, C. L., S. Mahanty, V. Kumaraswami, J. S. Abrams, J. Regunathan, K. Jayaraman, E. A. Ottesen, and T. B. Nutman. 1993. Cytokine control of parasite-specific anergy in human lymphatic filariasis. Preferential induction of a regulatory T helper type 2 lymphocyte subset. *The Journal of clinical investigation* 92: 1667-1673.
170. Maizels, R. M., H. H. Smits, and H. J. McSorley. 2018. Modulation of Host Immunity by Helminths: The Expanding Repertoire of Parasite Effector Molecules. *Immunity* 49: 801-818.
171. Schnoeller, C., S. Rausch, S. Pillai, A. Avagyan, B. M. Wittig, C. Loddenkemper, A. Hamann, E. Hamelmann, R. Lucius, and S. Hartmann. 2008. A helminth immunomodulator reduces allergic and inflammatory responses by induction of IL-10-producing macrophages. *Journal of immunology (Baltimore, Md. : 1950)* 180: 4265-4272.
172. Lu, B., K. Kwan, Y. A. Levine, P. S. Olofsson, H. Yang, J. Li, S. Joshi, H. Wang, U. Andersson, S. S. Chavan, and K. J. Tracey. 2014. alpha7 nicotinic acetylcholine receptor signaling inhibits inflammasome activation by preventing mitochondrial DNA release. *Molecular medicine (Cambridge, Mass.)* 20: 350-358.
173. Wessler, I. K., and C. J. Kirkpatrick. 2012. Activation of muscarinic receptors by non-neuronal acetylcholine. *Handbook of experimental pharmacology*: 469-491.
174. Fujii, T., M. Mashimo, Y. Moriwaki, H. Misawa, S. Ono, K. Horiguchi, and K. Kawashima. 2017. Expression and Function of the Cholinergic System in Immune Cells. *Front Immunol* 8: 1085.
175. Pionnier, N., E. Brotin, G. Karadjian, P. Hemon, F. Gaudin-Nomé, N. Vallarino-Lhermitte, A. Nieguitsila, F. Fercoq, M. L. Aknin, V. Marin-Esteban, S. Chollet-Martin, G. Schlecht-Louf, F. Bachelerie, and C. Martin. 2016. Neutropenic Mice Provide Insight into the Role of Skin-Infiltrating Neutrophils in the Host Protective Immunity against Filarial Infective Larvae. *PLoS neglected tropical diseases* 10: e0004605.
176. Fox, E. M., C. P. Morris, M. P. Hübner, and E. Mitre. 2015. Histamine 1 Receptor Blockade Enhances Eosinophil-Mediated Clearance of Adult Filarial Worms. *PLoS neglected tropical diseases* 9: e0003932.
177. Ritter, M., R. S. Tamadaho, J. Feid, W. Vogel, K. Wiszniewsky, S. Perner, A. Hoerauf, and L. E. Layland. 2017. IL-4/5 signalling plays an important role during Litomosoides sigmodontis infection, influencing both immune system regulation and tissue pathology in the thoracic cavity. *International journal for parasitology* 47: 951-960.
178. Carmona-Rivera, C., M. M. Purmalek, E. Moore, M. Waldman, P. J. Walter, H. M. Garraffo, K. A. Phillips, K. L. Preston, J. Graf, M. J. Kaplan, and P. C. Grayson. 2017. A role for

muscarinic receptors in neutrophil extracellular trap formation and levamisole-induced autoimmunity. *JCI insight* 2: e89780.
179. Soderberg, D., and M. Segelmark. 2018. Neutrophil extracellular traps in vasculitis, friend or foe? *Current opinion in rheumatology* 30: 16-23.
180. Haben, I., W. Hartmann, S. Specht, A. Hoerauf, A. Roers, W. Müller, and M. Breloer. 2013. T-cell-derived, but not B-cell-derived, IL-10 suppresses antigen-specific T-cell responses in Litomosoides sigmodontis-infected mice. *European journal of immunology* 43: 1799-1805.
181. Cox, M. A., C. Bassi, M. E. Saunders, R. Nechanitzky, I. Morgado-Palacin, C. Zheng, and T. W. Mak. 2020. Beyond neurotransmission: acetylcholine in immunity and inflammation. *Journal of internal medicine* 287: 120-133.
182. Taylor, M. D., A. Harris, M. G. Nair, R. M. Maizels, and J. E. Allen. 2006. F4/80+ alternatively activated macrophages control CD4+ T cell hyporesponsiveness at sites peripheral to filarial infection. *Journal of immunology (Baltimore, Md. : 1950)* 176: 6918-6927.
183. Nair, M. G., I. J. Gallagher, M. D. Taylor, P. Loke, P. S. Coulson, R. A. Wilson, R. M. Maizels, and J. E. Allen. 2005. Chitinase and Fizz family members are a generalized feature of nematode infection with selective upregulation of Ym1 and Fizz1 by antigen-presenting cells. *Infection and immunity* 73: 385-394.
184. Gavaldà, A., M. Miralpeix, I. Ramos, R. Otal, C. Carreño, M. Viñals, T. Doménech, C. Carcasona, B. Reyes, D. Vilella, J. Gras, J. Cortijo, E. Morcillo, J. Llenas, H. Ryder, and J. Beleta. 2009. Characterization of Aclidinium Bromide, a Novel Inhaled Muscarinic Antagonist, with Long Duration of Action and a Favorable Pharmacological Profile. *Journal of Pharmacology and Experimental Therapeutics* 331: 740.
185. Kistemaker, L. E., S. T. Bos, W. M. Mudde, M. N. Hylkema, P. S. Hiemstra, J. Wess, H. Meurs, H. A. Kerstjens, and R. Gosens. 2014. Muscarinic M(3) receptors contribute to allergen-induced airway remodeling in mice. *American journal of respiratory cell and molecular biology* 50: 690-698.
186. Layland, L. E., J. Ajendra, M. Ritter, A. Wiszniewsky, A. Hoerauf, and M. P. Hübner. 2015. Development of patent Litomosoides sigmodontis infections in semi-susceptible C57BL/6 mice in the absence of adaptive immune responses. *Parasites & vectors* 8: 396.
187. Vandoorne, K., Y. Addadi, and M. Neeman. 2010. Visualizing vascular permeability and lymphatic drainage using labeled serum albumin. *Angiogenesis* 13: 75-85.
188. Endo, M., M. Hori, H. Ozaki, T. Oikawa, H. Odaguchi, and T. Hanawa. 2018. Possible anti-inflammatory role of Zingiberis processum rhizoma, one component of the Kampo formula daikenchuto, against neutrophil infiltration through muscarinic acetylcholine receptor activation. *Journal of pharmacological sciences* 137: 379-386.
189. Gavaldà, A., I. Ramos, C. Carcasona, E. Calama, R. Otal, J. L. Montero, S. Sentellas, M. Aparici, D. Vilella, J. Alberti, J. Beleta, and M. Miralpeix. 2014. The in vitro and in vivo profile of aclidinium bromide in comparison with glycopyrronium bromide. *Pulmonary pharmacology & therapeutics* 28: 114-121.
190. Graham, A. L., M. D. Taylor, L. Le Goff, T. J. Lamb, M. Magennis, and J. E. Allen. 2005. Quantitative appraisal of murine filariasis confirms host strain differences but reveals that BALB/c females are more susceptible than males to Litomosoides sigmodontis. *Microbes and infection* 7: 612-618.
191. Balamayooran, G., S. Batra, S. Cai, J. Mei, G. S. Worthen, A. L. Penn, and S. Jeyaseelan. 2012. Role of CXCL5 in leukocyte recruitment to the lungs during secondhand smoke exposure. *American journal of respiratory cell and molecular biology* 47: 104-111.
192. Fulkerson, P. C., and M. E. Rothenberg. 2018. Eosinophil Development, Disease Involvement, and Therapeutic Suppression. *Advances in immunology* 138: 1-34.
193. Yang, M., S. P. Hogan, S. Mahalingam, S. M. Pope, N. Zimmermann, P. Fulkerson, L. A. Dent, I. G. Young, K. I. Matthaei, M. E. Rothenberg, and P. S. Foster. 2003. Eotaxin-2 and IL-5 cooperate in the lung to regulate IL-13 production and airway eosinophilia and hyperreactivity. *The Journal of allergy and clinical immunology* 112: 935-943.
194. Schultz, J., and K. Kaminker. 1962. Myeloperoxidase of the leucocyte of normal human blood. I. Content and localization. *Archives of biochemistry and biophysics* 96: 465-467.

195. Khan, A. A., M. A. Alsahli, and A. H. Rahmani. 2018. Myeloperoxidase as an Active Disease Biomarker: Recent Biochemical and Pathological Perspectives. *Medical sciences (Basel, Switzerland)* 6.
196. Metzler, K. D., T. A. Fuchs, W. M. Nauseef, D. Reumaux, J. Roesler, I. Schulze, V. Wahn, V. Papayannopoulos, and A. Zychlinsky. 2011. Myeloperoxidase is required for neutrophil extracellular trap formation: implications for innate immunity. *Blood* 117: 953-959.
197. Volkmann, L., O. Bain, M. Saeftel, S. Specht, K. Fischer, F. Brombacher, K. I. Matthaei, and A. Hoerauf. 2003. Murine filariasis: interleukin 4 and interleukin 5 lead to containment of different worm developmental stages. *Medical microbiology and immunology* 192: 23-31.
198. Le Goff, L., P. Loke, H. F. Ali, D. W. Taylor, and J. E. Allen. 2000. Interleukin-5 is essential for vaccine-mediated immunity but not innate resistance to a filarial parasite. *Infection and immunity* 68: 2513-2517.
199. Margraf, A., K. Ley, and A. Zarbock. 2019. Neutrophil Recruitment: From Model Systems to Tissue-Specific Patterns. *Trends in immunology* 40: 613-634.
200. Papayannopoulos, V., K. D. Metzler, A. Hakkim, and A. Zychlinsky. 2010. Neutrophil elastase and myeloperoxidase regulate the formation of neutrophil extracellular traps. *The Journal of cell biology* 191: 677-691.
201. Gentil, K., C. S. Lentz, R. Rai, M. Muhsin, A. D. Kamath, O. Mutluer, S. Specht, M. P. Hübner, and A. Hoerauf. 2014. Eotaxin-1 is involved in parasite clearance during chronic filarial infection. *Parasite Immunol* 36: 60-77.
202. Herbert, D. R., B. Douglas, and K. Zullo. 2019. Group 2 Innate Lymphoid Cells (ILC2): Type 2 Immunity and Helminth Immunity. *International journal of molecular sciences* 20.
203. Jiang, W., D. Li, R. Han, C. Zhang, W. N. Jin, K. Wood, Q. Liu, F. D. Shi, and J. Hao. 2017. Acetylcholine-producing NK cells attenuate CNS inflammation via modulation of infiltrating monocytes/macrophages. *Proceedings of the National Academy of Sciences of the United States of America* 114: E6202-e6211.
204. Babayan, S., T. Attout, S. Specht, A. Hoerauf, G. Snounou, L. Renia, M. Korenaga, O. Bain, and C. Martin. 2005. Increased early local immune responses and altered worm development in high-dose infections of mice susceptible to the filaria Litomosoides sigmodontis. *Med Microbiol Immunol* 194: 151-162.
205. Bonne-Année, S., L. A. Kerepesi, J. A. Hess, J. Wesolowski, F. Paumet, J. B. Lok, T. J. Nolan, and D. Abraham. 2014. Extracellular traps are associated with human and mouse neutrophil and macrophage mediated killing of larval Strongyloides stercoralis. *Microbes and infection* 16: 502-511.
206. Bonilla, M. C., L. Fingerhut, A. Alfonso-Castro, A. Mergani, C. Schwennen, M. von Köckritz-Blickwede, and N. de Buhr. 2020. How Long Does a Neutrophil Live?-The Effect of 24 h Whole Blood Storage on Neutrophil Functions in Pigs. *Biomedicines* 8: 278.
207. Neavin, D. R., D. Liu, B. Ray, and R. M. Weinshilboum. 2018. The Role of the Aryl Hydrocarbon Receptor (AHR) in Immune and Inflammatory Diseases. *International journal of molecular sciences* 19.
208. Safe, S., U. H. Jin, H. Park, R. S. Chapkin, and A. Jayaraman. 2020. Aryl Hydrocarbon Receptor (AHR) Ligands as Selective AHR Modulators (SAhRMs). *International journal of molecular sciences* 21.
209. Yeste, A., I. D. Mascanfroni, M. Nadeau, E. J. Burns, A. M. Tukpah, A. Santiago, C. Wu, B. Patel, D. Kumar, and F. J. Quintana. 2014. IL-21 induces IL-22 production in CD4+ T cells. *Nature communications* 5: 3753.
210. Vorderstrasse, B. A., J. A. Cundiff, and B. P. Lawrence. 2006. A dose-response study of the effects of prenatal and lactational exposure to TCDD on the immune response to influenza a virus. *Journal of toxicology and environmental health. Part A* 69: 445-463.
211. Shi, L. Z., N. G. Faith, Y. Nakayama, M. Suresh, H. Steinberg, and C. J. Czuprynski. 2007. The aryl hydrocarbon receptor is required for optimal resistance to Listeria monocytogenes infection in mice. *Journal of immunology (Baltimore, Md. : 1950)* 179: 6952-6962.
212. Stehle, C., D. C. Hernández, and C. Romagnani. 2018. Innate lymphoid cells in lung infection and immunity. *Immunological reviews* 286: 102-119.

213. Mao, K., A. P. Baptista, S. Tamoutounour, L. Zhuang, N. Bouladoux, A. J. Martins, Y. Huang, M. Y. Gerner, Y. Belkaid, and R. N. Germain. 2018. Innate and adaptive lymphocytes sequentially shape the gut microbiota and lipid metabolism. *Nature* 554: 255-259.
214. Bonne-Année, S., and T. B. Nutman. 2018. Human innate lymphoid cells (ILCs) in filarial infections. *Parasite immunology* 40.
215. Huang, L., and J. A. Appleton. 2016. Eosinophils in Helminth Infection: Defenders and Dupes. *Trends in parasitology* 32: 798-807.
216. Capron, M., G. Torpier, and A. Capron. 1979. In vitro killing of S. mansoni schistosomula by eosinophils from infected rats: role of cytophilic antibodies. *Journal of immunology (Baltimore, Md. : 1950)* 123: 2220-2230.
217. Buys, J., R. Wever, R. van Stigt, and E. J. Ruitenberg. 1981. The killing of newborn larvae of Trichinella spiralis by eosinophil peroxidase in vitro. *European journal of immunology* 11: 843-845.
218. Scott, D. L., F. Wolfe, and T. W. Huizinga. 2010. Rheumatoid arthritis. *Lancet (London, England)* 376: 1094-1108.
219. Caplazi, P., M. Baca, K. Barck, R. A. Carano, J. DeVoss, W. P. Lee, B. Bolon, and L. Diehl. 2015. Mouse Models of Rheumatoid Arthritis. *Veterinary pathology* 52: 819-826.
220. Tu, J., S. Stoner, P. D. Fromm, T. Wang, D. Chen, J. Tuckermann, M. S. Cooper, M. J. Seibel, and H. Zhou. 2018. Endogenous glucocorticoid signaling in chondrocytes attenuates joint inflammation and damage. *FASEB journal : official publication of the Federation of American Societies for Experimental Biology* 32: 478-487.
221. Ng, M., T. Fleming, M. Robinson, B. Thomson, N. Graetz, C. Margono, E. C. Mullany, S. Biryukov, C. Abbafati, S. F. Abera, J. P. Abraham, N. M. Abu-Rmeileh, T. Achoki, F. S. AlBuhairan, Z. A. Alemu, R. Alfonso, M. K. Ali, R. Ali, N. A. Guzman, W. Ammar, P. Anwari, A. Banerjee, S. Barquera, S. Basu, D. A. Bennett, Z. Bhutta, J. Blore, N. Cabral, I. C. Nonato, J. C. Chang, R. Chowdhury, K. J. Courville, M. H. Criqui, D. K. Cundiff, K. C. Dabhadkar, L. Dandona, A. Davis, A. Dayama, S. D. Dharmaratne, E. L. Ding, A. M. Durrani, A. Esteghamati, F. Farzadfar, D. F. Fay, V. L. Feigin, A. Flaxman, M. H. Forouzanfar, A. Goto, M. A. Green, R. Gupta, N. Hafezi-Nejad, G. J. Hankey, H. C. Harewood, R. Havmoeller, S. Hay, L. Hernandez, A. Husseini, B. T. Idrisov, N. Ikeda, F. Islami, E. Jahangir, S. K. Jassal, S. H. Jee, M. Jeffreys, J. B. Jonas, E. K. Kabagambe, S. E. Khalifa, A. P. Kengne, Y. S. Khader, Y. H. Khang, D. Kim, R. W. Kimokoti, J. M. Kinge, Y. Kokubo, S. Kosen, G. Kwan, T. Lai, M. Leinsalu, Y. Li, X. Liang, S. Liu, G. Logroscino, P. A. Lotufo, Y. Lu, J. Ma, N. K. Mainoo, G. A. Mensah, T. R. Merriman, A. H. Mokdad, J. Moschandreas, M. Naghavi, A. Naheed, D. Nand, K. M. Narayan, E. L. Nelson, M. L. Neuhouser, M. I. Nisar, T. Ohkubo, S. O. Oti, A. Pedroza, D. Prabhakaran, N. Roy, U. Sampson, H. Seo, S. G. Sepanlou, K. Shibuya, R. Shiri, I. Shiue, G. M. Singh, J. A. Singh, V. Skirbekk, N. J. Stapelberg, L. Sturua, B. L. Sykes, M. Tobias, B. X. Tran, L. Trasande, H. Toyoshima, S. van de Vijver, T. J. Vasankari, J. L. Veerman, G. Velasquez-Melendez, V. V. Vlassov, S. E. Vollset, T. Vos, C. Wang, X. Wang, E. Weiderpass, A. Werdecker, J. L. Wright, Y. C. Yang, H. Yatsuya, J. Yoon, S. J. Yoon, Y. Zhao, M. Zhou, S. Zhu, A. D. Lopez, C. J. Murray, and E. Gakidou. 2014. Global, regional, and national prevalence of overweight and obesity in children and adults during 1980-2013: a systematic analysis for the Global Burden of Disease Study 2013. *Lancet (London, England)* 384: 766-781.

List of abbreviations

AAMΦ	Alternatively activated macrophages
ACh	Acetylcholine
AChE	Acetylcholine esterase

AhR	Aryl Hydrocarbon receptor
BSA	Bovine serum albumin
°C	Degree Celsius
COPD	Chronic obstructive pulmonary disease
CNS	Central nervous system
CXCL	C-X-C motif ligand
CD	Cluster of differentiation
ConA	Concanavalin A
ChAt	Cholinacetyl transferase
DC	Dendritic cell
DEC	Diethylcarbamazine
DMSO	Dimethyl sulfoxide
DNA	Desoxyribonucleic acid
DOX	Doxycycline
dpi	Days post infection
EDTA	Ethylenediaminetraacetic acid
E/S	Excretory/secretory
ELISA	Enzyme-linked immunosorbent assay
EPO	Eosinophil peroxidase
FACS	Fluorescence activated automatic cell sorting
FMO	Fluorescence minus one
FSC	Forwards scatter
g	Gravity
GABA	gaba aminobutyric acid
IFNγ	Interferon gamma
Ig	Immunoglobulin
IL	Interleukin
ILC	Innate lymphoid cells
IL-R	Interleukin receptor
IMMIP	Institute of Medical Microbiology, Immunology and Parasitology

HPA	Hypothylamo-pyturitary adrenal axis
iv	Intravenous
IVM	Ivermectin
KO	Knock-out
L3	Third larval stage
LF	Lymphatic filariasis
LPS	Lipopolysaccharide
LsAg	*Litomosoides sigmodontis* crude extract
MACS	Magnetic activated cell sorting
mAChR	Muscarinic acetylcholine receptor
MBP	Major basic protein
MCP	Monocyte chemotactic protein
MDA	Mass drug administration
MPO	Myeloid peroxidase
M	Molarity (mol/L)
Med	Medium (RPMI 1640)
Min	Minutes
MF	Microfilariae
MFI	Mean fluorescence intensity
MHC	Mayor histocompatibilty complex
mL	Millilitre
nAChR	Nicotinic acetylcholine receptor
NETs	Neutrophil extracellular traps
OD	Optical density
PBS	Phosphate buffered saline
PCR	Polymerase chain reaction
PE	Phycoerythrin
PFA	Para-formaldehyde
PMA	Phorbol-12-myristat-13-acetat
PNS	Peripheral nervous system
RBC	Red blood cell

rpm	Rounds per minute
RPMI	Roswell Park Memorial Institute
RT	Room temperature
RT-PCR	Realtime PCR
ROS	Reactive oxygen species
SAE	Severe adverse events
SNS	Systemic nervous system
SSC	Side scatter
TSLP	Thymic stromal lymophopoietin
Th	T helper cell
TMB	Tetraethylbenzidine
T reg	Regulatory T cell
WHO	World health organisation
WT	Wild-type
+/-	Positive/negative

Publications in peer-reviewed journals

Published:

1) Ajendra J, Specht S, **Neumann AL,** Fabian Gondorf, David Schmidt, Katrin Gentil, Wolfgang H Hoffmann, Mark J Taylor, Achim Hoerauf, Marc P Hübner. ST2 deficiency does not impair type 2 immune responses during chronic filarial infection but leads to an increased microfilaremia due to an impaired splenic microfilarial clearance. PLoS One. 2014 Mar 24;9(3):e93072

2) Berbudi A, Ajendra J, Gondorf F, Schmidt D, **Neumann AL**, Laura E Layland, Achim Hoerauf, Marc P Hübner. Chronic Filarial Infection Provides Protection against Bacterial Sepsis by Functionally Reprogramming Macrophages. *PLOS Pathogen* 2015 Jan; 11(1): e1004616

3) Afiat Berbudi, Surendar J, Ajendra J, Gondorf F, Schmidt D, **Neumann AL**, Ajeng P F Wardani, Laura E Layland, Linda S Hoffmann, Alexander Pfeifer, Achim Hoerauf, Marc P Hübner. Filarial Infection or Antigen Administration Improves Glucose Tolerance in Diet-Induced Obese Mice. J Innate Immun. 2016;8(6):601-616

4) Muhsin M, Ajendra J, Gentil K, Berbudi A**, Neumann AL**, Lil Klaas, Kim E Schmidt, Achim Hoerauf, Marc P Hübner. IL-6 is required for protective immune responses against early filarial infection. Int J Parasitol. 2018 Oct;48(12):925-935.

5) Safi S, Frommholz D, Reimann S, Götz W, Bourauel C, **Neumann AL**, Achim Hoerauf, Harald Ilges, Ali-Farid Safi, Andreas Jäger, Marc P Hübner, Lina Gölz. Comparative study on serum-induced arthritis in the temporomandibular and limb joint of mice. Int J Rheum Dis. 2019 Apr;22(4):636-645.

6) Kuehn C, Tauchi M, Furtmair R, Urschel K, Raaz-Schrauder D, **Neumann AL**, ...Filarial extract of *Litomosoides sigmodontis* induces a type 2 immune response and attenuates plaque development in hyperlipidemic ApoE-knockout mice. FASEB J. 2019 May;33(5):6497-6513

7) Surendar J, Frohberger SJ, Karunakaran I, Schmitt V, Stamminger W, **Neumann AL**,... Adiponectin Limits IFN-γ and IL-17 Producing CD4 T Cells in Obesity by Restraining Cell Intrinsic Glycolysis. Front Immunol. 2019 Oct 29;10:2555. doi: 10.3389/fimmu.2019.02555. PMID: 31736971; PMCID: PMC6828851.

8) Frohberger SJ, Fercoq F, **Neumann AL**, Stefan J. Frohberger, Achim Hoerauf, Susanne Regus, Werner Lang, Tolga Atilla Sagban, Florian Matthias Stumpfe, Stephan Achenbach, Marc P Hübner, Barbara Dietel. S100A8/S100A9 deficiency increases neutrophil activation and protective immune responses against invading infective L3 larvae of the filarial nematode Litomosoides sigmodontis. PLoS Negl Trop Dis. 2020 Feb 27;14(2):e0008119. doi: 10.1371/journal.pntd.0008119. PMID: 32107497; PMCID: PMC7064255.

9) Ehrens A., Lenz B., **Neumann AL,** Samuela Giarrizzo, Julia J Reichwald, Stefan J Frohberger, Wiebke Stamminger, Benedikt C Buerfent, Frédéric Fercoq, Coralie Martin, Daniel Kulke, Achim Hoerauf, Marc p Hübner..Microfilaria Trigger Eosinophil Extracellular DNA Traps in a Dectin-1-Dependent Manner. 2021 Cell Reports, Volume 34, Issue 2, 108621

Under preparation:

10) Stefan J. Frohberger, **Anna-Lena Neumann,** Fabian Gondorf, Wiebke Stamminger, Jayagopi Surendar, Alexandra Ehrens, Achim Hoerauf, Irmgard Förster, Marc P. Hübner. Absence of the Aryl hydrocarbon receptor impairs protective immune responses and enhances vascular permeability during *Litomosoides sigmodontis* infection

11) Julia J. Reichwald, **Anna-Lena Neumann**, Frederic Risch, Stefan J. Frohberger, Johanna F. Scheunemann, Alexandra Ehrens, Wiebke Strutz, Achim Hoerauf, Beatrix Schumak, Marc P. Hübner. ILC2s control microfilaremia during *Litomosoides sigmodontis* infection.

12) **Anna-Lena Neumann,** Karunakaran I, Stefan J. Frohberger, Alexandra Ehrens, Achim Hoerauf, William GC Horsnell, Marc P. Hübner. Acetylcholine mediates protective immune responses against the rodent filarial nematode *Litomosoides sigmodontis*

Conferences

Oral presentation at the DGfl AK Infektionsimmunologie, Rothenfels, March 2017 (title of the talk: Contribution of acetylcholine in regulating immunity to a respiratory viral infection)

Oral presentation at the conference from Le Studium "Neurotransmitters: non-neuronal functions and therapeutic opportunities "Orleans, 26th - 28th March 2018; (title of the talk: Contribution of acetylcholine in regulating immunity to *Litomosoides sigmodontis* infection)

Poster presentation at the Cluster Science Days, Bonn, November 2019 (title of the poster: Acetylcholine regulates immunity to the rodent filarial nematode *Litomosoides sigmodontis*)

Oral presentation at the 29th Annual meeting of the German Society of Parasitology (DGP), Bonn, 15th - 17th March 2021; (title of the talk: Acetylcholine mediates protective immune responses against the rodent filarial nematode *Litomosoides sigmodontis*)

Acknowledgements

First of all I want to thank the Director of the Institute of Medical Microbiology, Immunology and Parasitology, Prof. Dr. Achim Hörauf, for giving me the opportunity to fulfil my PhD thesis at the University Hospital of Bonn. I would also like to extend my gratitude to my reviewers Prof. Dr. Marc Hübner and Prof. Dr. Walter Witke. Also many thanks to PD Dr. Gerlinde van Echten-Deckert and Prof. Dr. Ian Brock for accepting to be members of the examination committee.

My deepest gratitude goes to my group leader and primary supervisor Prof. Dr. Marc Hübner for his excellent guidance and supervision during my PhD. He was available at all times as an intensive consultant and motivated me a lot during my educational and professional career.

I am also very grateful to the former and current group members of AG Hübner for their support and the special moments and cheers during and after work: Dr. Stefan Julian Frohberger, Dr. Indulekha Karunakaran, Dr. Alexandra Ehrens, Wiebke Stamminger, Benjamin Lenz, Johanna Scheunemann, Julia Reichwald, Frederic Risch as well as Martina Fendler and Marianne Koschel. I would also like to share my appreciation with my (former) colleagues of the other research groups at the IMMIP (AG Layland, AG Adjobimey, AG Pfarr, AG Klarmann-Schulz) especially Anna, Kathi, Kirstin and Tine for scientific support and friendship.

Most credits are going to my partner Mike Gajdiss, my parents Jutta und Herbert Neumann and my brother Daniel von Horn for their unconditional support and endless encouragement during this unique and exciting phase of my life. Thank you so much that you believe in me all the time!